DOKUZ EYLÜL UNIVERSITY
GRADUATE SCHOOL OF NATURAL AND APPLIED SCIENCES

DYNAMIC STABILITY OF CRACKED COMPOSITE PLATES

by
Özgür SAYER

October, 2020
İZMİR

DYNAMIC STABILITY OF CRACKED COMPOSITE PLATES

A Thesis Submitted to the
Graduate School of Natural and Applied Sciences of Dokuz Eylül University
In Partial Fulfillment of the Requirements for the Degree of Master of Science
in Mechanical Engineering, Machine Theory and Dynamics Program

by
Özgür SAYER

October, 2020
İZMİR

M.Sc THESIS EXAMINATION RESULT FORM

We have read the thesis entitled **"DYNAMIC STABILITY OF CRACKED COMPOSITE PLATES"** completed by **ÖZGÜR SAYER** under supervision of **PROF. DR. HASAN ÖZTÜRK** and we certify that in our opinion it is fully adequate, in scope and in quality, as a thesis for the degree of Master of Science.

Prof. Dr. Hasan ÖZTÜRK

Supervisor

Dr. Öğr. Üyesi Aysun BALTACI

(Jury Member)

Prof. Dr. Çınar Emine YENİ

(Jury Member)

Prof. Dr. Özgür ÖZÇELİK
Director
Graduate School of Natural and Applied Sciences

ACKNOWLEDGMENTS

I would like to express my respect and gratitude to my thesis supervisor Prof. Dr. Hasan ÖZTÜRK for his guidance, encouragement, effort and patience throughout my education and this thesis.

I am remarkably thanks to my family for their patience and support during my education.

Özgür SAYER

DYNAMIC STABILITY OF CRACKED COMPOSITE PLATES

ABSTRACT

In recent decades, composite plates are widely used in a wide variety of engineering applications such as the automotive industry, aerospace, marine, rail vehicles and civil engineering structures. Composite plates are subjected to static and dynamic loads. In this study, the dynamic stability of cracked composite plates has been investigated numerically by using the finite element method. Isotropic thin plate based on the Kirchhoff's thin plate theory is modelled by using the principles of the finite element method. In addition to, a composite plate based on classical lamination theory is modelled by using the finite element method. It is assumed that the boundary condition of the thin plate is fixed on one side and the other sides are free. The thin plate is divided into square plate elements. These square plates have four nodes and each node have one translational and two rotational degrees of freedom, so these square plates have twelve degrees of freedom. Mathieu-Hill type motion equation which is used to calculate the dynamic stability of the plate, is created by using energy expressions obtained from the Lagrange equation. The developed MATLAB finite element code is used to examine the effect of crack on natural frequency, critical buckling load and dynamic stability for isotropic and composite plates. Furthermore, MATLAB results are compared with the results of ANSYS model and very good agreement between these results is observed.

Keywords: Dynamic stability, cracked composite plates, finite element method, natural frequency, critical buckling load

ÇATLAKLI KOMPOZİT PLAKALARIN DİNAMİK KARARLILIĞI

ÖZ

Son yıllarda, kompozit plakalar otomotiv endüstrisi, havacılık, deniz, demiryolu araçları ve inşaat mühendisliği yapıları gibi çok çeşitli mühendislik uygulamalarında yaygın olarak kullanılmaktadır. Kompozit plakalar statik ve dinamik yüklere maruz kalır. Bu çalışmada, sonlu elemanlar yöntemi kullanılarak çatlaklı kompozit plakaların dinamik kararlılığı sayısal olarak incelenmiştir. Kirchhoff'un ince plaka teorisine dayanan izotropik ince plaka, sonlu elemanlar metodu kullanılarak modellenmiştir. Ek olarak, klasik laminasyon teorisine dayanan kompozit plaka, sonlu elemanlar yöntemi kullanılarak modellenmiştir. İnce plakanın sınır şartlarının bir taraftan sabitlendiği, diğer tarafların serbest olduğu varsayılmaktadır. İnce plaka, kare plaka elemanlara bölünmüştür. Bu kare plaka elemanlar dört düğüme sahiptir ve her düğüm bir vektörel ve iki dönme serbestlik derecesine sahiptir, bu yüzden bu kare plaka elemanlar on iki serbestlik derecesine sahiptir. Plakanın dinamik kararlılığını hesaplamak için kullanılan Mathieu-Hill tipi hareket denklemi, Lagrange denkleminden elde edilen enerji ifadeleri kullanılarak oluşturulmuştur. Geliştirilen MATLAB sonlu elemanlar kodu kullanılarak çatlağın izotropik ve kompozit plakalar için doğal frekans, kritik burkulma yükü ve dinamik kararlılığı üzerindeki etkisi incelenmiştir. Ayrıca, MATLAB sonuçları ile ANSYS sonuçları karşılaştırılmış ve sonuçların çok yakın olduğu gözlemlenmiştir.

Anahtar kelimeler: Dinamik kararlılık, çatlaklı kompozit plakalar, sonlu elemanlar methodu, doğal frekans, kritik burkulma yükü

CONTENTS

LIST OF FIGURES

Page

LIST OF TABLES

CHAPTER ONE
INTRODUCTION

The requirements of modern society variationed over the centuries and especially in the last few years. In this new era, reliable structures with high performance, lightweight, toughness, strength and low cost sustainable products and processes are some of the requisitions. Using conventional materials, all requirements such as strength, toughness and low cost can not be satisfied. In particularly recent years, composite materials are created by combining two or more different materials to provide these properties. In many branches of engineering, composite plates are widely used such as the automotive industry, aerospace, spacecraft and solar panels.

Furthermore, the crack can occur on a plate because of various reasons such as mechanical damage, fatigue. The crack not only causes a reduction in local stiffness but also significantly affect the mechanical behavior of the entire plate. For this reason, the effect of crack on the dynamic behavior of plate has been investigated in many studies using numerical methods of fracture mechanics.

Composite plates are subjected to various loading types such as static and dynamic loads which are cause loss of static and dynamic instability. If the static buckling load is greater than the amplitudes of the pulses, vibrations occur in the plate, and for certain frequencies of the pulses resonance will occur. The loads are parametric loads. Thus, the buckling problem, the amplitude and frequency of the vibrating charge are calculated in a parametric valid differential equation rather than a compelling function as in normal resonance. This differential equation is known as the Mathieu-Hill type differential equation.

Up to now, many studies about composite material, crack, and dynamic stability features of plates have been carried out by other researchers can be summarized as follows:

Kwon & Bang (1996) investigated the finite element method on structures. Structures were examined using the finite element method by MATLAB computer program. Soedel (2004) examined the vibration of plate structures. Natural frequencies and mode shapes were investigated using the finite element method on plate and shell structures. Semie (2010) investigated on numerical modeling of thin plates by using the finite element method. This thin plate was modeled by using Kirchoff's thin plate theory. Analyzes are performed with ANSYS and FORTRAN computer programs.

Chen & Yang (1990) investigated the effects of various parameters on the dynamic stability of laminated composite plates owing to periodic loads by using the finite element method. Reddy (2003) examined the mechanics of the composite plate. This study investigated theories of the composite plate. Bending, buckling and vibration of composite plates were examined in this study. Voyiadjis & Kattan (2005) studied on mechanics of composite materials by using the MATLAB program. MATLAB code was written to create composite materials in this study. Daniel & Ishai (2006) studied classical lamination theory. Classical lamination theory has been expanded to include various applications to sandwich plates. Aggarwal (2013) investigated the method for determining the optimal ply angle distributions variable stiffness laminates by using the finite element method.

Krawczuk & Ostachowicz (1994) studied a method of creating internal, non-propagating and open crack on the stiffness matrix of a finite plate element. A cracked stiffness matrix was created by using the Castigliano theory. Avadutala (2005) studied vibrational responses from a specimen which different types of fractures in it at different locations on the composite plate. Khoei (2015) studied on extended finite element method theory. In the study, special functions were added to the finite element approximation using the partition of unity in the extended finite element method.

Timoshenko & Gere (1961) investigated the theory of elastic stability on elastic systems. Bolotin (1964) studied on dynamic stability of elastic systems. This study was examined the effects of various parameters on dynamic stability by applying various methods. Hutt (1968) studied on dynamic stability of plates by using the finite element method. This study investigated the development of the governing set of matrix differential equations and the procedure for the development of the elemental matrices. Radu & Chattopadhyay (2002) investigated the dynamic stability of composite plates with delaminations. The results of natural frequencies and critical buckling loads were calculated and compared with NASTRAN results. The effect of edge crack and crack growth on the stability was examined in this study. Abramovich (2017) studied on vibrations and stability of composite plate structures. The natural frequencies, the critical buckling loads, dynamic stability of composite structures were examined in this study.

The purpose of this thesis is "dynamic stability of cracked composite plates" theory and to examine the dynamic stability of cracked composite plates by using the finite element method. Firstly, the isotropic thin plate based on Kirchhoff's thin plate theory was modeled by using the finite element method. Furthermore, a composite plate based on classical laminate plate theory was modeled and then, the crack was created on thin-plate by using principles of the finite element method. Mathieu-Hill type motion equation was created by using energy expressions obtained in the Lagrange equation. Finally, it has been examined the effect of crack on the natural frequency, the critical buckling load analysis and the dynamic stability for the isotropic and composite plate by using MATLAB and ANSYS computer programs. This thesis is described in the following chapters:

Chapter 1 deals with the introduction of this thesis. Furthermore, previous studies on dynamic stability, composite plate and crack are examined in chapter 1.

Chapter 2 presents the finite element model of isotropic, composite and cracked plates. Elastic stiffness, geometric stiffness and mass matrices of thin plate element are obtained by using the energy equations. Moreover, the cracked plate element model is developed by using the finite element method for the isotropic and composite plate.

Chapter 3 presents the theory of stability for plate structures.

Chapter 4 presents the results of natural frequency analysis, buckling analysis and dynamic stability analysis for the isotropic and composite plate. Furthermore, the effect of crack on natural frequency, critical buckling load and dynamic stability for the isotropic and composite plate are examined in chapter 4.

Chapter 5 presents conclusions drawn from this thesis.

CHAPTER TWO
FINITE ELEMENT MODEL

2.1 Introduction to the Finite Element Method

Nowadays, it is preferred to find approximate numerical solutions to problems instead of the exact closed form solutions in engineering applications. Therefore, engineers have developed a number of approximate methods of numerical analysis to preserve the complexity of problem. In recent years, the most widely used numerical analysis method is the finite element method.

The finite element method can be used for accurate solution of complex structures, differential equation problems and various engineering applications. It was initially developed to examine stresses in complex airframe structures. Since then it is widely used in the engineering industry due to it is an applicable analysis tool in various fields.

A finite element model of a problem gives a piecewise approach to equations. Therefore, the finite element method provides a solution structure consisting of a plurality of small and interconnected elements. The main property of the finite element method is that complex structure can be analytically modeled by replacing it with a separate set of elements. These elements can be assembled in various shapes (such as rectangles, triangles) appropriate with the shape of the complex structure, they can be used to replace the complex structures.

If the finite element method is examined in a problem of any dimension the field variables (such as displacement, stress) have an infinite number of values, so the problem has an infinite number of unknown. The finite element method divides the complex structure into elements and reduces the problem to a limited number of unknowns by expressing it in terms of assumed interpolation functions within each element. These interpolation functions are defined in terms of values of field variables at the nodes.

As seen from figure 2.1, the cantilever plate is subjected to the load. The finite element method can be used to analyze the complex structure.

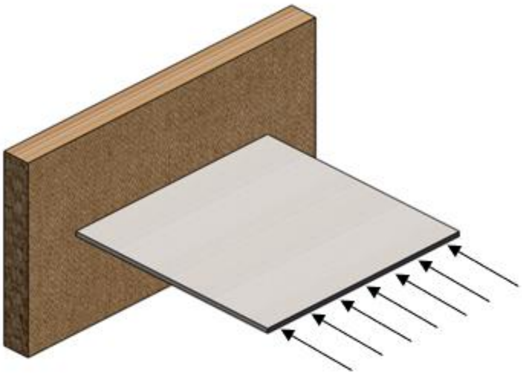

Figure 2.1 Cantilever plate is subjected to load

As seen from figure 2.2, the complex structure is divided into elements appropriate to the shape of the structure and adjacent elements are connected to each other by nodes. Each element is assumed to behave as a continuous structural member. In the solution process of the finite elements, the equilibrium of forces at the connection points and the suitability of the displacements between the elements are provided therefore the whole structure is made to behave as a single entity. As a result, a complex problem is simplified by divide into small elements in the finite element method.

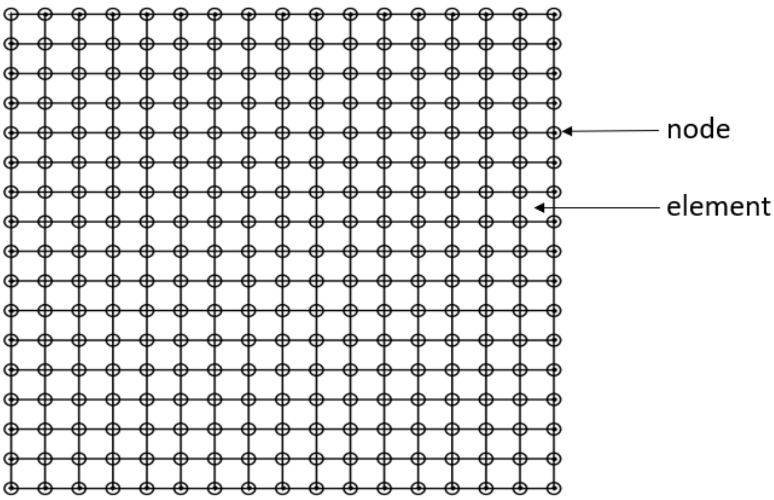

Figure 2.2 Plate divided into square elements with using the finite element method

The solution of the complex structure problem by using the finite element method always follows the step-by-step process (Öztürk, 1999, p.42):

The first step is to divide the continuum structure into small elements. In the example of figure 2.2, the plate is divided into square elements for analysis. If the finite element dimensions are selected smaller, these solutions will be more accurate (Öztürk, 1999).

The second step is to determine how many nodes to place on each element, and then choose the type of interpolation function to represent the variation of the field variable at the nodes (Öztürk, 1999).

In the third step, the matrices of each element (such as stiffness, mass) are determined and then these matrices are combined to obtain the matrix of the complex structure. According to the assembly procedure, in a node to which the elements are connected, the value of the field variable must be the same for each element that shares the node. In addition, the boundary conditions must be applied to the matrix obtained before the complex structure is analyzed.

In the final step, the analysis of the complex structure is usually done by digital computers and the problem of complex structure is solved.

2.2 Evaluation of the Displacement Matrix

In this thesis, the plate is divided into square elements because of the appropriate to square shape using the finite element method. These square elements are connected to each other by nodes. Degrees of freedom for these square elements are the displacements at the nodes.

According to Kirchhoff's thin plate theory, A plate's thickness is smaller than its other dimensions. This ratio is that a thickness ratio to length or width smaller than five percent.

The thin plate is taken as the reference plane (z = 0) for deriving kinematic equations. Therefore the axial straining is zero. The displacement can be expressed in terms of translations and rotations (Oñate, 2013, p.234).

As shown in figure 2.3, each square element has one translational and two rotational degrees of freedom at each corner. The two rotational components are situated on the x and y axes. The one translational component is situated on the z axes. Each square plate element has a total of twelve degrees of freedom.

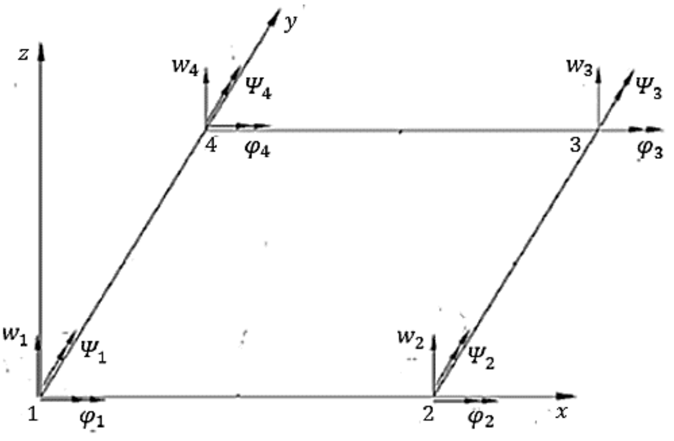

Figure 2.3 Generalized coordinates of a square plate element

Displacement matrix for corner 1 as

$$\{d_1\} = [w_1, \Psi_1, \varphi_1]^{\mathrm{T}} \tag{2.1}$$

The rotational components at corner 1 are

$$\Psi_1 = \frac{\partial w_1}{\partial y} \tag{2.2}$$

$$\varphi_1 = \frac{\partial w_1}{\partial x} \tag{2.3}$$

The displacement vector for an element square element is

$$\{q_e\}^{\mathrm{T}} = [w_1, \Psi_1, \varphi_1, w_2, \Psi_2, \varphi_2, w_3, \Psi_3, \varphi_3, w_4, \Psi_4, \varphi_4] \tag{2.4}$$

There are twelve displacement degrees of freedom in each of the square plate elements, the assumed polynomial $q_e(x, y)$ must also contain twelve constant terms.

Coefficient matrix is

$$[\alpha^e] = [\alpha_1^e, \alpha_2^e, \alpha_3^e, \alpha_4^e, \alpha_5^e, \alpha_6^e, \alpha_7^e, \alpha_8^e, \alpha_9^e, \alpha_{10}^e, \alpha_{11}^e, \alpha_{12}^e\ ]^{\mathrm{T}} \tag{2.5}$$

Maintain geometric isotropy, the displacement model is taken as

$$[C_e] = \ [1, x, y, x^2, xy, y^2, x^3, x^2y, xy^2, y^3, x^3y, xy^3] \tag{2.6}$$

Therefore the displacement function is

$$q_e(x, y) = [C_e] * [\alpha^e] \tag{2.7}$$

The displacement function is obtained;

$$\begin{aligned} q_e(x, y) = \alpha_1^e + \alpha_2^e x + \alpha_3^e y + \alpha_4^e x^2 + \alpha_5^e xy + \alpha_6^e y^2 + \alpha_7^e x^3 + \alpha_8^e x^2 y + \\ \alpha_9^e xy^2 + \alpha_{10}^e y^3 + \alpha_{11}^e x^3 y + \alpha_{12}^e xy^3 \end{aligned} \tag{2.8}$$

The displacement function is used to create a displacement matrix at corner 1. Displacement matrix at corner 1 as

$$\{d_1\} = \begin{bmatrix} 1 & x_1 & y_1 & x_1^2 & x_1y_1 & y_1^2 & x_1^3 & x_1^2y_1 & x_1y_1^2 & y_1^3 & x_1^3y_1 & x_1y_1^3 \\ 0 & 0 & 1 & 0 & x_1 & 2y_1 & 0 & x_1^2 & 2x_1y_1 & 3y_1^2 & x_1^3 & 3x_1y_1^2 \\ 0 & 1 & 0 & 2x_1 & y_1 & 0 & 3x_1^2 & 2x_1y_1 & y_1^2 & 0 & 3x_1^2y_1 & y_1^3 \end{bmatrix} * [\alpha^e] \tag{2.9}$$

The displacement matrix for the square plate element as

$$\{d_1, d_2, d_3, d_4\} = [A_e] * [\alpha^e] \tag{2.10}$$

Where

$$[A_e] = \begin{bmatrix} 1 & x_1 & y_1 & x_1^2 & x_1y_1 & y_1^2 & x_1^3 & x_1^2y_1 & x_1y_1^2 & y_1^3 & x_1^3y_1 & x_1y_1^3 \\ 0 & 0 & 1 & 0 & x_1 & 2y_1 & 0 & x_1^2 & 2x_1y_1 & 3y_1^2 & x_1^3 & 3x_1y_1^2 \\ 0 & 1 & 0 & 2x_1 & y_1 & 0 & 3x_1^2 & 2x_1y_1 & y_1^2 & 0 & 3x_1^2y_1 & y_1^3 \\ 1 & x_2 & y_2 & x_2^2 & x_2y_2 & y_2^2 & x_2^3 & x_2^2y_2 & x_2y_2^2 & y_2^3 & x_2^3y_2 & x_2y_2^3 \\ 0 & 0 & 1 & 0 & x_2 & 2y_2 & 0 & x_2^2 & 2x_2y_2 & 3y_2^2 & x_2^3 & 3x_2y_2^2 \\ 0 & 1 & 0 & 2x_2 & y_2 & 0 & 3x_2^2 & 2x_2y_2 & y_2^2 & 0 & 3x_2^2y_2 & y_2^3 \\ 1 & x_3 & y_3 & x_3^2 & x_3y_3 & y_3^2 & x_3^3 & x_3^2y_3 & x_3y_3^2 & y_3^3 & x_3^3y_3 & x_3y_3^3 \\ 0 & 0 & 1 & 0 & x_3 & 2y_3 & 0 & x_3^2 & 2x_3y_3 & 3y_3^2 & x_3^3 & 3x_3y_3^2 \\ 0 & 1 & 0 & 2x_3 & y_3 & 0 & 3x_3^2 & 2x_3y_3 & y_3^2 & 0 & 3x_3^2y_3 & y_3^3 \\ 1 & x_4 & y_4 & x_4^2 & x_4y_4 & y_4^2 & x_4^3 & x_4^2y_4 & x_4y_4^2 & y_4^3 & x_4^3y_4 & x_4y_4^3 \\ 0 & 0 & 1 & 0 & x_4 & 2y_4 & 0 & x_4^2 & 2x_4y_4 & 3y_4^2 & x_4^3 & 3x_4y_4^2 \\ 0 & 1 & 0 & 2x_4 & y_4 & 0 & 3x_4^2 & 2x_4y_4 & y_4^2 & 0 & 3x_4^2y_4 & y_4^3 \end{bmatrix} \tag{2.11}$$

2.2.1 Evaluation of the Element Elastic Stiffness Matrix

According to kirchhoff's thin plate theory, the stress-strain matrix form for an elastic isotropic plate as (Ventsel & Krauthammer, 2001)

$$\begin{Bmatrix} \sigma_{xx} \\ \sigma_{yy} \\ \tau_{xy} \end{Bmatrix} = \frac{E * \mathrm{h}^3}{1 - v^2} \begin{bmatrix} 1 & v & 0 \\ v & 1 & 0 \\ 0 & 0 & \frac{1-v}{2} \end{bmatrix} \begin{Bmatrix} \varepsilon_{xx} \\ \varepsilon_{yy} \\ \Upsilon_{xy} \end{Bmatrix} \tag{2.12}$$

E is young's modulus of the isotropic thin plate.

v is poisson's ratio of the isotropic thin plate.

h is thickness of the isotropic thin plate.

Shear modulus of the isotropic plate, G, is given by

$$G = \frac{E}{2 * (1 + v)} \tag{2.13}$$

The strain matrix for the elastic isotropic plate as

$$\{\mathcal{E}_e\} = \left\{-\frac{\partial^2 q_e}{\partial x^2}, -\frac{\partial^2 q_e}{\partial y^2}, -2\frac{\partial^2 q_e}{\partial x \partial y}\right\} \tag{2.14}$$

The strain matrix applied to the displacement matrix at each node. Substituting equation (2.6) into equation (2.14) and we obtain:

$$[\mathrm{H}_e] = \begin{bmatrix} 0 & 0 & 0 & -2 & 0 & 0 & -6x & -2y & 0 & 0 & -6xy & 0 \\ 0 & 0 & 0 & 0 & 0 & -2 & 0 & 0 & -2x & -6y & 0 & -6xy \\ 0 & 0 & 0 & 0 & -2 & 0 & 0 & -4x & -4y & 0 & -6x^2 & -6y^2 \end{bmatrix} \tag{2.15}$$

The strain matrix for an isotropic thin plate as

$$[\mathcal{E}_e] = [\mathrm{H}_e] * [\alpha^e] \tag{2.16}$$

The strain displacement matrix is

$$[\mathrm{B}_e] = [\mathrm{H}_e] * [A_e]^{-1} \tag{2.17}$$

For an elastic isotropic plate, the rigidity matrix is

$$[\mathrm{D}_e] = \frac{E * \mathrm{h}^3}{12(1 - v^2)} \begin{bmatrix} 1 & v & 0 \\ v & 1 & 0 \\ 0 & 0 & \frac{1 - v}{2} \end{bmatrix} \tag{2.18}$$

The local elastic stiffness matrix for an istoropic plate as

$$[K_e]^e = \iint [\mathrm{B}_e]^{\mathrm{T}} [\mathrm{D}_e][\mathrm{B}_e]\, dx\, dy \tag{2.19}$$

2.2.2 Evaluation of the Element Mass Matrix

According to Kirchhoff's thin plate theory, interpolation matrix as

$$[N_e] = [C_e] * [A_e]^{-1} \tag{2.20}$$

Local mass matrix is calculated which is represented $[M]^e$ as

$$[M]^e = \iint [N_e]^{\mathrm{T}} \rho [N_e] \, dx \, dy \tag{2.21}$$

2.2.3 Evaluation of the Element Geometrical Stiffness Matrix

In engineering applications, the critical buckling load is the greatest load that can be applied to a structural element in equilibrium without disturbing the stable equilibrium state. If a structural member is subjected to a load greater than the critical buckling load, the stable state of the structural member suddenly turns into the unstable state and simultaneously changes from the previous stable configuration of the equilibrium state to another stable configuration.

In this study, it is assumed that $\mathrm{N}_y = 0$ and $\mathrm{N}_{xy} = 0$ .The local geometric stiffness matrix formula is used to calculate the critical buckling load. The local geometric stiffness matrix formula is

$$\left[K_g^*\right]^e = \mathrm{h} \iint [S]^{\mathrm{T}} \mathrm{N}_x [S] dx dy \tag{2.22}$$

Where the matrix $[S]^{\mathrm{T}}$ is given by

$$[S]^{\mathrm{T}} = \begin{bmatrix} 1-\zeta\eta-(3-2\zeta)\zeta^2(1-\eta)-(1-\zeta)(3-2\eta)\eta^2 \\ (1-\zeta)\eta(1-\eta)^2 b \\ -\zeta(1-\zeta)^2(1-\eta)a \\ (1-\zeta)(3-2\eta)\eta^2+\zeta(1-\zeta)(1-2\zeta)\eta \\ -(1-\zeta)(1-\eta)\eta^2 b \\ -\zeta(1-\zeta)^2\eta a \\ (3-2\zeta)\zeta^2\eta-\zeta\eta(1-\eta)(1-2\eta) \\ -\zeta(1-\eta)\eta^2 b \\ (1-\zeta)\zeta^2\eta a \\ (3-2\zeta)\zeta^2(1-\eta)+\zeta\eta(1-\eta)(1-2\eta) \\ \zeta\eta(1-\eta)^2 b \\ (1-\zeta)\zeta^2(1-\eta)a \end{bmatrix} \tag{2.23}$$

Where,

$$\zeta = \frac{l_p}{a_e} \tag{2.24}$$

$$\eta = \frac{w_p}{b_e} \tag{2.25}$$

a_e = Length of the square plate element on the x-direction,

b_e = Width of the square plate element on the y-direction,

l_p = Length of plate

w_p = Width of plate

2.3 Composite Structures

2.3.1 Introduction to Composite Structures

Since the first eras, the development of humans has been related to the use of materials. In the stone age, mankind used materials such as stone and wood to make tools and weapons because it was easy to find them from nature. After that, with the development of mankind, fundamental materials such as steel, aluminum and iron were used to satisfy the needs of mankind. Nowadays, the needs of people have increased in proportion to the development of technology. Therefore, people want to use structures and vehicles that include high performance, lightweight, strength and low cost. When conventional materials are used, not all of these requirements can be satisfied. To satisfy these requirements, composite materials are used which are a combination of two or more materials that have appropriate properties. Composite plates are widely used in many engineering fields, such as marine, automotive industry, aircraft, spacecraft and solar panels.

As shown in figure 2.4, the main components of composite materials are matrix and fiber. The fiber is usually discontinuous and stronger. The matrix is continuous and acts as a binder for the fibers. The properties of a composite material depend on the geometries, volume ratios, properties and distribution of components.

One of the most important parameters is matrix and fiber volume ratio. In the composite material, the volume ratio of the fibers is generally from sixty percent to seventy percent. When the volume ratio of the fibers used in the composite material increases, the strength of composite materials increases.

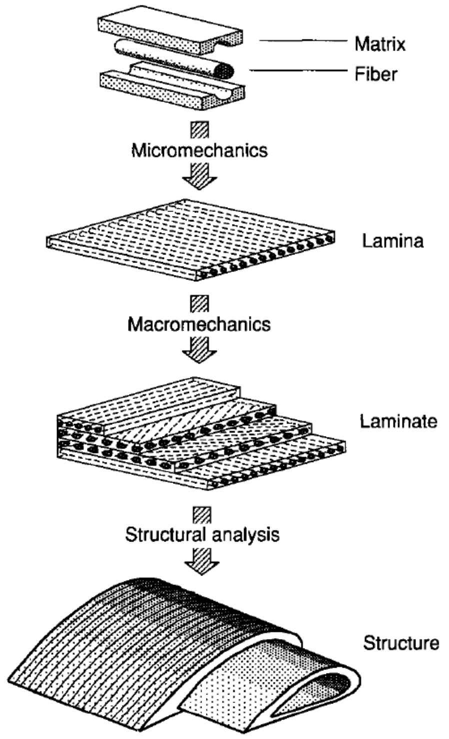

Figure 2.4 Levels of observation and types of analysis for composite materials (Daniel & Ishai, 2006)

Another parameter is the distribution of components. The distribution of the fibers determines the uniformity of the material system. As shown in figure 2.5, the fibers can be distributed as woven, bidirectional, discontinuous, unidirectional.

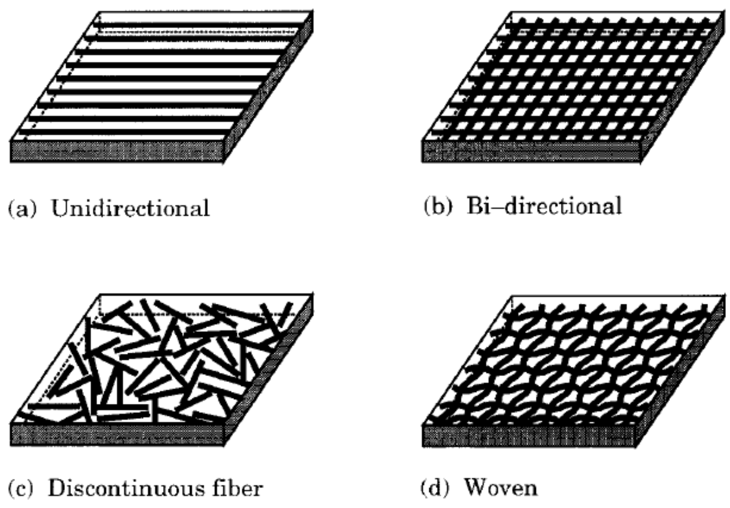

Figure 2.5 Various types of fiber-reinforced in composite lamina (Reddy, 2003)

The more uniform the fiber distribution, the more homogeneous the material is obtained. The unidirectional lamina can be shown as an example of a uniform distribution. Unidirectional lamina exhibit the greatest strength and modulus in the direction of the fibers. The more nonuniform the fiber distribution, the more heterogeneous the material and the probability of failure in the weakest places.

2.3.2 Classical Laminated Plate Theory

Unidirectional composites generally consist of two components, matrix and fiber. According to the rule of mixtures, the properties of the composite plate are depended on the properties and volume fracture of the materials.

E_1 is symbol of longitudinal modulus of the composite plate, E_1 can be written as (Abramovich, 2017)

$$E_1 = E_f V_f + E_m V_m \tag{2.26}$$

Where E_f is young's modulus of fiber material and E_m is young's modulus of matrix material. V_f is volume fraction of fiber material and V_m is volume fraction of matrix material. The total volume fraction is

$$V_f + V_m = 1 \tag{2.27}$$

The major poisson's ratio, v_{12}, is given by

$$v_{12} = v_f V_f + v_m V_m \tag{2.28}$$

Where v_f is poisson's ratio of fiber material and v_m is poisson's ratio of matrix material. The minor poisson's ratio, v_{21}, is calculated

$$\frac{v_{12}}{E_1} = \frac{v_{21}}{E_2} \rightarrow v_{21} = v_{12}\frac{E_2}{E_1} \tag{2.29}$$

The transverse modulus of the composite plate, E_2, is given as

$$\frac{1}{E_2} = \frac{V_f}{E_f} + \frac{V_m}{E_m} \quad \rightarrow \quad E_2 = \frac{E_m}{V_f \frac{E_m}{E_f} + V_m} \tag{2.30}$$

The shear modulus of the composite plate, G_{12}, is given by

$$\frac{1}{G_{12}} = \frac{V_f}{G_f} + \frac{V_m}{G_m} \quad \rightarrow \quad G_{12} = \frac{G_m}{V_f \frac{G_m}{G_f} + V_m} \tag{2.31}$$

Where G_f is shear modulus of fiber material and G_m is shear modulus of matrix material.

$$G_f = \frac{E_f}{2 * (1 + v_f)} \tag{2.32}$$

$$G_m = \frac{E_m}{2 * (1 + v_m)} \tag{2.33}$$

In the classical laminated plate theory, all three transverse strain components ($\varepsilon_{xz}, \varepsilon_{yz}, \varepsilon_{zz}$) are equal to zero. Calculation of the stresses functions in terms of strains functions;

$$\begin{Bmatrix} \sigma_{11} \\ \sigma_{22} \\ \tau_{12} \end{Bmatrix} = \begin{bmatrix} Q_{11} & Q_{12} & 0 \\ Q_{21} & Q_{22} & 0 \\ 0 & 0 & Q_{66} \end{bmatrix} \begin{Bmatrix} \varepsilon_{11} \\ \varepsilon_{22} \\ \Upsilon_{12} \end{Bmatrix} \tag{2.34}$$

The stress is obtained;

$$\begin{Bmatrix} \sigma_{11} \\ \sigma_{22} \\ \tau_{12} \end{Bmatrix} = \begin{bmatrix} \frac{E_1}{(1-\ v_{12}v_{21})} & \frac{v_{21}E_1}{(1-\ v_{12}v_{21})} & 0 \\ \frac{v_{12}E_2}{(1-\ v_{12}v_{21})} & \frac{E_2}{(1-\ v_{12}v_{21})} & 0 \\ 0 & 0 & G_{12} \end{bmatrix} \begin{Bmatrix} \varepsilon_{11} \\ \varepsilon_{22} \\ \Upsilon_{12} \end{Bmatrix} \tag{2.35}$$

As seen in figure 2.6, two coordinate systems are described. The coordinate system with indexes 1 and 2 describes the layer coordinate system, this coordinate system is rotated by angle Θ and obtaining in a new coordinate system containing x and y.

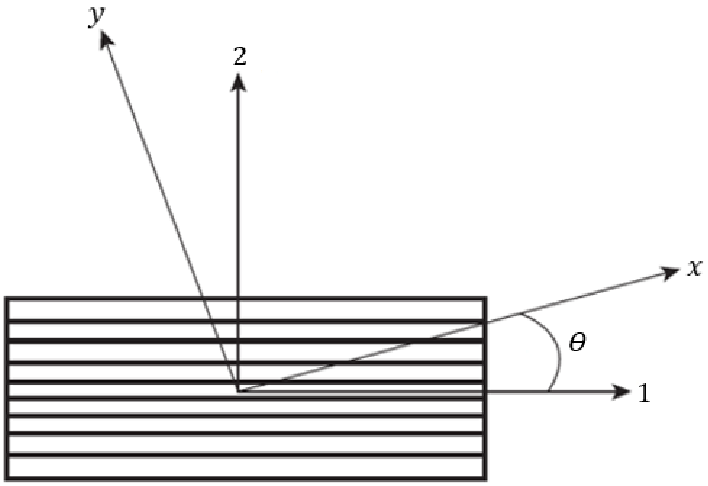

Figure 2.6 The coordinate system of the composite plate

The stresses and strains are multiplied by the transformation matrix $[T]$ for the transformation of the stresses and strains on the x, y coordinate system. (Abramovich, 2017)

$$\begin{Bmatrix} \sigma_{11} \\ \sigma_{22} \\ \tau_{12} \end{Bmatrix}^{\mathrm{k}} = [T] \begin{Bmatrix} \sigma_{xx} \\ \sigma_{yy} \\ \tau_{xy} \end{Bmatrix}^{\mathrm{k}} \tag{2.36}$$

$$\begin{Bmatrix} \varepsilon_{11} \\ \varepsilon_{22} \\ \dfrac{\gamma_{12}}{2} \end{Bmatrix}^{\mathrm{k}} = [T] \begin{Bmatrix} \varepsilon_{xx} \\ \varepsilon_{yy} \\ \dfrac{\gamma_{xy}}{2} \end{Bmatrix}^{\mathrm{k}} \tag{2.37}$$

The number of the ply is described k and the transformation matrix $[T]$ is given by

$$[T] = \begin{bmatrix} c^2 & s^2 & 2cs \\ s^2 & c^2 & -2cs \\ -cs & cs & c^2 - s^2 \end{bmatrix} \tag{2.38}$$

Where $c = cos\theta$ and $s = sin\theta$

The inverse of the transformation matrix $[T]$ is given by

$$[T]^{-1} = [T(-\theta)] = \begin{bmatrix} c^2 & s^2 & -2cs \\ s^2 & c^2 & 2cs \\ cs & -cs & c^2 - s^2 \end{bmatrix} \tag{2.39}$$

The ply strain-stress relationship is (Abramovich, 2017)

$$\begin{Bmatrix} \sigma_{11} \\ \sigma_{22} \\ \tau_{12} \end{Bmatrix}^{\mathrm{k}} = [T]^{-1}[Q]^{\mathrm{k}}[T] \begin{Bmatrix} \varepsilon_{xx} \\ \varepsilon_{yy} \\ \gamma_{xy} \end{Bmatrix}^{\mathrm{k}} \tag{2.40}$$

Where

$$[Q]^{\mathrm{k}} = \begin{bmatrix} Q_{11} & Q_{12} & 0 \\ Q_{12} & Q_{22} & 0 \\ 0 & 0 & 2Q_{66} \end{bmatrix}^{\mathrm{k}} \tag{2.41}$$

We obtain this equation

$$\begin{Bmatrix} \sigma_{11} \\ \sigma_{22} \\ \tau_{12} \end{Bmatrix}^{k} = [\bar{Q}]^{k} \begin{Bmatrix} \varepsilon_{11} \\ \varepsilon_{22} \\ \gamma_{12} \end{Bmatrix}^{k} \tag{2.42}$$

Where

$$[\bar{Q}]^{k} = \begin{bmatrix} \bar{Q}_{11} & \bar{Q}_{12} & \bar{Q}_{16} \\ \bar{Q}_{12} & \bar{Q}_{22} & \bar{Q}_{26} \\ \bar{Q}_{16} & \bar{Q}_{26} & \bar{Q}_{66} \end{bmatrix}^{k} \tag{2.43}$$

$$\bar{Q}_{11} = Q_{11}cos^4\theta + 2(Q_{12} + 2Q_{66})sin^2\theta cos^2\theta + Q_{22}sin^4\theta \tag{2.44}$$

$$\bar{Q}_{12} = (Q_{11} + Q_{22} - 4Q_{66})sin^2\theta cos^2\theta + Q_{12}(sin^4\theta + cos^4\theta) \tag{2.45}$$

$$\bar{Q}_{22} = Q_{11}sin^4\theta + 2(Q_{12} + 2Q_{66})sin^2\theta cos^2\theta + Q_{22}cos^4\theta \tag{2.46}$$

$$\bar{Q}_{16} = (Q_{11} - Q_{12} - 2Q_{66})sin\theta cos^3\theta + (Q_{12} - Q_{22} + 2Q_{66})sin^3\theta cos\theta \tag{2.47}$$

$$\bar{Q}_{26} = (Q_{11} - Q_{12} - 2Q_{66})sin^3\theta cos\theta + (Q_{12} - Q_{22} + 2Q_{66})sin\theta cos^3\theta \tag{2.48}$$

$$\bar{Q}_{66} = (Q_{11} + Q_{22} - 2Q_{12} - 2Q_{66})sin^2\theta cos^2\theta + Q_{66}(sin^4\theta + cos^4\theta) \tag{2.49}$$

Then the strains $(\varepsilon_{xx}, \varepsilon_{yy}, \gamma_{xy})$ and the curvatures (K_{xx}, K_{yy}, K_{xy}) can be written as

$$\varepsilon_{xx} = \varepsilon_{xx}^{0} + zK_{xx} \tag{2.50}$$

$$\varepsilon_{yy} = \varepsilon_{yy}^{0} + zK_{yy} \tag{2.51}$$

$$\gamma_{xy} = \gamma_{xy}^{0} + zK_{xy} \tag{2.52}$$

Where

$$K_{xx} = \frac{\partial^2 q}{\partial x^2} \qquad K_{yy} = \frac{\partial^2 q}{\partial y^2} \qquad K_{xy} = 2\frac{\partial^2 q}{\partial x \partial y} \tag{2.53}$$

This matrix is obtained

$$\begin{Bmatrix} \varepsilon_{xx} \\ \varepsilon_{yy} \\ \gamma_{xy} \end{Bmatrix} = \begin{Bmatrix} \varepsilon_{xx}^0 \\ \varepsilon_{yy}^0 \\ \gamma_{xy}^0 \end{Bmatrix} + z \begin{Bmatrix} K_{xx} \\ K_{yy} \\ K_{xy} \end{Bmatrix} \rightarrow \{\varepsilon\} = \{\varepsilon^0\} + z\{K\} \tag{2.54}$$

At the ply level, the stresses are given by

$$\{\sigma\}^{\mathrm{k}} = [\bar{Q}]^{\mathrm{k}}\{\varepsilon^0\} + z[\bar{Q}]^{\mathrm{k}}\{K\} \tag{2.55}$$

Force (N_{xx}, N_{yy}, N_{xy}) and moment (M_{xx}, M_{yy}, M_{xy}) are given by

$$N_{xx} = \int_{-\mathrm{h}/2}^{\mathrm{h}/2} \sigma_{xx}\, dz \qquad N_{yy} = \int_{-\mathrm{h}/2}^{\mathrm{h}/2} \sigma_{yy}\, dz \qquad N_{xy} = \int_{-\mathrm{h}/2}^{\mathrm{h}/2} \tau_{xy}\, dz \tag{2.56}$$

$$M_{xx} = \int_{-\mathrm{h}/2}^{\mathrm{h}/2} \sigma_{xx} z\, dz \qquad M_{yy} = \int_{-\mathrm{h}/2}^{\mathrm{h}/2} \sigma_{yy}\, zdz \qquad M_{xy} = \int_{-\mathrm{h}/2}^{\mathrm{h}/2} \tau_{xy}\, zdz \tag{2.57}$$

The total thickness of the composite plate is described h

The force and moment matrix expressions are

$$\begin{Bmatrix} \{N\} \\ \{M\} \end{Bmatrix} = \begin{bmatrix} [A] & [B] \\ [B] & [D] \end{bmatrix} \begin{Bmatrix} \{\varepsilon^0\} \\ \{K\} \end{Bmatrix} \tag{2.58}$$

A function of the strain on the midplane is ε^0 and curvature is K.

The long-written expressions are

$$\begin{Bmatrix} \begin{Bmatrix} N_{xx} \\ N_{yy} \\ N_{xy} \end{Bmatrix} \\ \begin{Bmatrix} M_{xx} \\ M_{yy} \\ M_{xy} \end{Bmatrix} \end{Bmatrix} = \begin{bmatrix} \begin{bmatrix} A_{11} & A_{12} & A_{16} \\ A_{12} & A_{22} & A_{26} \\ A_{16} & A_{26} & A_{66} \end{bmatrix} & \begin{bmatrix} B_{11} & B_{12} & B_{16} \\ B_{12} & B_{22} & B_{26} \\ B_{16} & B_{26} & B_{66} \end{bmatrix} \\ \begin{bmatrix} B_{11} & B_{12} & B_{16} \\ B_{12} & B_{22} & B_{26} \\ B_{16} & B_{26} & B_{66} \end{bmatrix} & \begin{bmatrix} D_{11} & D_{12} & D_{16} \\ D_{12} & D_{22} & D_{26} \\ D_{16} & D_{26} & D_{66} \end{bmatrix} \end{bmatrix} \begin{Bmatrix} \begin{Bmatrix} \varepsilon_{xx}^{0} \\ \varepsilon_{yy}^{0} \\ \gamma_{xy}^{0} \end{Bmatrix} \\ \begin{Bmatrix} K_{xx} \\ K_{yy} \\ K_{xy} \end{Bmatrix} \end{Bmatrix} \qquad (2.59)$$

Where the various constant defined as

$$A_{ij} = \int_{-\mathrm{h}/2}^{\mathrm{h}/2} \bar{Q}_{ij}^{\mathrm{k}}\, dz = \sum_{\mathrm{k}=1}^{\mathrm{n}} \bar{Q}_{ij}^{\mathrm{k}} \left(\mathrm{h_k} - \mathrm{h_{k-1}}\right) \qquad (2.60)$$

$$B_{ij} = \int_{-\mathrm{h}/2}^{\mathrm{h}/2} \bar{Q}_{ij}^{\mathrm{k}}\, zdz = \frac{1}{2}\sum_{\mathrm{k}=1}^{\mathrm{n}} \bar{Q}_{ij}^{\mathrm{k}} \left(\mathrm{h_k^2} - \mathrm{h_{k-1}^2}\right) \qquad (2.61)$$

$$D_{ij} = \int_{-\mathrm{h}/2}^{\mathrm{h}/2} \bar{Q}_{ij}^{\mathrm{k}}\, z^2 dz = \frac{1}{3}\sum_{\mathrm{k}=1}^{\mathrm{n}} \bar{Q}_{ij}^{\mathrm{k}} \left(\mathrm{h_k^3} - \mathrm{h_{k-1}^3}\right) \qquad (2.62)$$

Where *i, j* = 1, 1; 1, 2; 2, 2; 1, 6; 2, 6; 6, 6

$$[\mathrm{D}_e^c] = \begin{bmatrix} [A] & [B] \\ [B] & [D] \end{bmatrix} \qquad (2.63)$$

Equation (2.59) is according to the notations in figure 2.7.

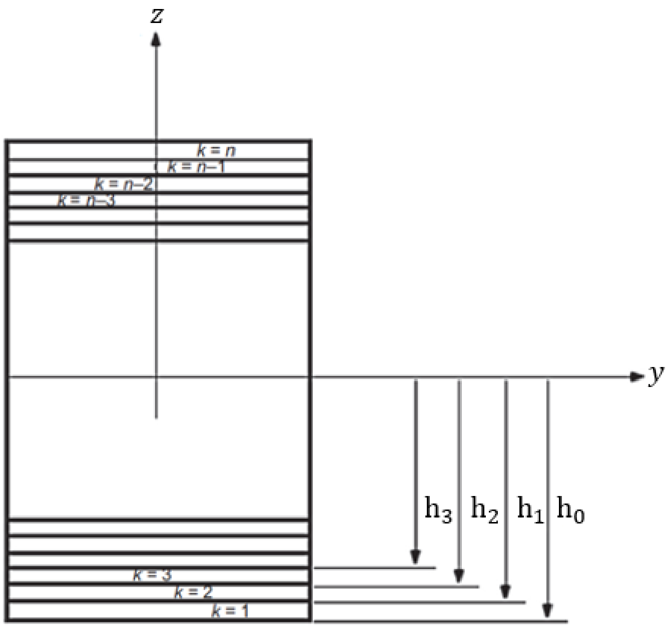

Figure 2.7 Lamina notations within a given laminate (Abramovich, 2017)

As shown in figure 2.8, the fibers can be oriented in the angle directions for each ply.

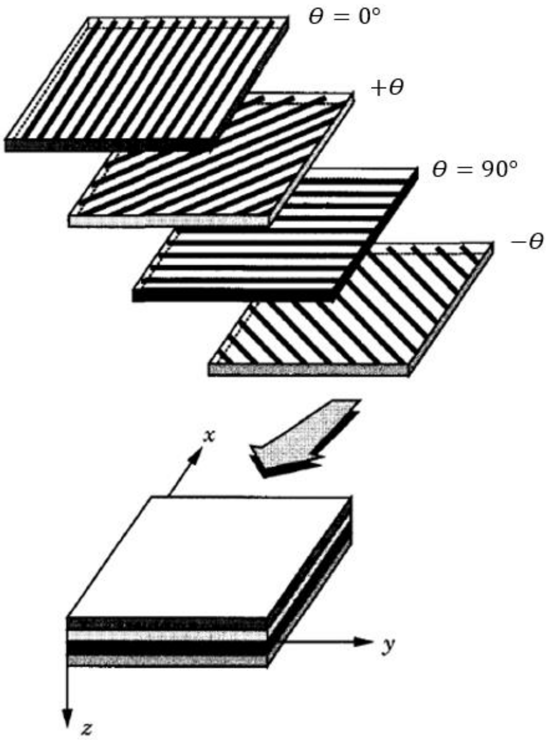

Figure 2.8 A laminate made up of lamina with different fiber orientations (Reddy, 2003)

Consequently, the fiber orientation of the laminate can be given by applying these formulations. The ability to combine different fiber orientations in different layers provides spectacular design flexibility for laminated composite structures. The composite structure can be created to suit specific design requirements by using the classical laminated plate method.

As a result of these operations, the local elastic stiffness matrix of the plate is changed. Equations (2.17) and (2.63) are used and the local elastic stiffness matrix for a composite plate is obtained.

The local elastic stiffness matrix for a composite plate as

$$[K_e]^e = \iint [\mathrm{B}_e]^\mathrm{T} \left[\mathrm{D}_e^c\right][\mathrm{B}_e]\, dx\, dy \tag{2.64}$$

2.4 Crack Finite Element Model

2.4.1 Crack Modes

Throughout the years, engineering designs are developed and it has provided advantages for human life, but these developments have occurred in many problems. In the nineteenth century, with the development of metalworking skills, metals used greatly increased in structures. Subsequently, it is observed that unexpected defects occurred occasionally in the structures made of metal materials. Some of these defects cause a crack formation. Cracks may be caused by corrosion, fatigue strength of materials and mechanical damage.

Crack in the structure causes reduction in local stiffness therefore it reduces the structure's strength. Any changes in the stiffness of structure have an influence on the modal parameters, such as natural frequencies, critical buckling load and dynamic stability. Therefore, it is very important to crack’s location and size in the machine.

A crack separates a structure into two or more pieces under the action of stress. As shown in figure 2.9, cracks can be stressed in three different types of mode.

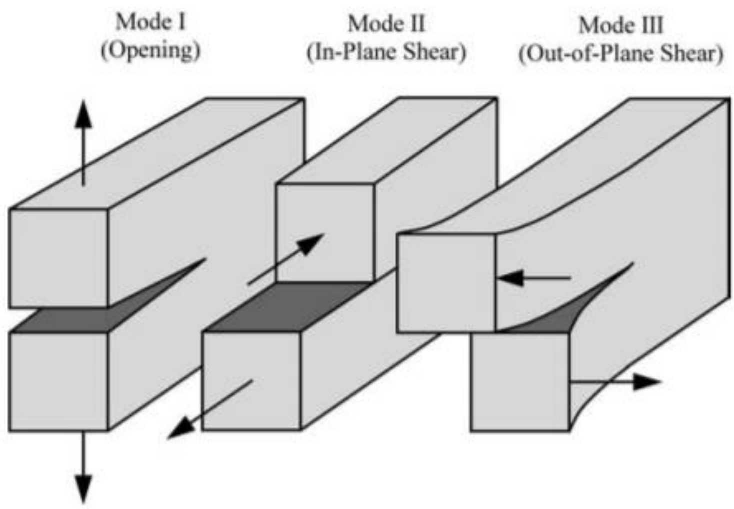

Figure 2.9 The three modes of loading that can be applied to a crack (Anderson, 2005)

Mode I of (Opening mode) crack: Applied tensile stresses are perpendicular to the crack and pulling the crack open. Crack is horizontal to plane and the tensile stresses are vertical to plane. This case is called as opening mode.

Mode II of (Sliding mode) crack: Applied in-plane shear stresses are parallel to crack. One stress pushes the upper half of the crack backward, and the other pulls the lower half of the crack forward along the same line. This case is called as sliding mode.

Mode III of (Tearing mode) crack: Applied out-plane shear stresses are perpendicular to the crack. The crack is in the front-back direction, the stresses are pulling right and left side. This case is called as tearing mode.

2.4.2 The Finite Element Method for a Crack Model

In recent years, several methods have been developed to simulate crack problems associated with the creation of cracks. These methods have been successfully used to model cracks. Each of the methods provided advantages and disadvantages of certain parts of the simulation.

In this thesis, the finite element method is used to design the crack in the structure. This method is similar to the extended finite element method. The creation of cracks in the finite element method is basically the disruption of the unity of the structure assuming that there is a crack in a certain area of the structure.

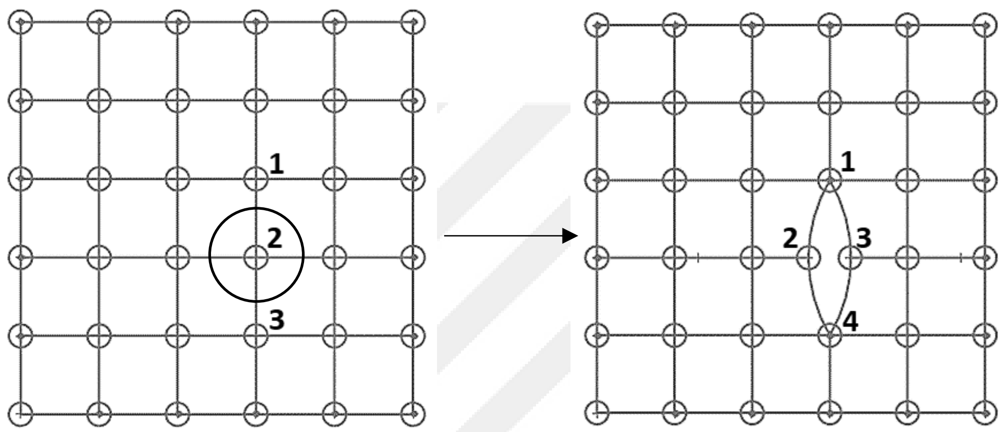

Figure 2.10 Finite element model converts into crack finite element model

According to this theory, firstly, the finite element method is applied to the structure. The structure is divided into elements appropriate to the shape of the structure and these elements are connected to each other at certain points known as nodes.

As shown in figure 2.10, the node in the circle and the four elements that contact this node are removed from the structure. And then, two nodes and four elements are added to this removed region. Consequently, a void is created in the structure by using the finite element method and performing these operations. In this way, a cracked effect is achieved in the structure.

CHAPTER THREE
THEORY OF STABILITY

3.1 Introduction to Stability

In recent years, complex structures have begun to be used to benefit human life with the development of the engineering field. As a result of complex structures (such as bridges, airplanes and ships) are subjected to dynamic loads, the problem of elastic instability has arisen in complex structures. This problem in complex structures can cause serious troubles unless precaution is taken. Stability formulations have been developed for the elements (such as plates, beams and bars) of the complex structure to prevent these problems. Stability problems can be defined by using energy conservation law.

To describe the stability from energy equations, total potential energy (Π) must be formulated. Total potential energy is expressed as (Öztürk, 1999)

$$\Pi = \mathrm{U} + \Lambda \tag{3.1}$$

Internal potential energy is described U and the potential energy of the external forces is desccribed Λ.

The loss of potential energy is equal to the work done on the system by external forces ($\Lambda = -\mathrm{W_e}$). Therefore, equation (3.1) is reformulated as

$$\Pi = \mathrm{U} - \mathrm{W_e} \tag{3.2}$$

The total potential energy must be stationary for balance, therefore its variation must be equal to zero,

$$\delta\Pi = \delta\mathrm{U} - \delta\mathrm{W_e} \tag{3.3}$$

However, equation (3.3) can not satisfy the condition for the stability of balance. Therefore, the higher orders terms of Taylor’s expansion should be examined. Taylor’s expansion is: (Öztürk, 1999)

$$\Delta\Pi = \delta\Pi + \frac{1}{2!}\delta^2\Pi + \frac{1}{3!}\delta^3\Pi + \cdots \tag{3.4}$$

In order to determine the equilibrium state in linear elastic systems, it is sufficient to examine the second term of Taylor's expansion.

$\delta^2\Pi > 0$ for stable state

$\delta^2\Pi = 0$ for neutral state associated with the critical load

$\delta^2\Pi < 0$ for unstable state

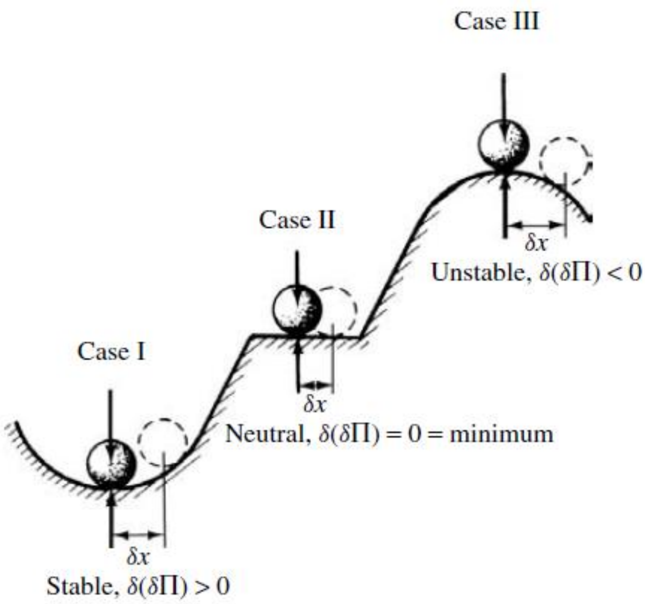

Figure 3.1 Analogy of various states of equilibrium (Szilard, 2004)

These expressions may be clarified in figure 3.1. The second derivative of the total potential energy of the ball determines the type of equilibrium.

The ball stands on the concave spherical surface (case I), and then this equilibrium condition is disturbed by introducing displacement δx. If the ball returns to its original position after oscillations, its equilibrium is said to be stable.

The ball stands on the horizontal plane (case II), and then this equilibrium condition is disturbed by introducing displacement δx. If that does not change the potential energy of the ball, its equilibrium is said to be neutral.

The ball stands on the convex spherical surface (case III), and then this equilibrium condition is disturbed by introducing displacement δx. If the ball does not return to its original position after oscillations, its equilibrium is said to be unstable.

3.2 Dynamic Stability

The theory of dynamic stability is generally examined the vibration and stability of elastic systems. The theory of dynamic stability can be illustrated by the following examples: (Bolotin, 1964)

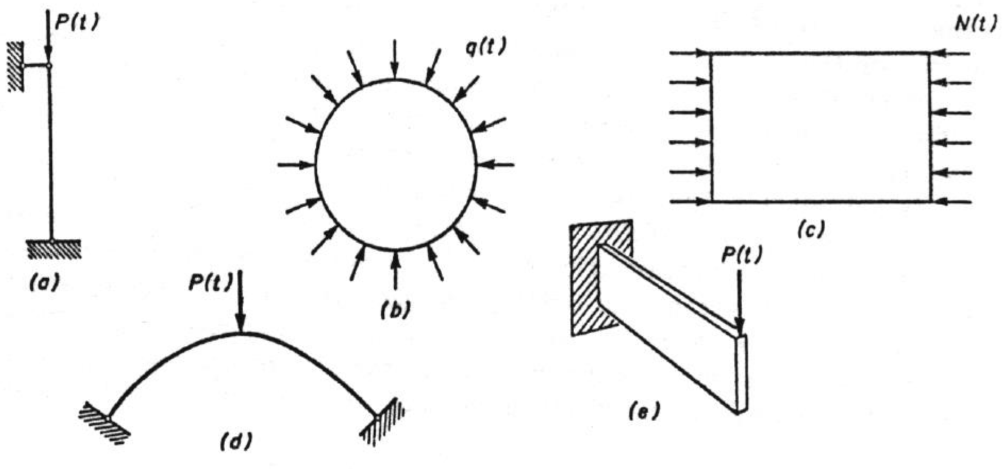

Figure 3.2 Different loads types (Bolotin, 1964)

As shown in figure 3.2, different elastic systems (such as beam, ring, plate) are subjected to parametric load. If this parametric loading is above a certain level, it will cause the stability loss of the elastic system. Therefore, the theory of dynamic stability can be defined as the study of vibrations caused by parametric loading. (Bolotin, 1964)

The parametric excitation occurs because of the periodic change in the rigidity, load and inertia of the system. It is demanded that parametric excitation can be used practically in most situation. In order to parametric excitation define practically, Mathieu-Hill differential equations have been developed. Mathieu-Hill differential equation is;

$$\frac{\partial^2 f}{\partial ч^2} + (\mathrm{a} - 2\mathrm{b}\cos 2ч)f = 0 \tag{3.5}$$

a and b are constant value.

ч is the symbol of dimensionless time.

The solutions of the Mathieu-Hill equation are oscillatory and depend decisively on the values of constant parameters (a, b). In some situations, while the vibrations of a given combination of a and b have limited amplitude, if this combination can not be achieved, the vibrations have increasing amplitude. If the amplitude increases, parametric resonance occurs so the system becomes unstable otherwise the system remains stable.

Figure 3.3 shows the results of solving equation (3.5) for two different situations. The parameter b (b=0.1) is the same in both situations. However, the vibrations of the system are considerably different due to different values of the parameter a (a=1; a=1.2). In the first situation, the vibration increases so that the system is dynamically unstable, however in the second situation, the vibration remains limited therefore the system is dynamically stable.

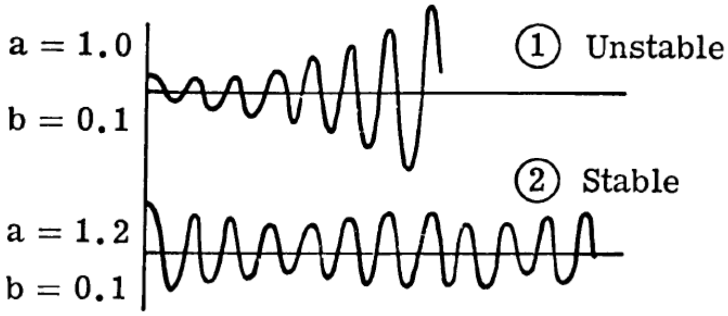

Figure 3.3 Two Solutions of Mathieu's Equation (Abbas, 1977)

3.3 The Formulation of Stability

The local elastic stiffness, local geometrical stiffness and local mass matrix of the square plate elements are obtained from the divided plate using the finite element method. The local elastic stiffness, local geometrical stiffness and local mass matrix of the square plate elements are converted to the global elastic stiffness, global geometrical stiffness and global mass matrix of the whole structure. The resulting global geometric stiffness, global elastic stiffness and global mass matrix are associated with each other using the following energy equations.

Strain energy of the system;

$$\mathrm{U} = \frac{1}{2}\{q\}^{\mathrm{T}}[K_e]\{q\} \tag{3.6}$$

In this thesis, it is assumed that $\mathrm{N}_y = 0$ and $\mathrm{N}_{xy} = 0$ so, the potential energy of the external forces

$$\Lambda = \frac{1}{2}\{q\}^{\mathrm{T}}\left[K_g^*\right]\{q\} \tag{3.7}$$

Where

$$\left[K_g^*\right] = \mathrm{N}_x * \left[K_g\right] \tag{3.8}$$

If small displacements are given to the system, the total potential energy of the system is constant so its variation is equal to zero.

$$\delta(\Pi) = 0 \tag{3.9}$$

Where Π and δ define respectively, the total potential energy of the system and the change of the virtual displacements.

The static stability formula is

$$\left[[K_e] - \mathrm{N}_x * [K_g] - \mathrm{N}_y * [K_g] - \mathrm{N}_{xy} * [K_g]\right]\{q\} = 0 \tag{3.10}$$

In this thesis, it is assumed that $\mathrm{N}_y = 0$ and $\mathrm{N}_{xy} = 0$. The static stability formula is

$$\left[[K_e] - \mathrm{N}_x[K_g]\right]\{q\} = 0 \tag{3.11}$$

The kinetic energy of the system;

$$V = \frac{1}{2}\{\dot{q}\}^{\mathrm{T}}[M]\{\dot{q}\} \tag{3.12}$$

By using Lagrange's equation for energies, the dynamic equilibrium of the system is obtained

$$[M]\{\ddot{q}\} + [K_e]\{q\} - \mathrm{N}_x[K_g]\{q\} = 0 \tag{3.13}$$

The periodic force is

$$\mathrm{N}_x = \mathrm{N}_s + \mathrm{N}_d ø(t) \tag{3.14}$$

The static and time dependent components of the load can be represented as a fraction of the fundamental static buckling load N_{cr} ,and periodic force is rewritten $\mathrm{N}_x = \alpha\mathrm{N}_{cr} + \beta\mathrm{N}_{cr}\varnothing(t)$ equation (3.13) becomes

$$[M]\{\ddot{q}\} + \left[[K_e] - \alpha\mathrm{N}_{cr}\left[K_{g_s}\right] - \beta\mathrm{N}_{cr}\varnothing(t)\left[K_{g_d}\right]\right]\{q\} = 0 \qquad (3.15)$$

Where the matrices $\left[K_{g_s}\right]$ and $\left[K_{g_d}\right]$ reflect the influence of N_s and N_d respectively. (Abbas,1997)

The boundaries between stable and unstable regions are formed by periodic solutions of period T_p and $2T_p$. Those situations are also valid for multi-degree of freedom systems (see also Bolotin, 1967 & Abbas, 1977).

The periodic force is

$$\mathrm{N}_x = \mathrm{N}_s + \mathrm{N}_d \cos\Omega t \qquad (3.16)$$

Where Ω is the exciting frequency, equation (3.15) becomes

$$[M]\{\ddot{q}\} + \left[[K_e] - \alpha\mathrm{N}_{cr}\left[K_{g_s}\right] - \beta\mathrm{N}_{cr}\cos\Omega t\left[K_{g_d}\right]\right]\{q\} = 0 \qquad (3.17)$$

Equation (3.17) can be defined as a periodic solution of periods T_p and $2T_p$ where $T_p = 2\pi/\Omega$.

If a solution of period $2T_p$ exists, it can be expressed by the Fourier series

$$\{q\} = \sum_{k=1,3,5}^{\infty}\left[\{a\}_k \sin\frac{k\Omega t}{2} + \{b\}_k \cos\frac{k\Omega t}{2}\right] \qquad (3.18)$$

Where $\{a\}_k$ and $\{b\}_k$ are time-independent vectors.

Equation's (3.18) second derivative with respect to time is

$$\{\ddot{q}\} = \sum_{k=1,3,5}^{\infty} -\left(\frac{k\Omega}{2}\right)^2 \left[\{a\}_k \sin\frac{k\Omega t}{2} + \{b\}_k \cos\frac{k\Omega t}{2}\right] \tag{3.19}$$

Substituting equations (3.18) and (3.19) into equation (3.17) and using the trigonometric relations

$$\begin{aligned}
\sin A + \sin B &= 2\sin\frac{A+B}{2}\cos\frac{A-B}{2} \\
\sin A - \sin B &= 2\cos\frac{A+B}{2}\sin\frac{A-B}{2} \\
\cos A + \cos B &= 2\cos\frac{A+B}{2}\cos\frac{A-B}{2} \\
\cos A - \cos B &= 2\sin\frac{A+B}{2}\sin\frac{A-B}{2}
\end{aligned} \tag{3.20}$$

And comparing the coefficients of $\sin\frac{k\Omega t}{2}$ and $\cos\frac{k\Omega t}{2}$ lead to the following matrix equations relating the vectors $\{a\}_k$ and $\{b\}_k$

$$\begin{bmatrix}
[K_e] - \alpha N_{cr}[K_{g_s}] + \frac{1}{2}\beta N_{cr}[K_{g_d}] - \frac{\Omega^2}{4}[M] & -\frac{1}{2}\beta N_{cr}[K_{g_d}] & 0 & \cdots \\
-\frac{1}{2}\beta N_{cr}[K_{g_d}] & [K_e] - \alpha N_{cr}[K_{g_s}] - \frac{9\Omega^2}{4}[M] & -\frac{1}{2}\beta N_{cr}[K_{g_d}] & \cdots \\
0 & -\frac{1}{2}\beta N_{cr}[K_{g_d}] & [K_e] - \alpha N_{cr}[K_{g_s}] - \frac{25\Omega^2}{4}[M] & \cdots \\
\cdots & \cdots & \cdots & \cdots
\end{bmatrix}
\begin{Bmatrix} \{a\}_1 \\ \{a\}_2 \\ \{a\}_3 \\ \cdots \end{Bmatrix} = 0 \tag{3.21}$$

and

$$\begin{bmatrix}
[K_e] - \alpha N_{cr}[K_{g_s}] - \frac{1}{2}\beta N_{cr}[K_{g_d}] - \frac{\Omega^2}{4}[M] & -\frac{1}{2}\beta N_{cr}[K_{g_d}] & 0 & \cdots \\
-\frac{1}{2}\beta N_{cr}[K_{g_d}] & [K_e] - \alpha N_{cr}[K_{g_s}] - \frac{9\Omega^2}{4}[M] & -\frac{1}{2}\beta N_{cr}[K_{g_d}] & \cdots \\
0 & -\frac{1}{2}\beta N_{cr}[K_{g_d}] & [K_e] - \alpha N_{cr}[K_{g_s}] - \frac{25\Omega^2}{4}[M] & \cdots \\
\cdots & \cdots & \cdots & \cdots
\end{bmatrix}
\begin{Bmatrix} \{b\}_1 \\ \{b\}_2 \\ \{b\}_3 \\ \cdots \end{Bmatrix} = 0 \tag{3.22}$$

The order of matrices in equations (3.21) and (3.22) are infinite. If $2T_p$ exist, then the determinants of these matrices must vanish. Combining these two determinants and rewritten as

$$\begin{vmatrix} [K_e]-\alpha N_{cr}[K_{g_s}]\pm\frac{1}{2}\beta N_{cr}[K_{g_d}]-\frac{\Omega^2}{4}[M] & -\frac{1}{2}\beta N_{cr}[K_{g_d}] & 0 & \cdots \\ -\frac{1}{2}\beta N_{cr}[K_{g_d}] & [K_e]-\alpha N_{cr}[K_{g_s}]-\frac{9\Omega^2}{4}[M] & -\frac{1}{2}\beta N_{cr}[K_{g_d}] & \cdots \\ 0 & -\frac{1}{2}\beta N_{cr}[K_{g_d}] & [K_e]-\alpha N_{cr}[K_{g_s}]-\frac{25\Omega^2}{4}[M] & \cdots \\ \cdots & \cdots & \cdots & \cdots \end{vmatrix}=0 \tag{3.23}$$

If a solution to equation (3.17) exists with $T_p = 2\pi/\Omega$ then it can be expressed as a Fourier series

$$\{q\} = \frac{1}{2}b_0 + \sum_{k=2,4,6}^{\infty}\left[\{a\}_k \sin\frac{k\Omega t}{2} + \{b\}_k \sin\frac{k\Omega t}{2}\right] \tag{3.24}$$

Substituting into equation (3.17), the following conditions for the existence of solution with period T_p are obtained:

$$\begin{vmatrix} [K_e]-\alpha N_{cr}[K_{g_s}] & -\frac{1}{2}\beta N_{cr}[K_{g_d}] & 0 & 0 & \cdots \\ -\frac{1}{2}\beta N_{cr}[K_{g_d}] & [K_e]-\alpha N_{cr}[K_{g_s}]-\Omega^2[M] & -\frac{1}{2}\beta N_{cr}[K_{g_d}] & 0 & \cdots \\ 0 & -\frac{1}{2}\beta N_{cr}[K_{g_d}] & [K_e]-\alpha N_{cr}[K_{g_s}]-4\Omega^2[M] & -\frac{1}{2}\beta N_{cr}[K_{g_d}] & \cdots \\ 0 & 0 & 0 & [K_e]-\alpha N_{cr}[K_{g_s}]-9\Omega^2[M] & \cdots \\ \cdots & \cdots & \cdots & \cdots & \cdots \end{vmatrix}=0 \tag{3.25}$$

and

$$\begin{vmatrix} [K_e]-\alpha N_{cr}[K_{g_s}]-\Omega^2[M] & -\frac{1}{2}\beta N_{cr}[K_{g_d}] & 0 & \cdots \\ -\frac{1}{2}\beta N_{cr}[K_{g_d}] & [K_e]-\alpha N_{cr}[K_{g_s}]-4\Omega^2[M] & -\frac{1}{2}\beta N_{cr}[K_{g_d}] & \cdots \\ 0 & -\frac{1}{2}\beta N_{cr}[K_{g_d}] & [K_e]-\alpha N_{cr}[K_{g_s}]-9\Omega^2[M] & \cdots \\ \cdots & \cdots & \cdots & \cdots \end{vmatrix}=0 \tag{3.26}$$

Bolotin proved that solutions with a period of $2T_p$ are considerably practical importance and the boundaries of the dynamic instability regions can be determined with Equation (3.27).

$$\left[[K_e] - \alpha N_{cr}[K_{g_s}] \pm \frac{1}{2}\beta N_{cr}[K_{g_d}] - \frac{\Omega^2}{4}[M]\right]\{q\} = 0 \tag{3.27}$$

When the static and time dependent components of the loads are applied in the same manner, $[K_{g_s}]$ and $[K_{g_d}]$ will be identical. If $[K_{g_s}] \equiv [K_{g_d}] \equiv [K_g]$, in this situation equation (3.27) becomes

$$\left[[K_e] - (\alpha \pm \frac{1}{2}\beta)N_{cr}[K_g] - \frac{\Omega^2}{4}[M]\right]\{q\} = 0 \tag{3.28}$$

Equation (3.28) represents solutions to three related problems

1) Free vibration with ω, in case of $N_{cr} = 0$

$$\left[[K_e] - \omega^2[M]\right]\{q\} = 0 \tag{3.29}$$

2) Static stability with $\alpha = 1,\ \beta = 0$ and $\Omega = 0$

$$\left[[K_e] - N_{cr}[K_g]\right]\{q\} = 0 \tag{3.30}$$

3) Dynamic stability when all terms are present

$$\left[[K_e] - (\alpha \pm \frac{1}{2}\beta)N_{cr}[K_g] - \frac{\Omega^2}{4}[M]\right]\{q\} = 0 \tag{3.31}$$

CHAPTER FOUR
RESULTS AND DISCUSSIONS

In this study, two different plates in which are isotropic and composite materials are used. Boundary conditions, material properties and geometric properties have been specified before carrying out the theoretical analysis. As shown in figure 4.1, it is assumed for the composite and isotropic plates that the boundary condition of the thin plate is fixed on one side and the other sides are free. It is also assumed for the composite and isotropic plates that the cantilever thin plate's length (l_p) and width (w_p) are 400 mm. The cantilever isotropic plate's thickness (h) is 4 mm. The cantilever composite plate is formed four layers and each of the layer's thickness is 1 mm so that the cantilever composite plate's thickness (h) is 4 mm. The composite plates have been investigated for the five different orientation angles. The orientation angles are denoted by C1, C2, C3, C4, C5 as follows:

C1= [0°/0°/0°/0°]
C2= [0°/30°/-30°/0°]
C3= [0°/45°/-45°/0°]
C4= [0°/60°/-60°/0°]
C5= [0°/90°/90°/0°]

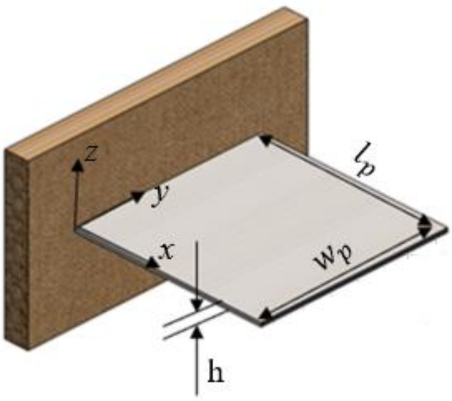

Figure 4.1 Cantilever thin plate

The material properties of the cantilever isotropic plate are given in table 4.1.

Table 4.1 Material properties of the isotropic plate

Properties	Quantities
Elastic modulus, $\boldsymbol{E}$ (GPa)	200
Poisson's ratio, $\boldsymbol{v}$	0.3
Density, $\boldsymbol{\rho}$ (kg/m^3)	8000

The material properties of the cantilever composite plate are given in table 4.2. The material properties are used for each lamina of the composite plate.

Table 4.2 Material properties of the composite plate

Properties	Quantities
Elastic modulus of matrix, $\boldsymbol{E_m}$ (GPa)	73
Elastic modulus of fiber, $\boldsymbol{E_f}$ (GPa)	190
Poisson's ratio of matrix, $\boldsymbol{v_m}$	0.33
Poisson's ratio of fiber, $\boldsymbol{v_f}$	0.29
Fiber volume fraction, $\boldsymbol{V_f}$ %	70
Density, $\boldsymbol{\rho}$ (kg/m^3)	8000

In this thesis, in order to verify the present work results, a comparison made between the natural frequencies and critical buckling loads of composite and isotropic plates obtained using the present model with the results obtained from the ANSYS software.

Table 4.3 gives the comparison of the natural frequencies of the cantilever isotropic and composite plate obtained by using present work with the results obtained from the ANSYS software.

Table 4.4 gives the comparison of the critical buckling loads of the cantilever isotropic and composite plate obtained by using present work with the results obtained from the ANSYS software.

It is seen from tables 4.3 and 4.4 that there is very good agreement between the results of the present work and the ANSYS software. It is observed from these tables, C1, C2, C3, C4 and C5 orientation angles of the composite plate have close results.

Table 4.3 Comparison of the natural frequency results between present work and ANSYS

The Natural Frequency			
	Isotropic		
Mode	Present Work (Hz)	ANSYS (Hz)	Error %
1	20.8965	20.8978	0.0062
2	51.2120	51.1767	0.0689
3	128.1805	128.5151	0.2610
4	163.7126	163.9772	0.1616
5	186.3643	186.6200	0.1372
	Composite		
Ply angle [0/0/0/0]			
Mode	Present Work (Hz)	ANSYS (Hz)	Error %
1	20.9421	20.9430	0.0043
2	43.5812	43.5457	0.0815
3	123.6408	123.7972	0.1265
4	136.8141	137.1750	0.2638
5	168.7500	168.9751	0.1334
Ply angle [0/90/90/0]			
Mode	Present Work (Hz)	ANSYS (Hz)	Error %
1	20.6239	20.4429	0.8776
2	43.4615	43.2402	0.5092
3	123.4649	123.5331	0.0552
4	137.1168	137.3513	0.1710
5	167.6049	166.6514	0.5689
Ply angle [0/30/-30/0]			
Mode	Present Work (Hz)	ANSYS (Hz)	Error %
1	20.8390	20.6895	0.7174
2	43.6890	43.8781	0.4328
3	123.4249	123.1233	0.2444
4	136.7944	136.9100	0.0845
5	168.7339	168.8041	0.0416

Table 4.3 continues

Ply angle [0/45/-45/0]			
Mode	Present Work (Hz)	ANSYS (Hz)	Error %
1	20.7279	20.5418	0.8978
2	43.7183	43.9511	0.5325
3	123.2188	122.8574	0.2933
4	136.7866	136.9051	0.0866
5	168.3587	168.4521	0.0555

Ply angle [0/60/-60/0]			
Mode	Present Work (Hz)	ANSYS (Hz)	Error %
1	20.6572	20.4625	0.9425
2	43.6078	43.7237	0.2658
3	123.3129	122.9412	0.3014
4	136.8805	137.0232	0.1043
5	168.0848	167.7171	0.2188

Table 4.4 Comparison of the critical buckling load results between present work and ANSYS

The Critical Buckling Load			
Isotropic material	Present Work (N)	ANSYS (N)	Error %
Critical Buckling Load	6976.5736	6987.2766	0.1534
Composite material			
Ply angle [0/0/0/0]	Present Work (N)	ANSYS (N)	Error %
Critical Buckling Load	6832.5320	6851.0846	0.2715
Ply angle [0/90/90/0]	Present Work (N)	ANSYS (N)	Error %
Critical Buckling Load	6563.6448	6457.5238	1.6168
Ply angle [0/30/-30/0]	Present Work (N)	ANSYS (N)	Error %
Critical Buckling Load	6790.4207	6707.6529	1.2189
Ply angle [0/45/-45/0]	Present Work (N)	ANSYS (N)	Error %
Critical Buckling Load	6749.7506	6662.7037	1.2896
Ply angle [0/60/-60/0]	Present Work (N)	ANSYS (N)	Error %
Critical Buckling Load	6709.2592	6615.3423	1.3998

Figures 4.2, 4.3, 4.4, 4.5 and 4.6 show the five mode shapes of cantilever thin plate for five modes obtained using the ANSYS software. When isotropic material

and composite material are used for the cantilever thin plate, the same mode shapes are obtained. When a crack occurs in the cantilever thin plate, it is observed that there are no changes in the mode shapes.

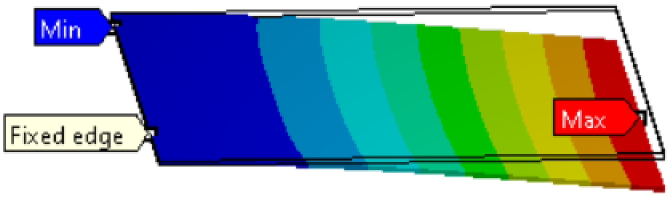

Figure 4.2 Mode shape of the cantilever thin plate for the first mode

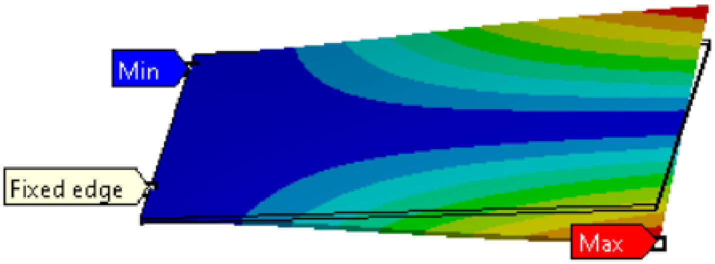

Figure 4.3 Mode shape of the cantilever thin plate for the second mode

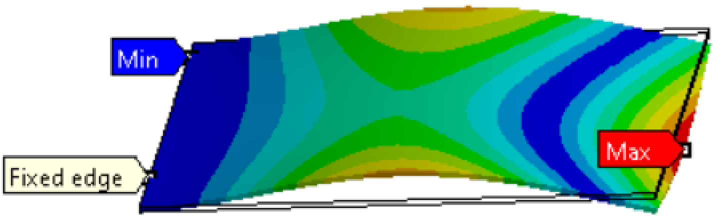

Figure 4.4 Mode shape of the cantilever thin plate for the third mode

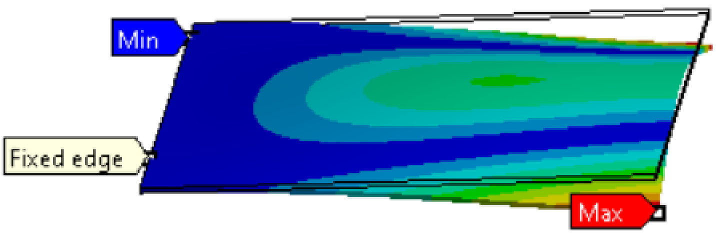

Figure 4.5 Mode shape of the cantilever thin plate for the fourth mode

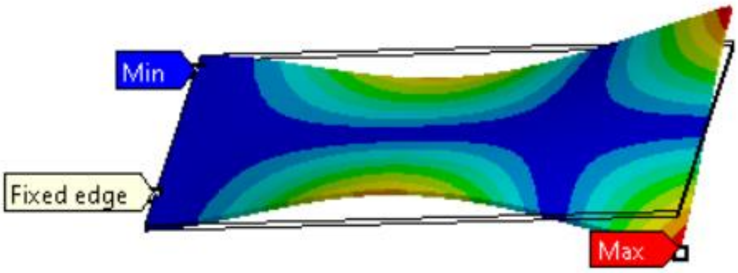

Figure 4.6 Mode shape of the cantilever thin plate for the fifth mode

As seen from figure 4.7, It is assumed that the crack occurs in the plate and the crack's length is 32 mm. The crack is moved along the *x* and *y* axes. In this thesis, the natural frequency and critical buckling analyses are made for the different crack locations on the cantilever plate.

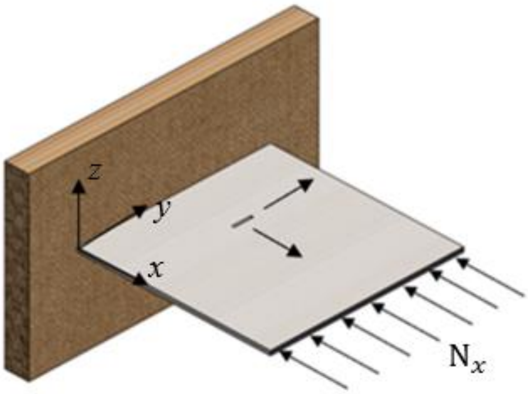

Figure 4.7 Cantilever cracked thin plate (crack is moved along the *x* and *y* axes)

Figures 4.8, 4.9, 4.10, 4.11 and 4.12 show the effect of crack on the natural frequency of the cantilever isotropic plate. In these figures, the crack is moved along the *x* and *y* axes of the cantilever isotropic plate. It has been observed that the crack decreases the first five modes of natural frequencies, albeit with different effects at each location on the cantilever isotropic plate. As seen from figure 4.8, if the crack is moved along the *y* axis, it is observed that the crack effect on the first natural frequency is approximately the same at each location on the cantilever isotropic plate. If the crack is moved away from the fixed support on the *x* axis direction, the first natural frequency increases. As shown in figure 4.9, if the crack is moved along the y axis at the location close to the fixed support, it is observed that the effect of the crack is maximum at the edge side regions of the cantilever isotropic plate therefore, the second natural frequency is minimum at these regions. As seen from figure 4.10, if the crack is moved along the y axis in a location close to a fixed support, the third natural frequency is minimum at the edge side regions of the cantilever isotropic plate. If the crack occurs in the middle area of the cantilever isotropic plate, the third natural frequency decreases. As seen from figure 4.11, the fourth natural frequency is minimum in the middle of the cantilever isotropic plate. Additionally, the fourth natural frequency decreases if the crack is close to the fixed support in the middle of the y axis. As shown in figure 4.12, If the crack occurs 50 mm or 350 mm on the x axis and in the middle area of the cantilever isotropic plate, the fifth natural frequency is minimum. It is also observed that if the crack is located at the 50 mm or 350 mm points of the region close to a fixed support, the fifth natural frequency decreases.

Figure 4.13 shows the effect of crack on the critical buckling load of cantilever isotropic plate. The crack is moved along the x and y axes of the isotropic plate. It is observed that the critical buckling load decreases due to crack occurs on the isotropic plate. As seen from this figure, the effect of a crack is maximum in the middle of the region close to a fixed support so that the critical buckling load is minimum at this region. If the crack is occurred the edge sides at close to the fixed support region, the effect of the crack reduces. It is also observed that if the crack is moved away from the fixed support on the x axis direction, the effect of crack decreases.

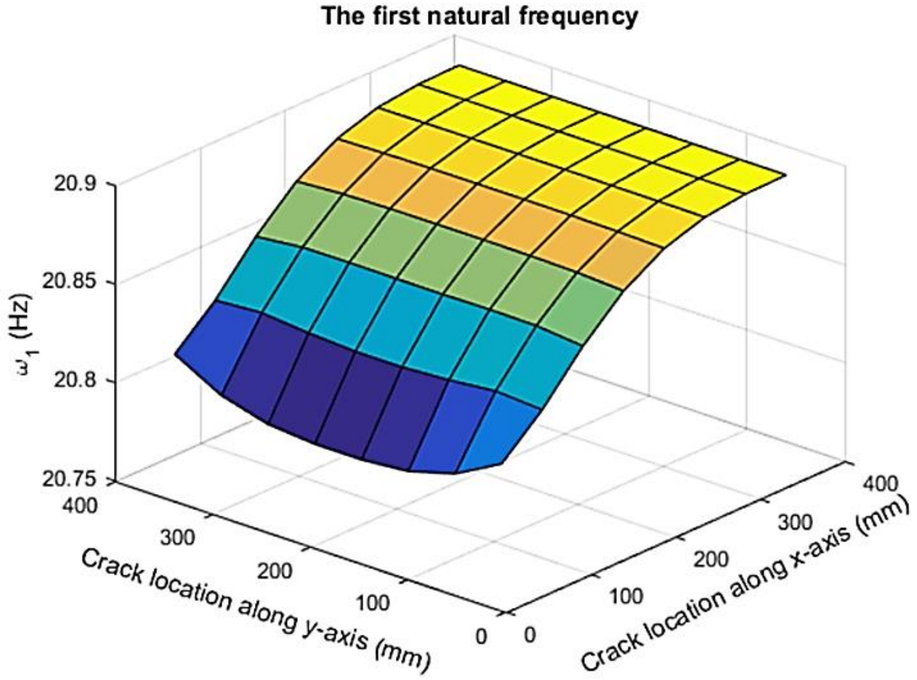

Figure 4.8 The effect of crack on the first natural frequency of the isotropic plate

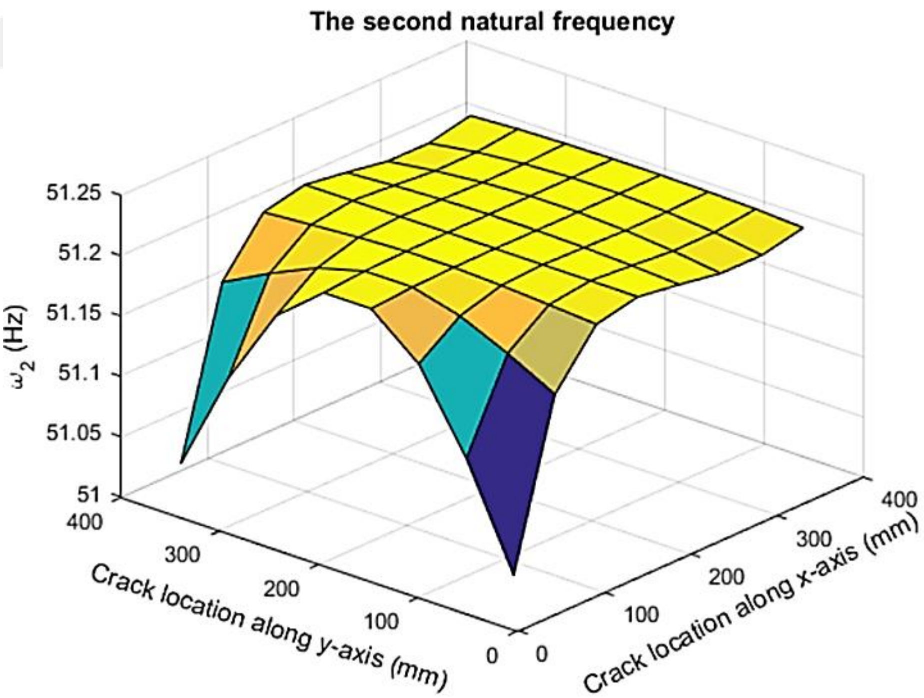

Figure 4.9 The effect of crack on the second natural frequency of the isotropic plate

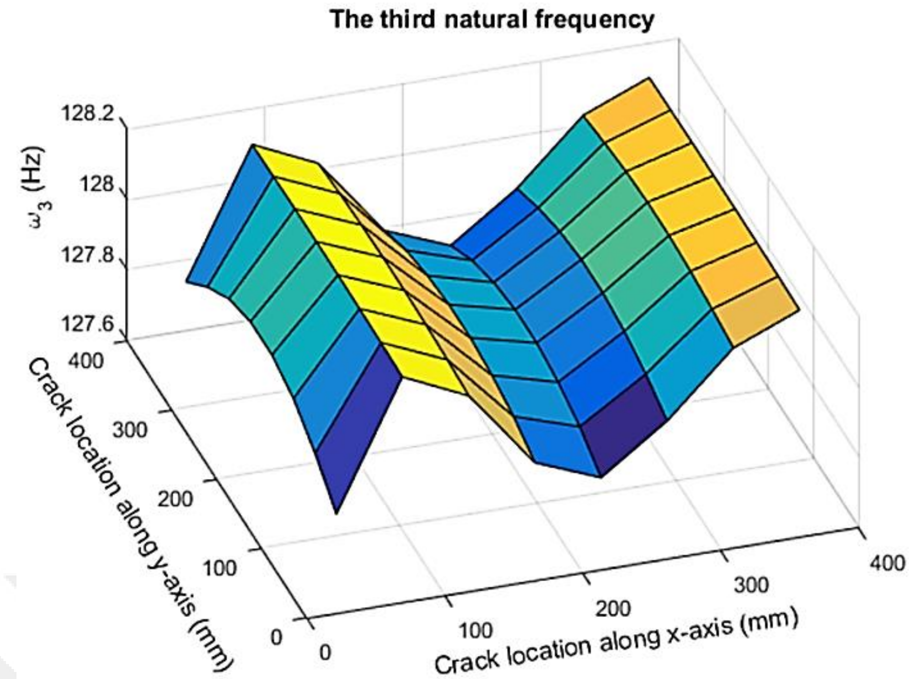

Figure 4.10 The effect of crack on the third natural frequency of the isotropic plate

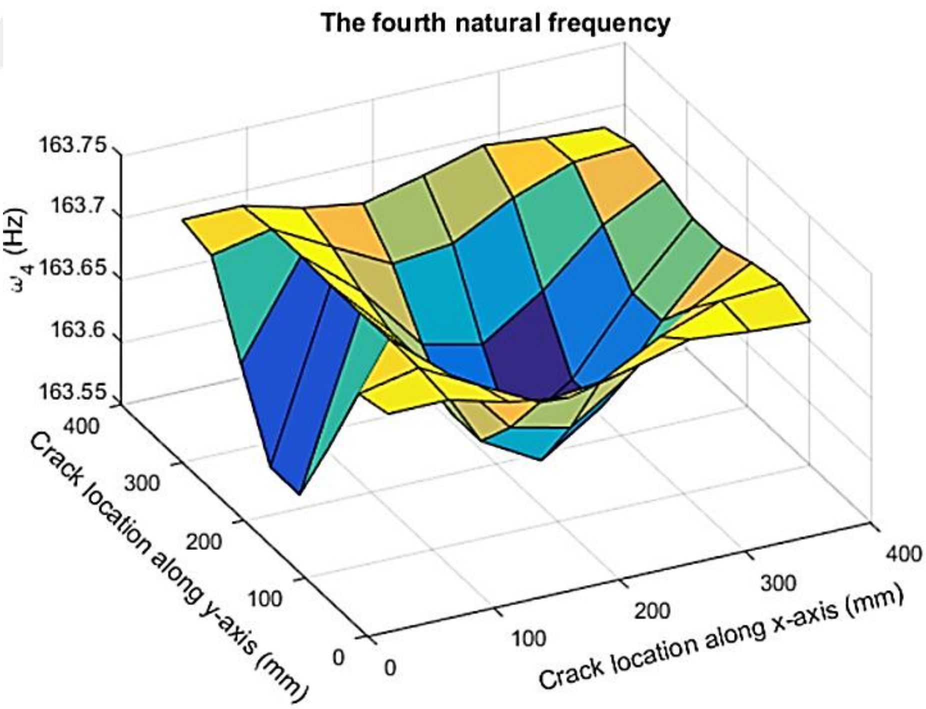

Figure 4.11 The effect of crack on the fourth natural frequency of the isotropic plate

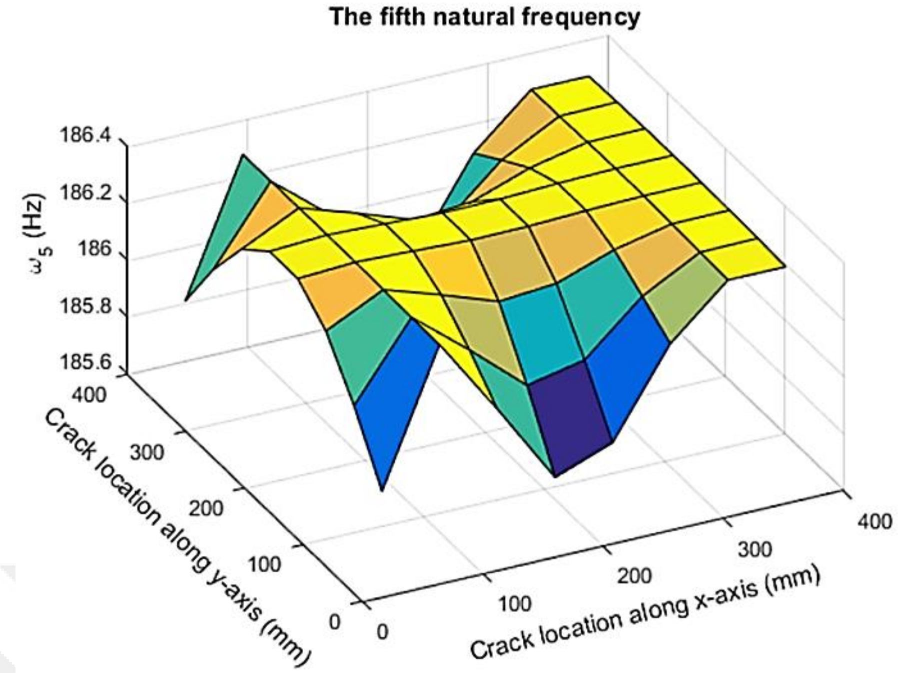

Figure 4.12 The effect of crack on the fifth natural frequency of the isotropic plate

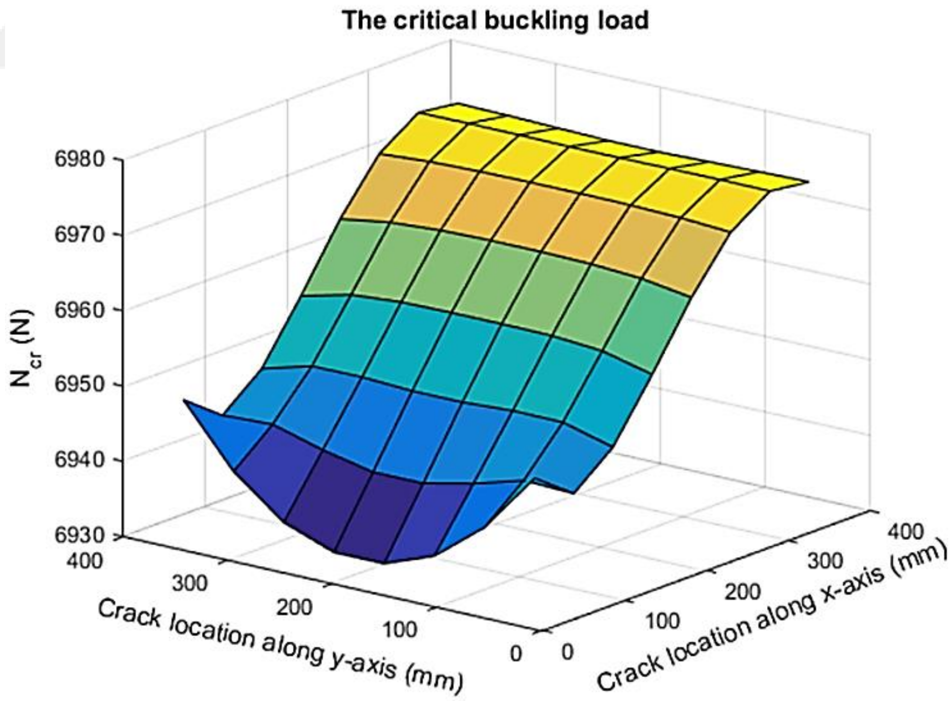

Figure 4.13 The effect of crack on the critical buckling load of the isotropic plate

Figures 4.14, 4.20, 4.26, 4.32 and 4.38 show the effect of crack on the first natural frequency of the cantilever composite plate. The composite plates have been examined for the five different orientation angles which are denoted by C1, C2, C3, C4, C5. In these figures, it is assumed that the crack is occurred on the cantilever composite plate. The crack is moved along *x* and *y* axes of composite plate. It can be noticed from these figures that the effect of crack on the first natural frequency is approximately the same. If the crack is moved away from the fixed support on the *x* axis direction, the effect of crack decreases so that the first natural frequency increases. If the composite plate is used to C1 orientation and the crack location is close to 400 mm, the first natural frequency is the maximum value. If the crack location is close to middle of fixed support and the cantilever composite plate is used to C5 orientation, the first natural frequency is the minimum value. When the crack is moved along the *y* axis, it is observed that the crack effect on the first natural frequency is approximately the same.

Figures 4.15, 4.21, 4.27, 4.33 and 4.39 show the effect of crack on the second natural frequency of the cantilever composite plate. In these figures, the crack is moved along the *x* and *y* axes of the composite plate. It has been observed that the crack decreases the second natural frequency, albeit with different effects at each location on the composite plate. The composite plates have been investigated for the five different orientation angles. if the crack occurs 50 mm or 350 mm on the *y* axis and the crack location is between 0 and 150 mm on the *x* axis direction, it is observed that the effect of crack decreases rapidly, especially for C1, C4, C5. It is also observed that if the crack is moved along the *y* axis in a location close to a fixed support, the second natural frequency is minimum at the edge side regions of the composite plate for C1, C2, C3, C4, C5. When the crack is moved towards the middle of the *y* axis, the effect of the crack is reduced so that the second natural frequency increases for each of five different orientation angles.

The effect of crack on the third natural frequency of the cantilever composite plate is examined in figures 4.16, 4.22, 4.28, 4.34 and 4.40. The crack is moved along *x* and *y* axes of composite plate. If the crack is moved along the *y* axis in a location close to a fixed support, the third natural frequency is minimum at the edge side regions of the composite plate. The third natural frequency of C3 is less than the other orientation angles at these regions. It is observed that if crack location is moved from these points to 200 mm on the *y* axis, the third natural frequency increases. The change of the third natural frequency of C4 is slower than the other orientaion in this region. If the crack is occurred on the *x* axis direction close to 100 mm, the effect of crack decreases. Therefore, the third natural frequency is maximum in this area. If the crack is moved away from 100 to 250 mm on the *x* direction, the third natural frequency decreases. It is also observed that if the crack is moved from 250 to 400 mm on the *x* direction, the third natural frequency increases.

Figures 4.17, 4.23, 4.29, 4.35 and 4.41 show the effect of crack on the fourth natural frequency of cantilever composite plate. In these figures, the crack is moved along the *x* and *y* axes of the composite plate. The fourth natural frequency decreases due to crack occurs at each point on the composite plate. As seen from these figures, the effect of a crack is maximum in the middle of the plate. Therefore, it is observed that the fourth natural frequency in this region is lower than the other regions. The fourth natural frequency of C2 is less than the other orientation angles at this region. In addition, it is observed that the fourth natural frequency decreases when the crack location is closed to the fixed side in the middle of the *y* axis. If the crack is moved from this region to the edge side regions, the fourth natural frequency increases rapidly. If the crack is occurred on the *x* axis direction close to 100 mm, the fourth natural frequency increases. In this area, the fourth natural frequency of C5 is the greatest among orientation values. If the crack is moved away from 100 to 200 mm on the *x* direction, the effect of crack increases so that the fourth natural frequency decreases. It is also observed that if the crack is moved from 200 to 400 mm on the *x* direction, the fourth natural frequency increases.

The effect of crack on the fifth natural frequency of the cantilever composite plate is investigated in figures 4.18, 4.24, 4.30, 4.36 and 4.42. In these figures, the crack is moved along the *x* and *y* axes of the composite plate which has been examined for C1, C2, C3, C4, C5. If the crack occurs in the middle of the *y* axis and is moved along the *x* axis, the effect of crack is no change and it is observed that the effect of the crack is less in this region. The effect of crack increases if the crack is located at the edge sides of the region close to a fixed support. When the crack is moved from these points to middle of the *y* axis, the effect of crack decreases. It is also observed that if the crack is located at the 50 mm or 350 mm points on the *y* axis and 185 mm on the *x* axis, the fifth natural frequency is minimum for all five different orientations. The fifth natural frequency of C5 is less than the other orientation angles at these points.

Figures 4.19, 4.25, 4.31, 4.37 and 4.43 show the effect of crack on the critical buckling load of cantilever composite plate. In these figures, the crack is moved along the *x* and *y* axes of the composite plate which has been examined for the five different orientation angles. If the crack is moved away from the fixed support on the *x* axis direction, the critical buckling load increases due to the effect of crack decreases. If the crack location is closed to the middle of fixed support, the critical buckling load decreases. The cantilever composite plate for C5 orientation, the critical buckling load is the minimum at this region. If the crack is located at the 50 mm or 350 mm points on the *y* axis and 50 mm on the *x* axis, the effect of crack decreases rapidly so that the critical buckling load increases for C1, C2, C3, C4 and C5.

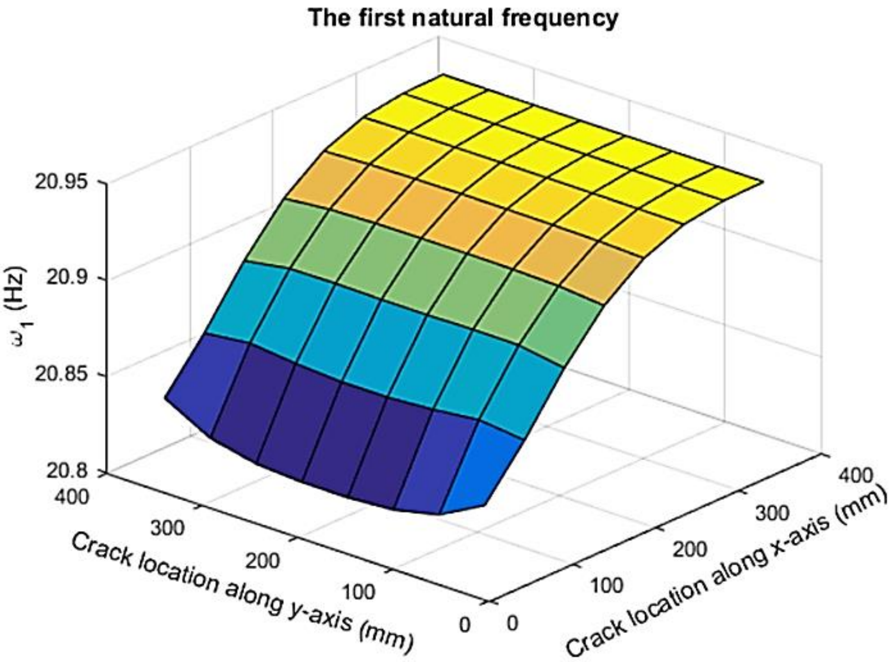

Figure 4.14 The effect of crack on the first natural frequency of the laminated composite plate [0°/0°/0°/0°]

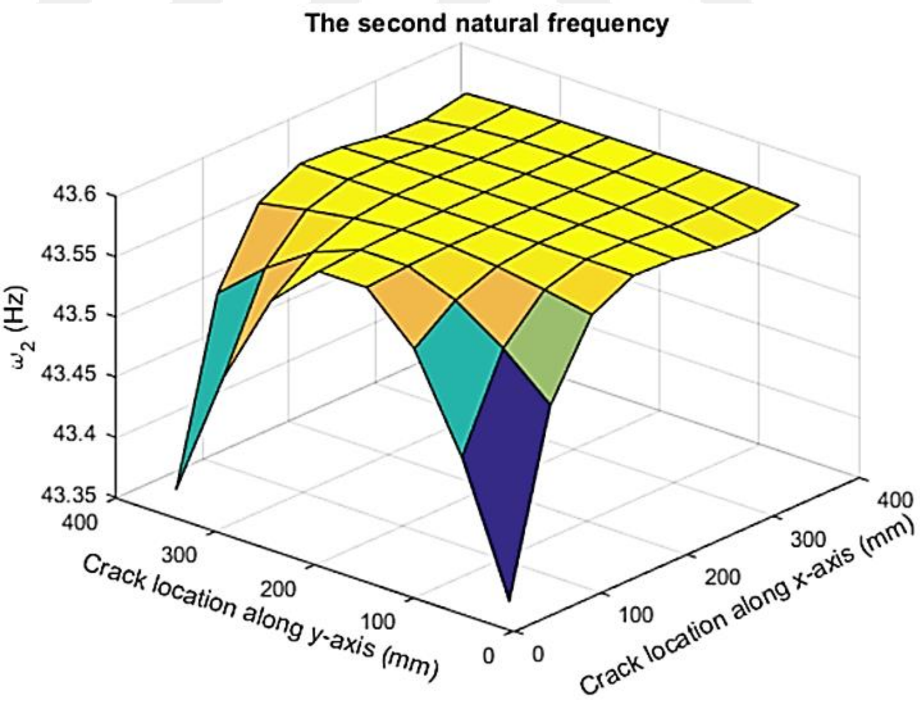

Figure 4.15 The effect of crack on the second natural frequency of the laminated composite plate [0°/0°/0°/0°]

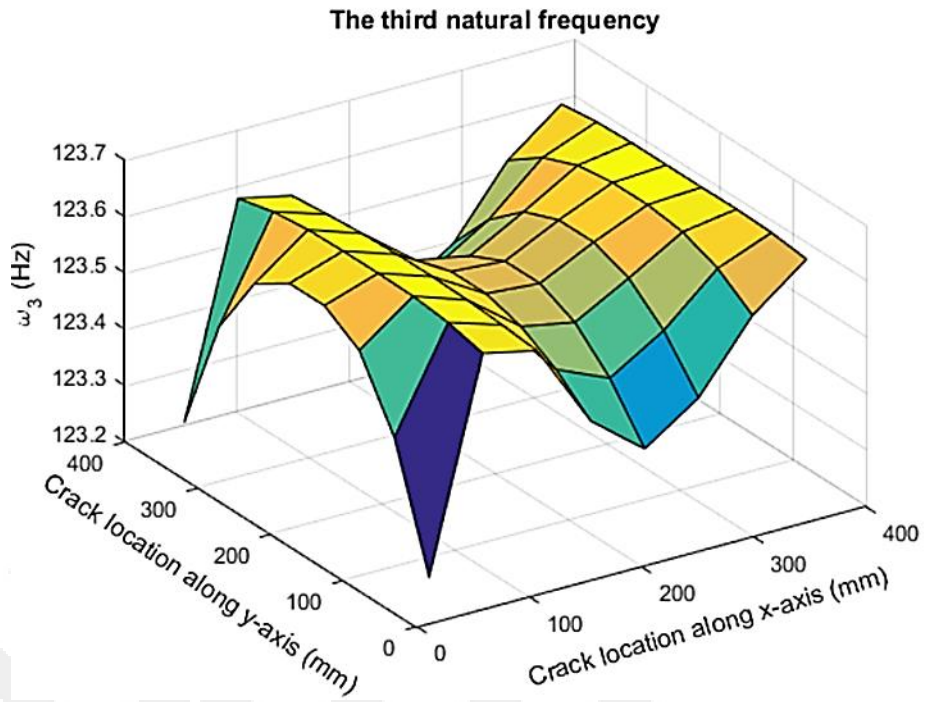

Figure 4.16 The effect of crack on the third natural frequency of the laminated composite plate [0°/0°/0°/0°]

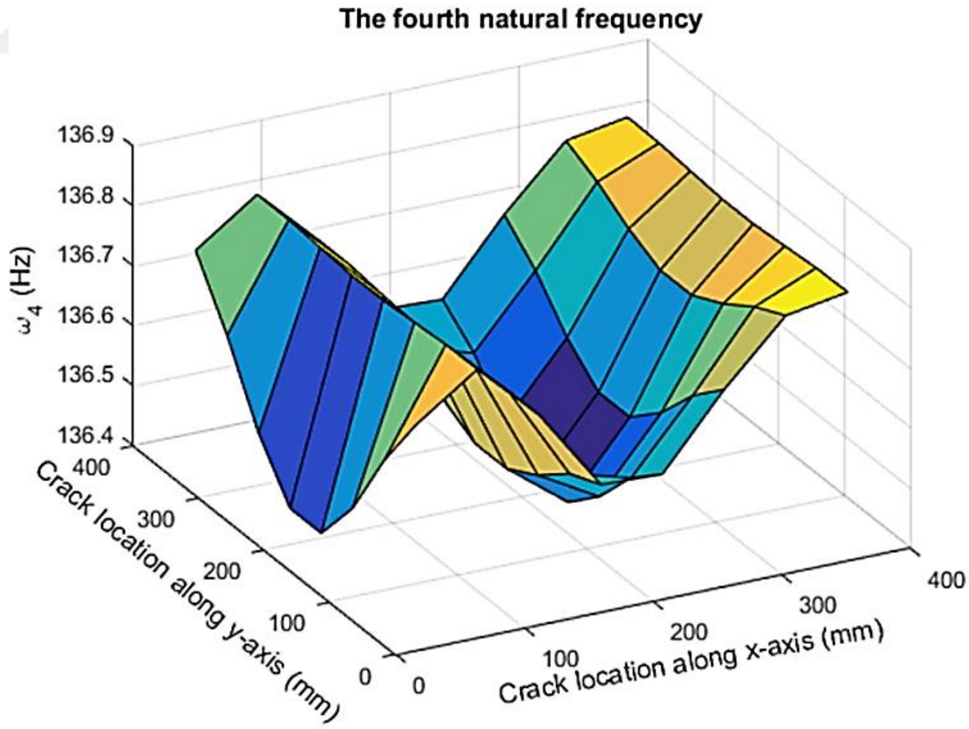

Figure 4.17 The effect of crack on the fourth natural frequency of the laminated composite plate [0°/0°/0°/0°]

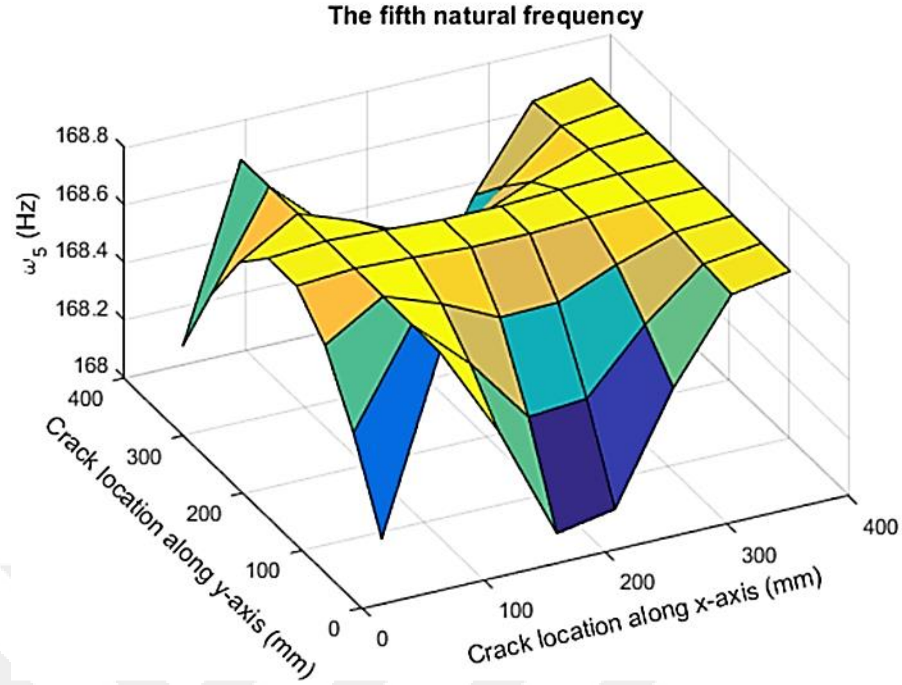

Figure 4.18 The effect of crack on the fifth natural frequency of the laminated composite plate [0°/0°/0°/0°]

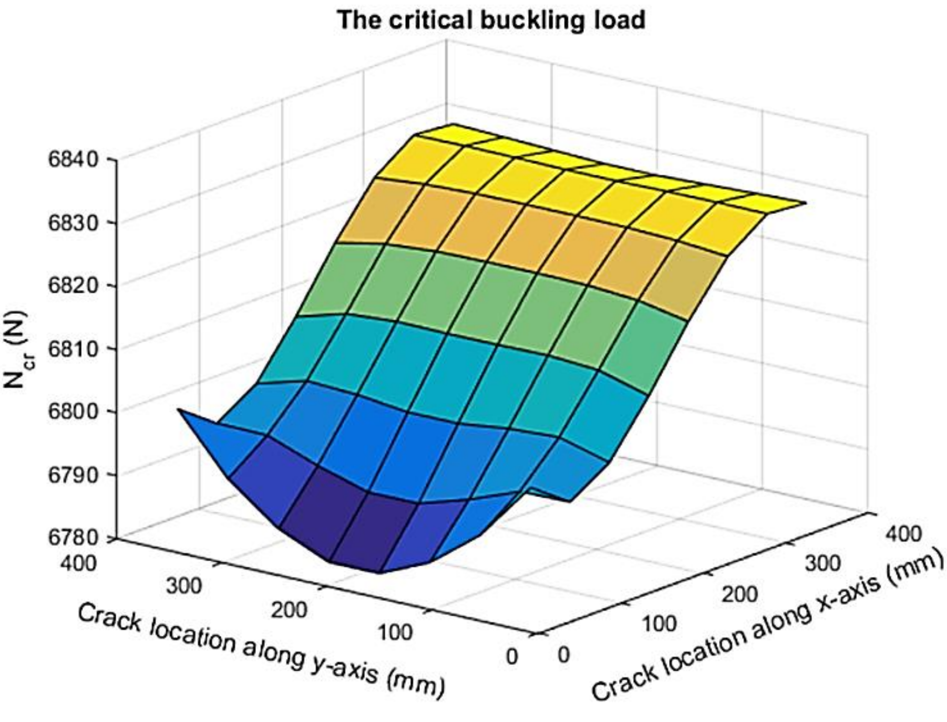

Figure 4.19 The effect of crack on the critical buckling load of the laminated composite plate [0°/0°/0°/0°]

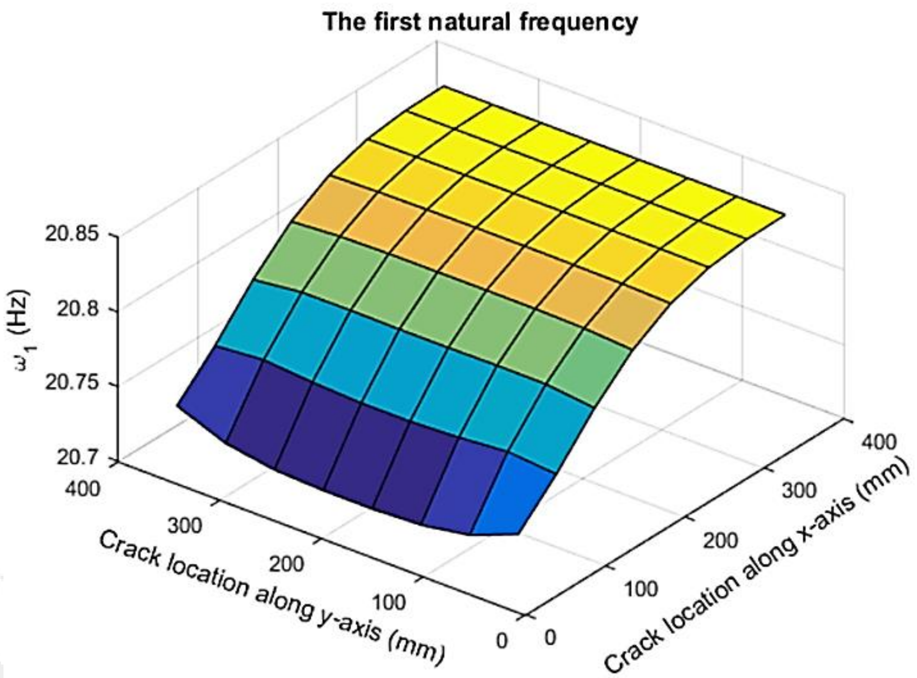

Figure 4.20 The effect of crack on the first natural frequency of the laminated composite plate [0°/30°/-30°/0°]

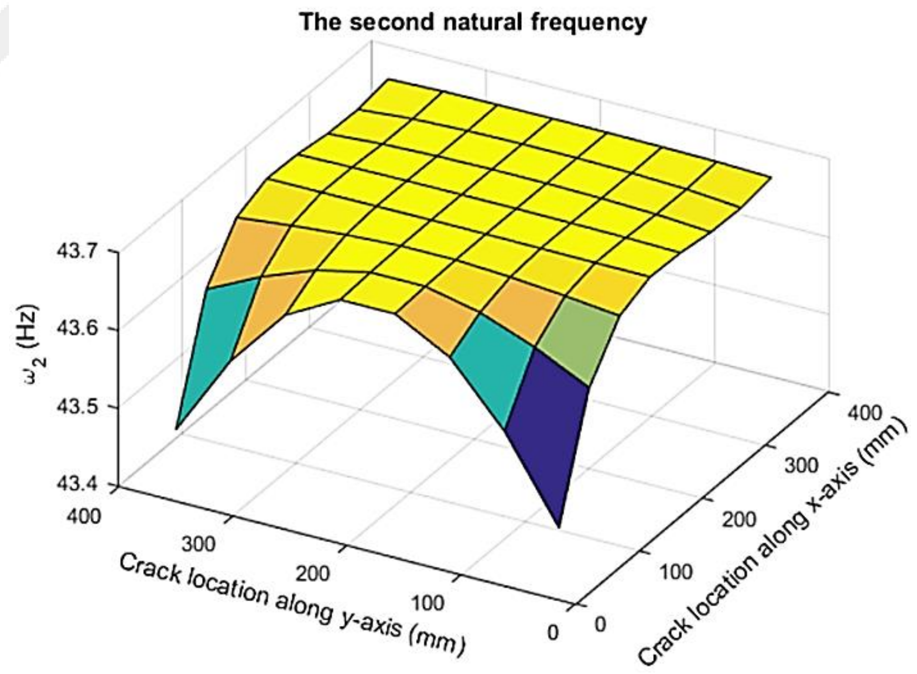

Figure 4.21 The effect of crack on the second natural frequency of the laminated composite plate [0°/30°/-30°/0°]

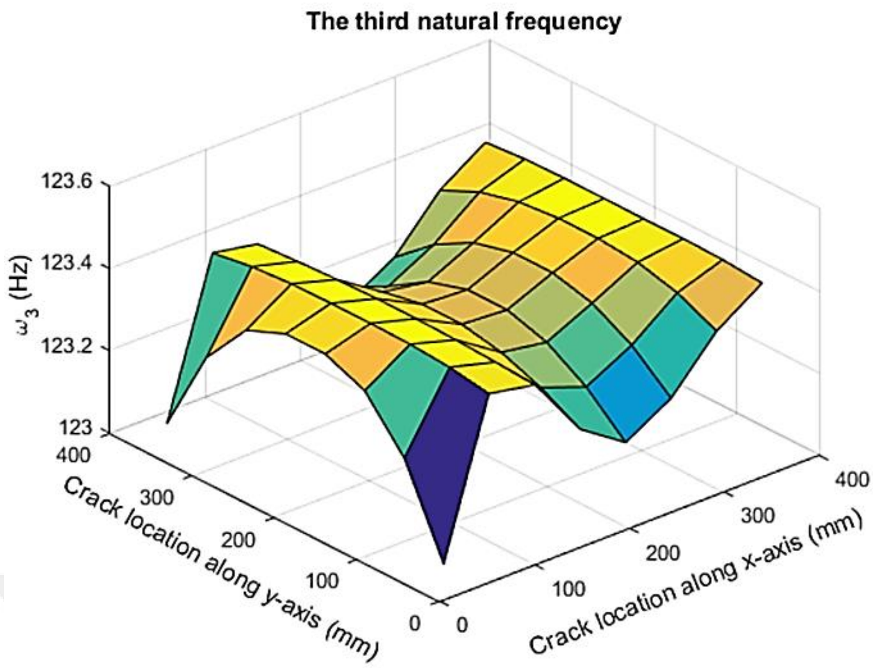

Figure 4.22 The effect of crack on the third natural frequency of the laminated composite plate [0°/30°/-30°/0°]

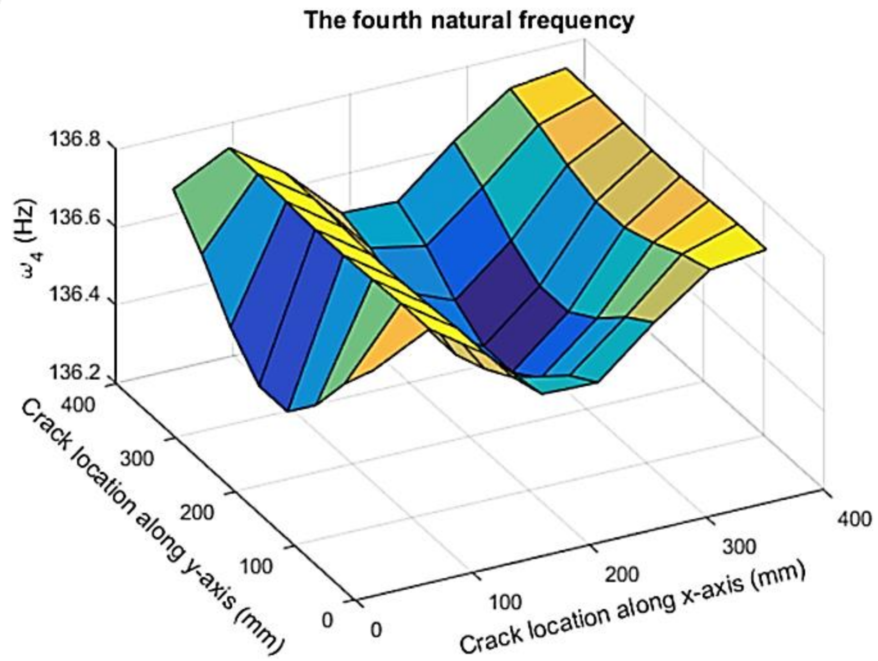

Figure 4.23 The effect of crack on the fourth natural frequency of the laminated composite plate [0°/30°/-30°/0°]

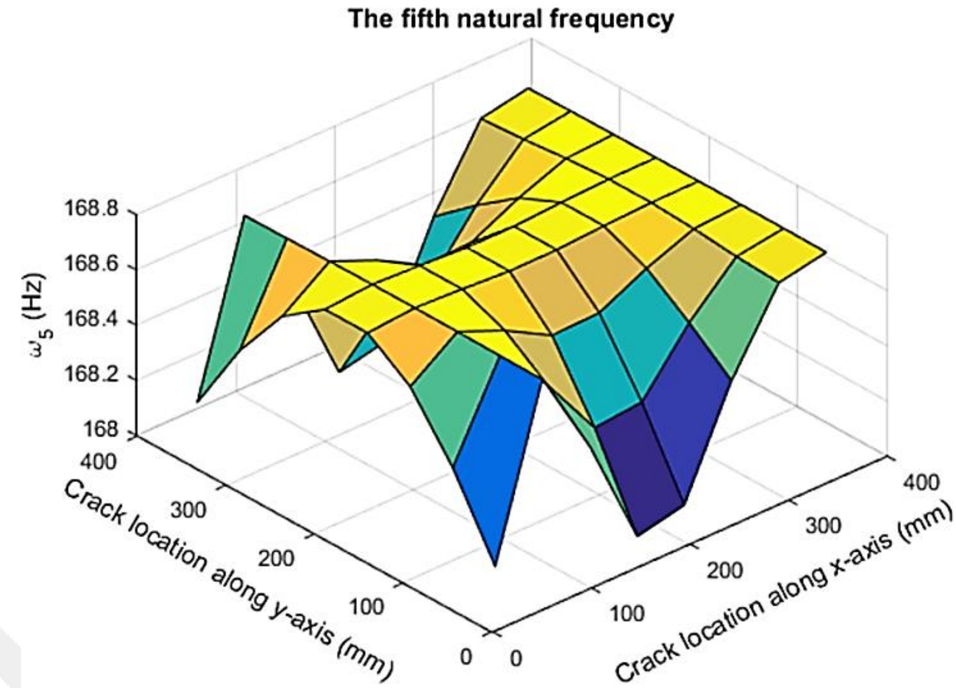

Figure 4.24 The effect of crack on the fifth natural frequency of the laminated composite plate [0°/30°/-30°/0°]

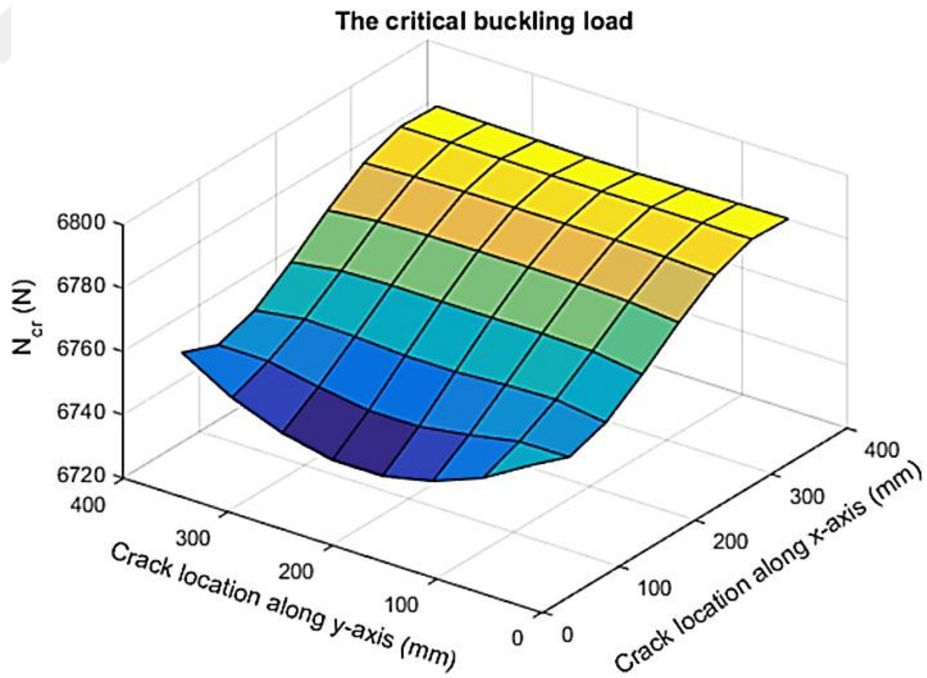

Figure 4.25 The effect of crack on the critical buckling load of the laminated composite plate [0°/30°/-30°/0°]

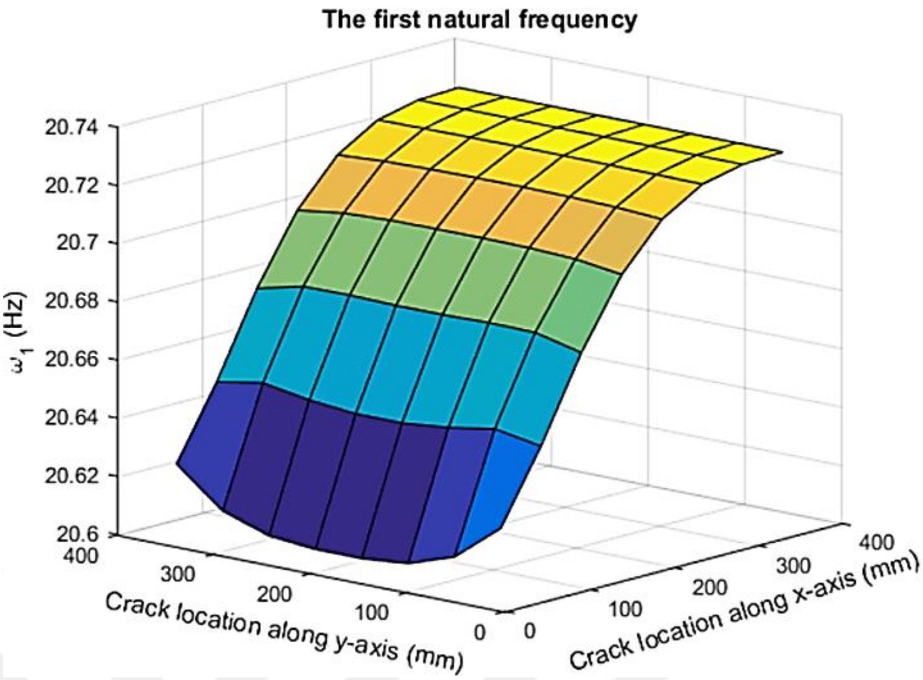

Figure 4.26 The effect of crack on the first natural frequency of the laminated composite plate [0°/45°/-45°/0°]

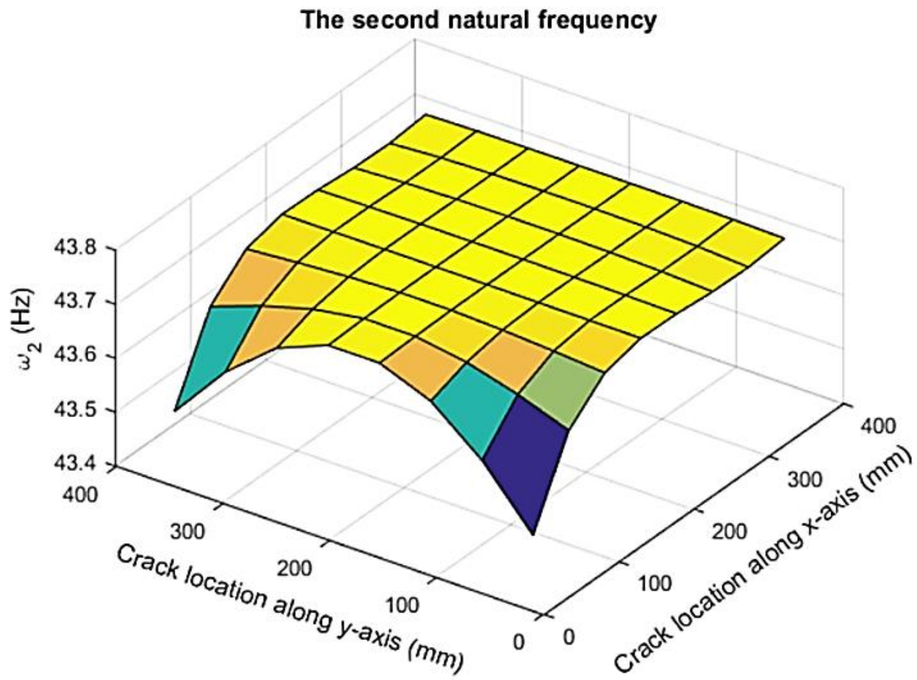

Figure 4.27 The effect of crack on the second natural frequency of the laminated composite plate [0°/45°/-45°/0°]

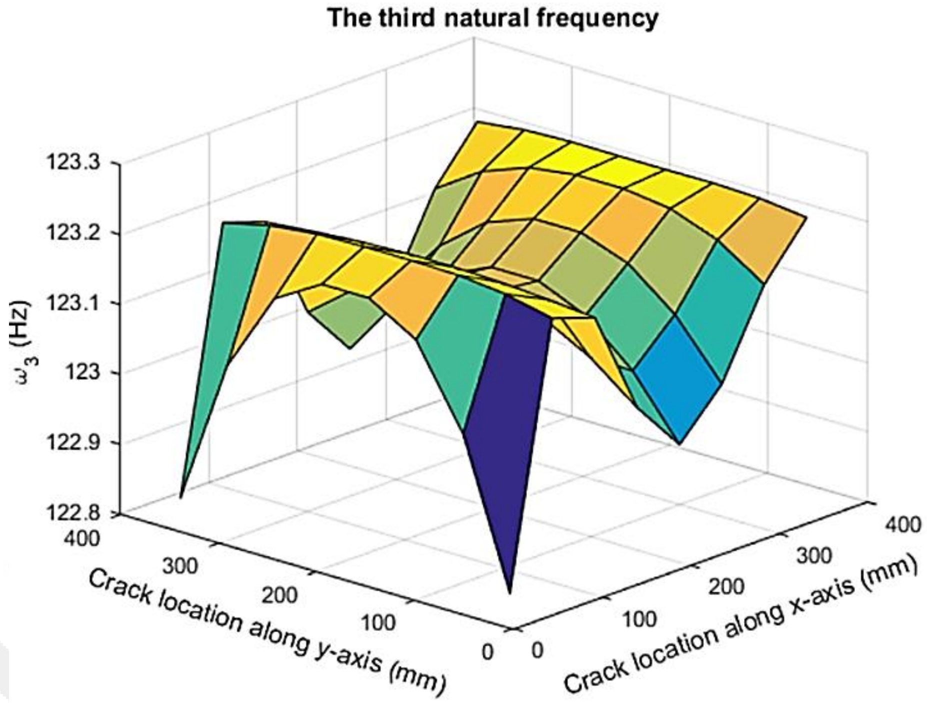

Figure 4.28 The effect of crack on the third natural frequency of the laminated composite plate [0°/45°/-45°/0°]

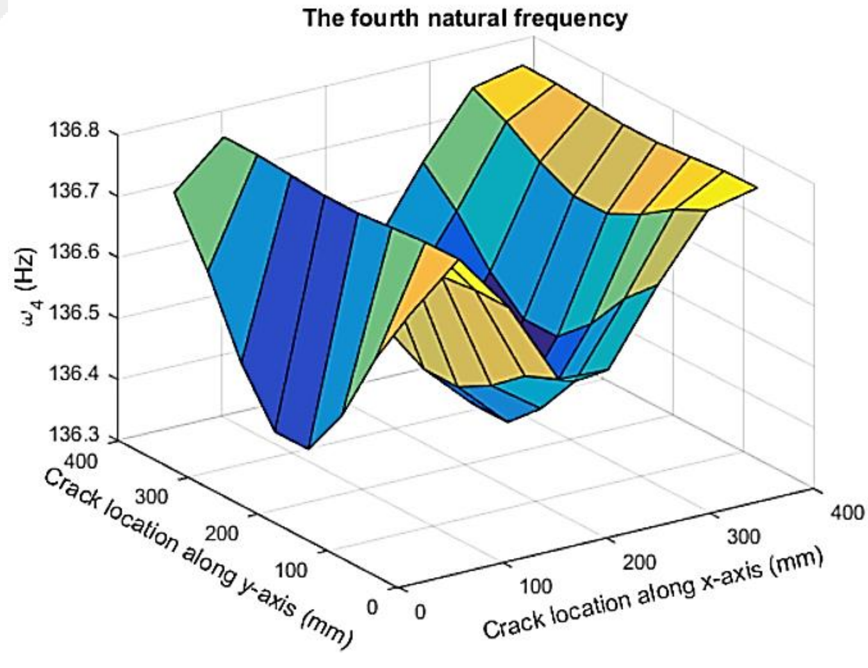

Figure 4.29 The effect of crack on the fourth natural frequency of the laminated composite plate [0°/45°/-45°/0°]

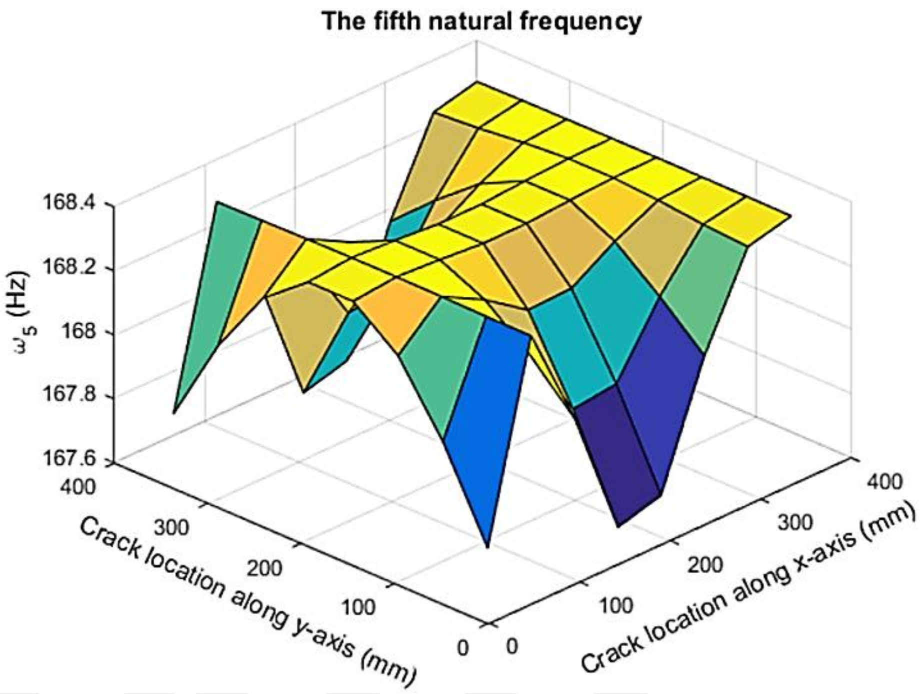

Figure 4.30 The effect of crack on the fifth natural frequency of the laminated composite plate [0°/45°/-45°/0°]

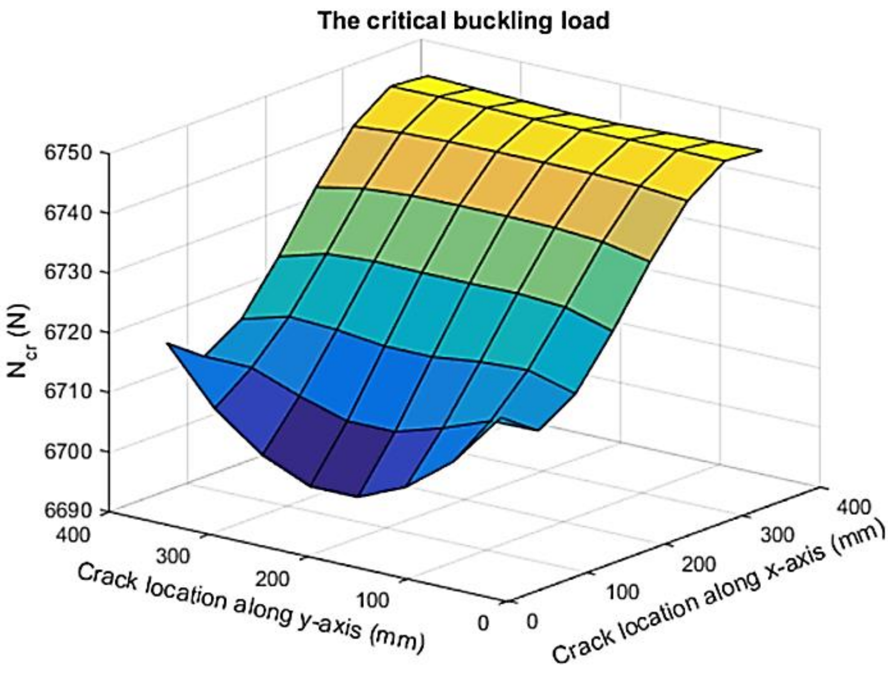

Figure 4.31 The effect of crack on the critical buckling load of the laminated composite plate [0°/45°/-45°/0°]

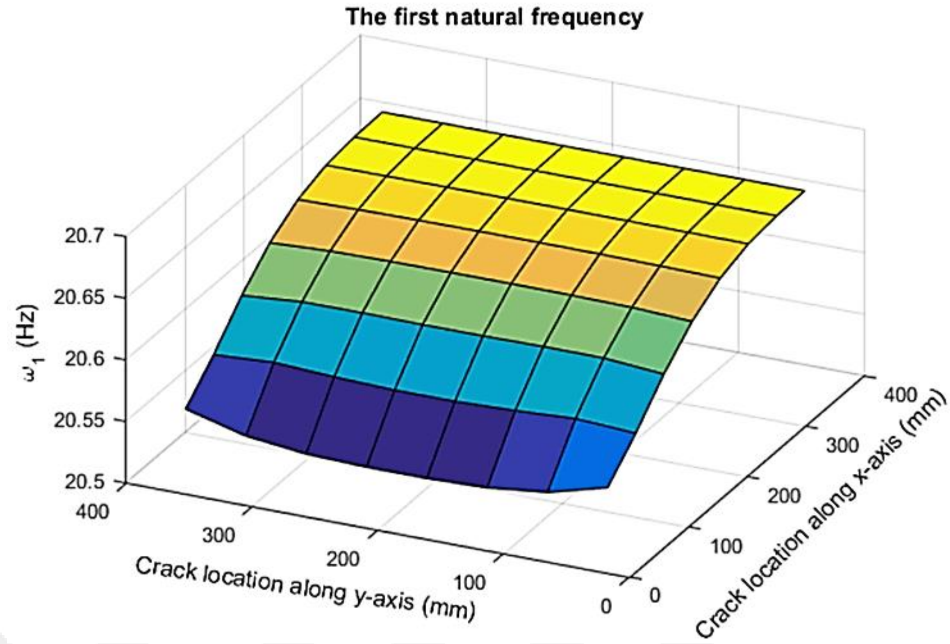

Figure 4.32 The effect of crack on the first natural frequency of the laminated composite plate [0°/60°/-60°/0°]

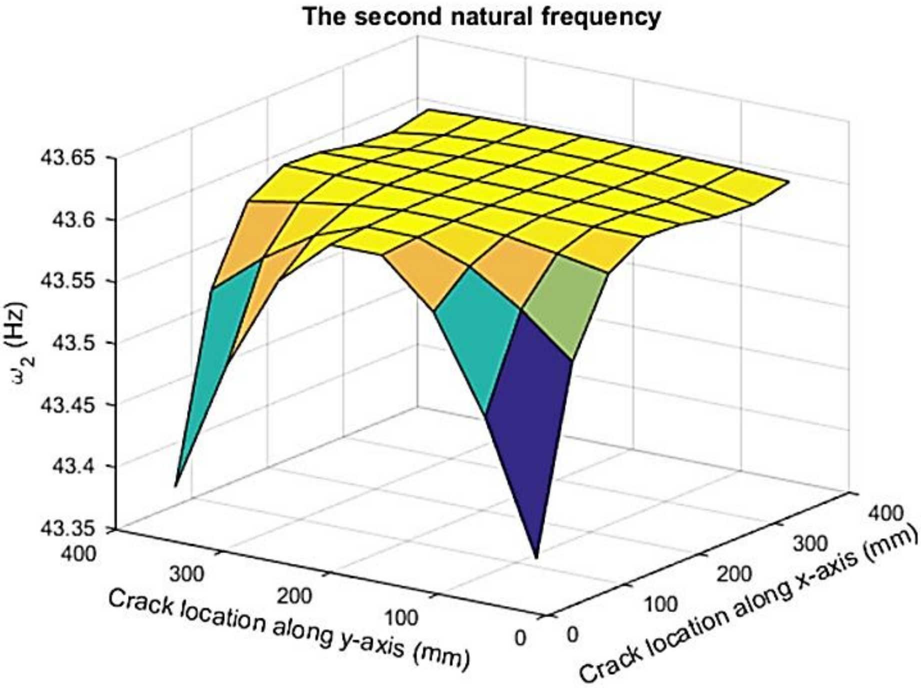

Figure 4.33 The effect of crack on the second natural frequency of the laminated composite plate [0°/60°/-60°/0°]

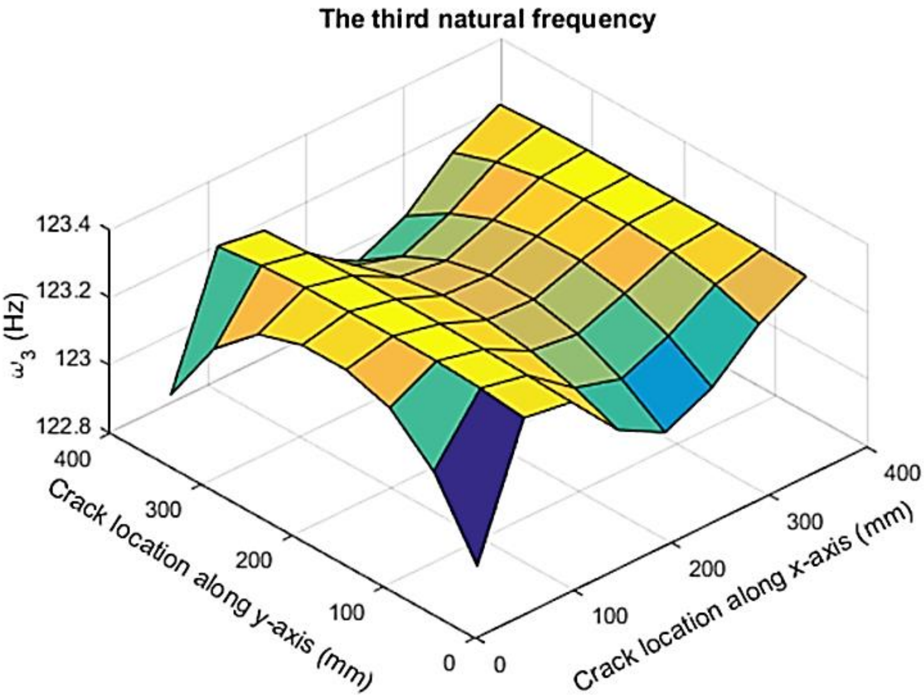

Figure 4.34 The effect of crack on the third natural frequency of the laminated composite plate [0°/60°/-60°/0°]

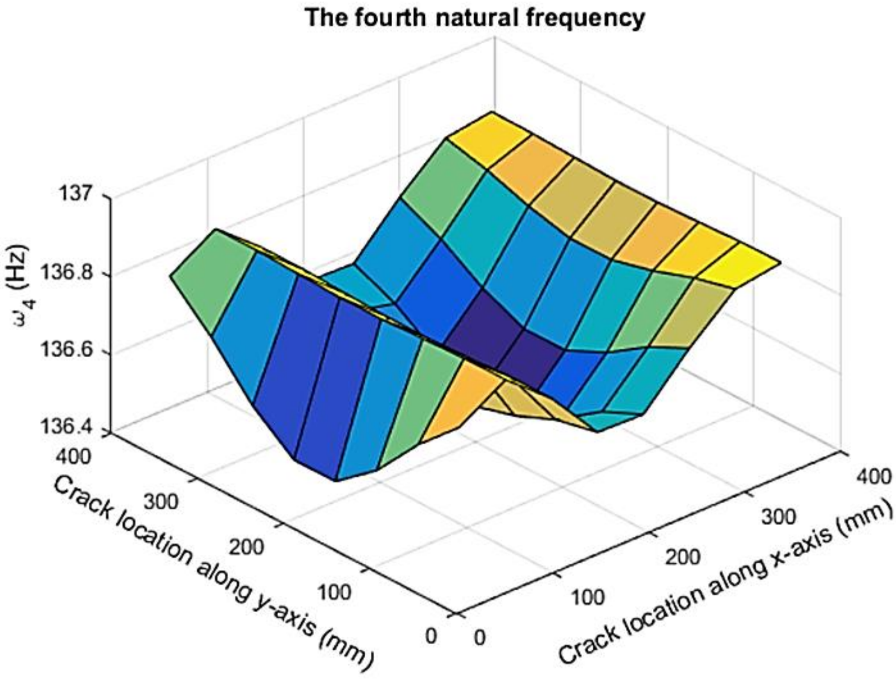

Figure 4.35 The effect of crack on the fourth natural frequency of the laminated composite plate [0°/60°/-60°/0°]

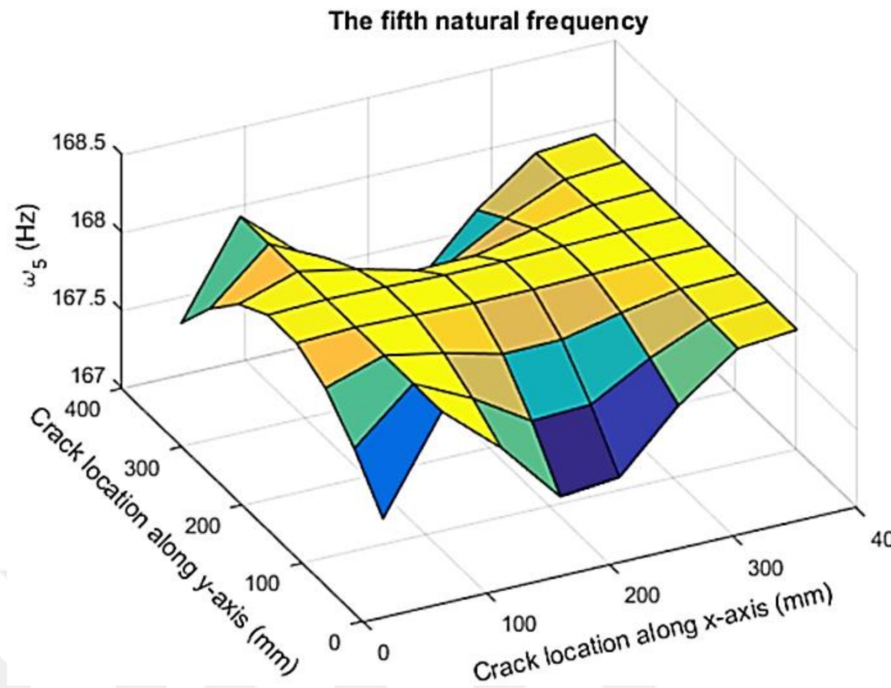

Figure 4.36 The effect of crack on the fifth natural frequency of the laminated composite plate [0°/60°/-60°/0°]

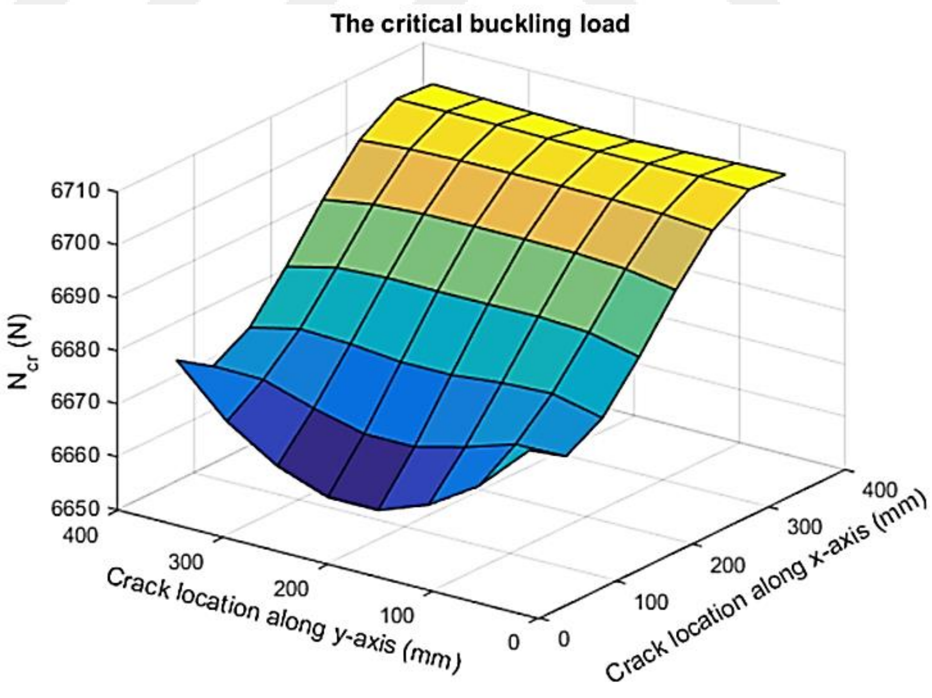

Figure 4.37 The effect of crack on the critical buckling load of the laminated composite plate [0°/60°/-60°/0°]

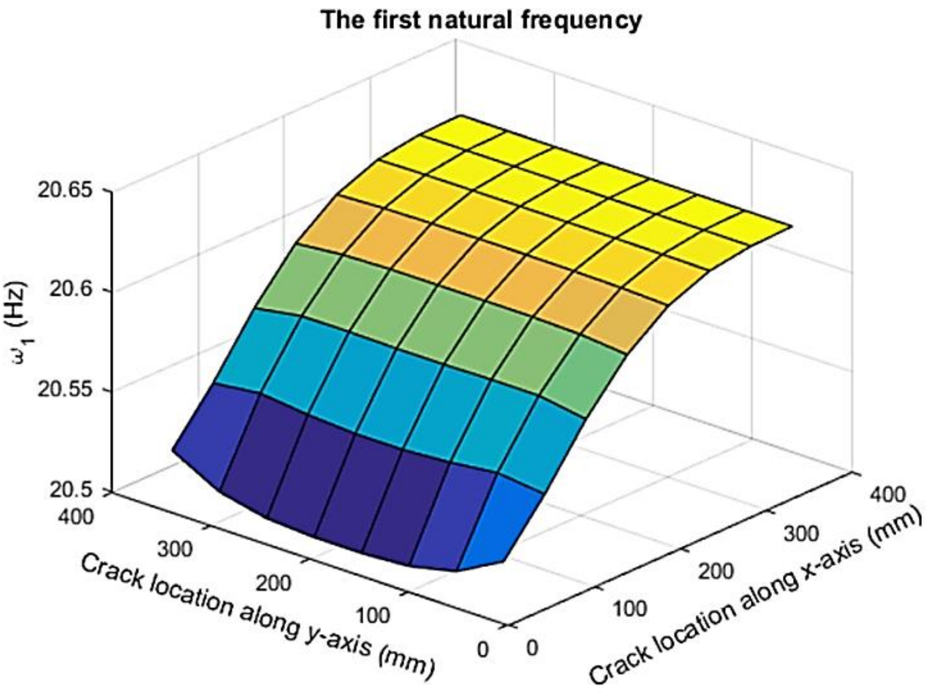

Figure 4.38 The effect of crack on the first natural frequency of the laminated composite plate [0°/90°/90°/0°]

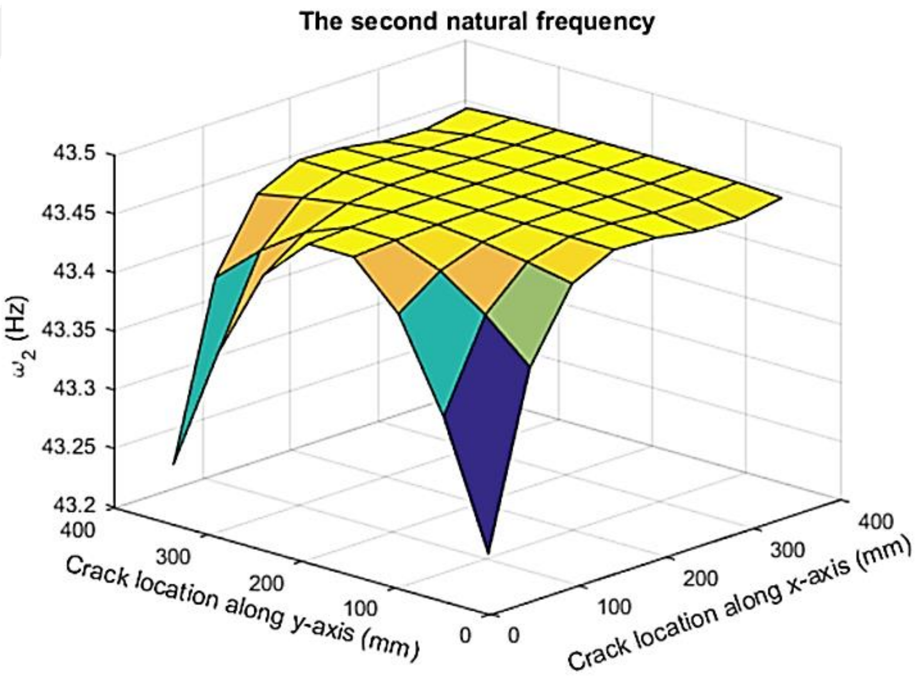

Figure 4.39 The effect of crack on the second natural frequency of the laminated composite plate [0°/90°/90°/0°]

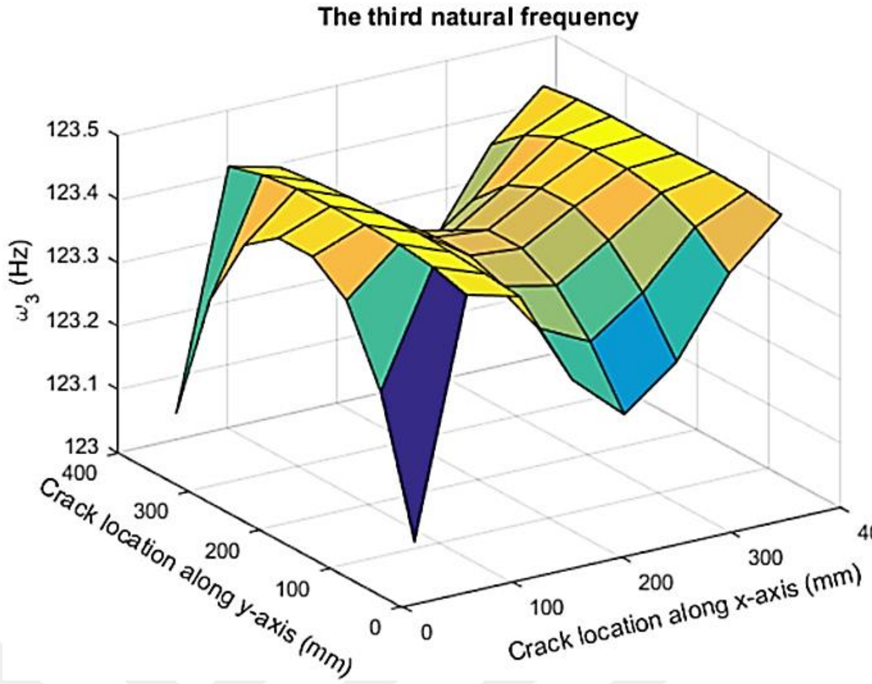

Figure 4.40 The effect of crack on the third natural frequency of the laminated composite plate [0°/90°/90°/0°]

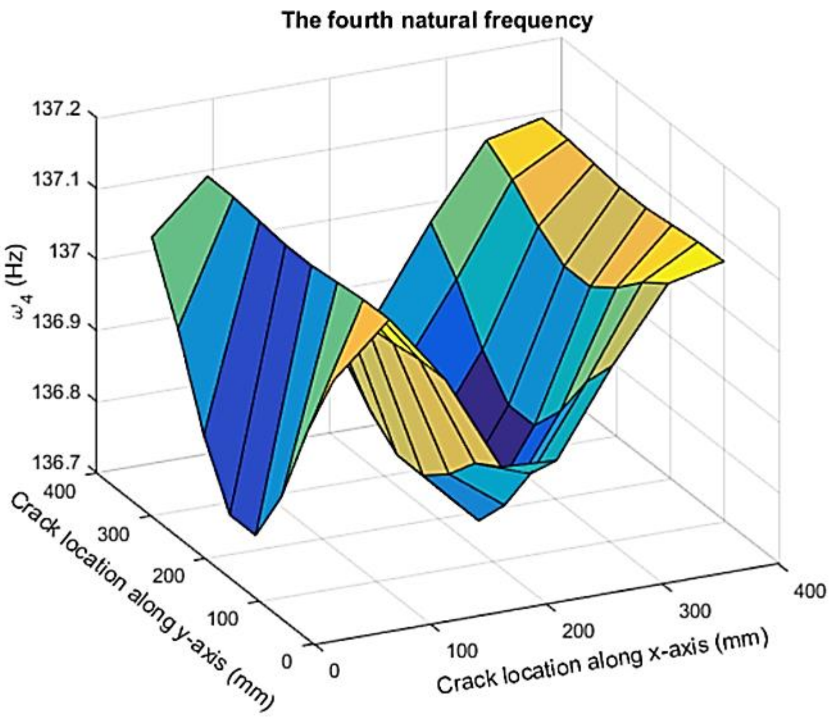

Figure 4.41 The effect of crack on the fourth natural frequency of the laminated composite plate [0°/90°/90°/0°]

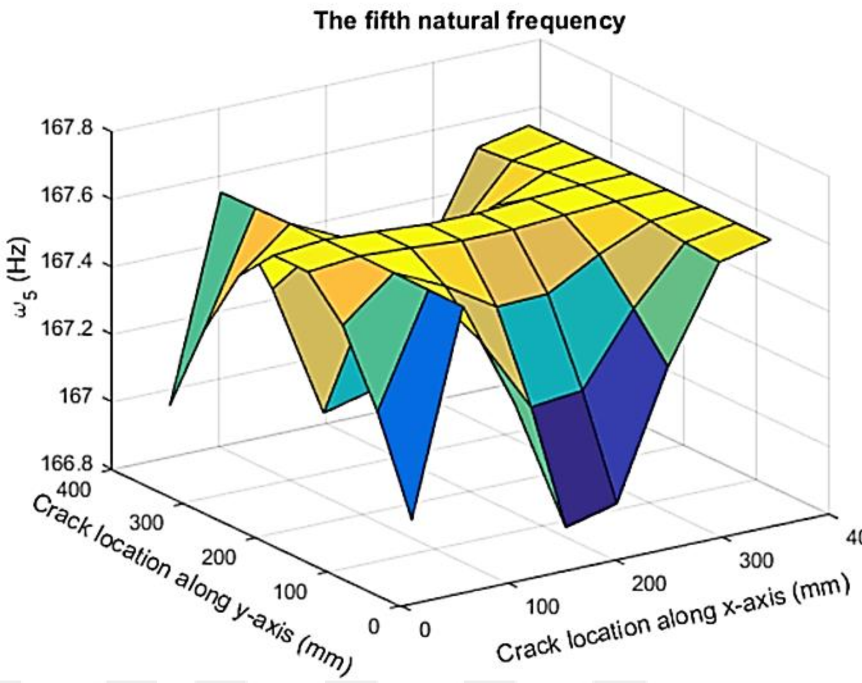

Figure 4.42 The effect of crack on the fifth natural frequency of the laminated composite plate [0°/90°/90°/0°]

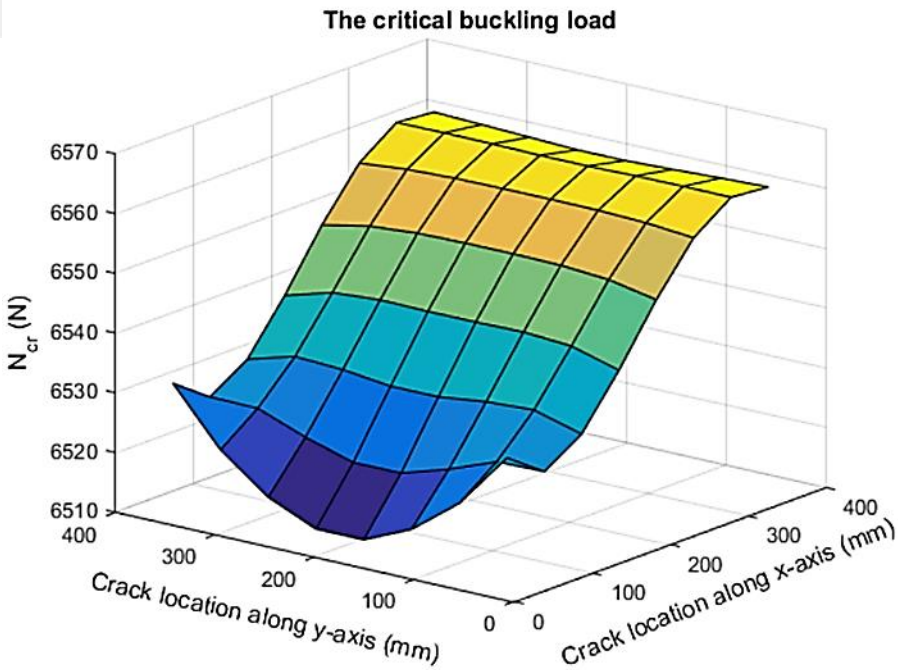

Figure 4.43 The effect of crack on the critical buckling load of the laminated composite plate [0°/90°/90°/0°]

Figure 4.44 shows the effect of static and dynamic load factor on the first dynamic stability of the cantilever isotropic plate. It is observed that the dynamic load factor (β) increases, the unstable region widens. When the static load factor (α) is equal to 0, the dynamic load factor (β) is bounded between the values of 0 and 2. If the static load factor (α) is equal to 0.5, the dynamic load factor (β) is bounded between the values of 0 and 1. When the static load factor (α) is equal to 0 and 0.5, the first exciting frequencies constructing the lower border of the unstable region reach zero values at which dynamic load factor (β) corresponds to the values of 1 and 2, respectively,

Figure 4.45 shows the effect of static and dynamic load factor on the second dynamic stability of cantilever isotropic plate. When the dynamic load factor (β) decreases, the exciting frequency's borders move towards the origin, therefore the unstable region becomes narrower. If the dynamic load factor (β) is equal to 0, the second exciting frequency is greater than the first exciting frequency. The unstable region of the first exciting frequency is wider than the unstable region of the second exciting frequency.

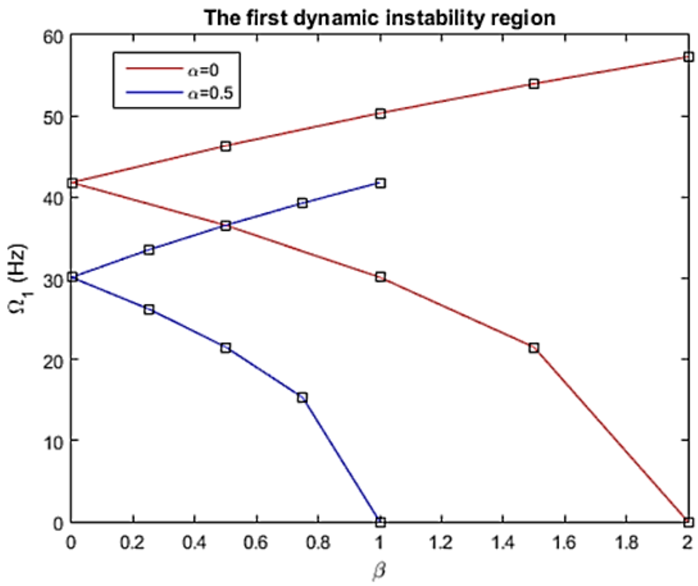

Figure 4.44 The effect of static and dynamic load factors on the first dynamic instability region of the isotropic plate

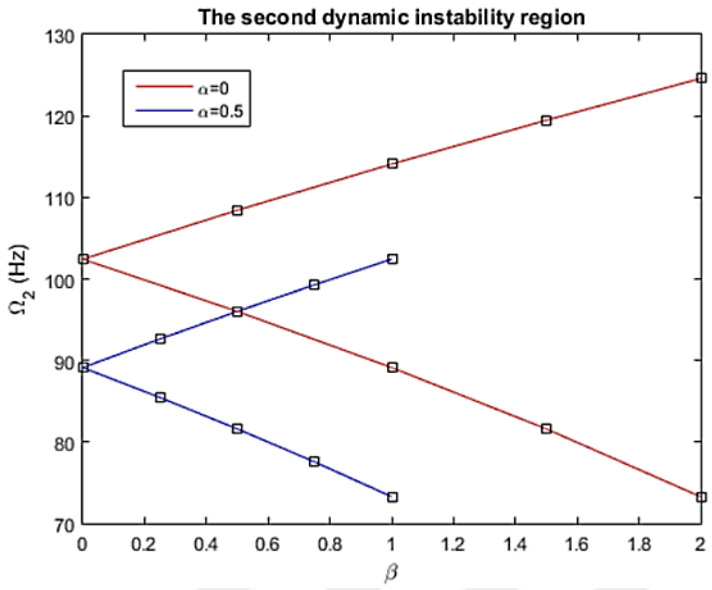

Figure 4.45 The effect of static and dynamic load factors on the second dynamic instability region of the isotropic plate

The first and second exciting frequency values are given approximately the same for each of five different orientations of laminates in composite plates. Therefore, C1 is examined for the composite plate in figures 4.46 and 4.47. The effect of static and dynamic load factor on the first dynamic stability of cantilever composite plate is examined in figure 4.46. When the static load factor (α) is equal to 0, 0.5 and dynamic load factor (β) is equal to 1, 2, respectively, the first exciting frequencies constructing the lower border of the unstable region is equal to 0. When the static load factor (α) is equal to 0.5, the dynamic load factor (β) is bounded between the values of 0 and 1. If the static load factor (α) is equal to 0, the dynamic load factor (β) is bounded between the values of 0 and 2. Figure 4.47 shows the effect of static and dynamic load factor on the second dynamic stability of cantilever composite plate. As seen from these figures, the dynamic load factor (β) increases, the unstable region widens. The unstable region of the second exciting frequency narrower than the unstable region of the first exciting frequency. When the dynamic load factor (β) is equal to 0, the first exciting frequency is less than the second exciting frequency.

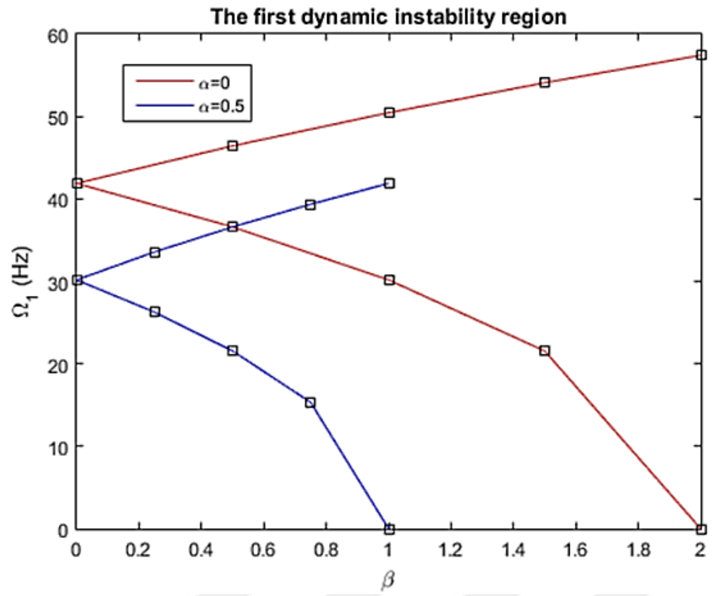

Figure 4.46 The effect of static and dynamic load factors on the first dynamic instability region of the composite plate [0°/0°/0°/0°]

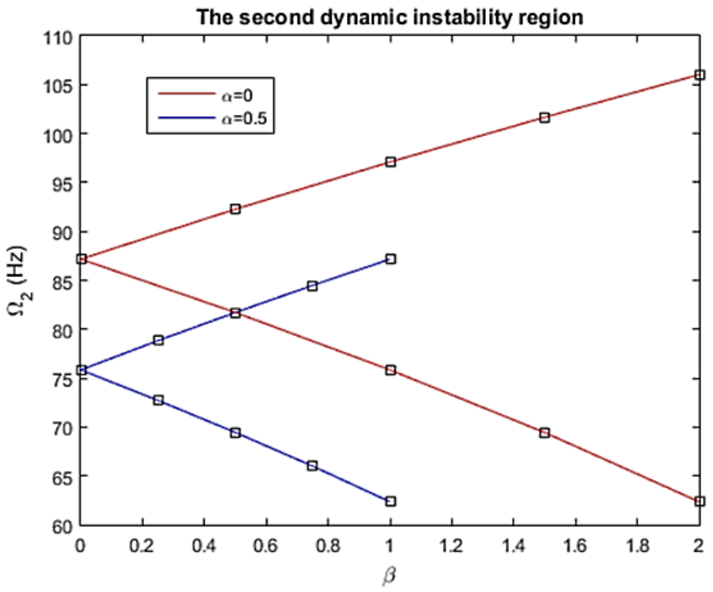

Figure 4.47 The effect of static and dynamic load factors on the second dynamic instability region of the composite plate [0°/0°/0°/0°]

As seen from figure 4.48, crack is located in the middle of y the axis and crack is moved along the x axis. In this thesis, the dynamic stability is analyzed for each of the different crack locations on the cantilever plate.

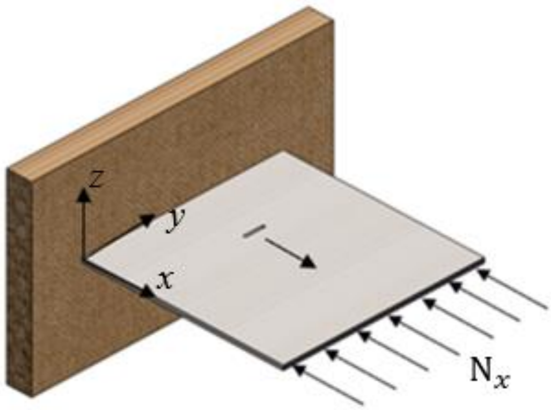

Figure 4.48 Cantilever cracked thin plate (crack is moved along the *x* axis)

Figures 4.49, 4.50, 4.51, 4.52 show the effects of the dynamic load factor, static load factor and the crack location on the first and second dynamic stability of cantilever isotropic plate, as 3D plots. In these figures, the crack is located in the middle of the y axis and the crack is moved along the x axis of the cantilever isotropic plate. When the static load factor (α) is equal to 0, 0.5 and dynamic load factor (β) is equal to 1, 2, respectively, the first exciting frequencies constructing the lower border of the unstable region reach zero. If the dynamic load factor (β) increases, the unstable region widens. When the static load factor (α) is equal to 0, the dynamic load factor (β) is bounded between the values of 0 and 2. If the static load factor (α) is equal to 0.5, the dynamic load factor (β) is bounded between the values of 0 and 1.It is observed that the crack has no effect on these situations.

In these figures, the crack changes the unstable region of the cantilever isotropic plate. It is observed that if the crack is moved away from the fixed support on the x axis direction, the first exciting frequency increases for each static load factor (α). It is also observed that if static load factor (α) is equal to 0, the effect of crack is less on the second exciting frequency. If static load factor (α) is equal to 0.5, the crack decreases the second exciting frequency but the crack occurs on the middle of the x axis, the second exciting frequency increase rapidly. When the crack moved away from the middle region of the cantilever isotropic plate, the second exciting frequency continues to decrease.

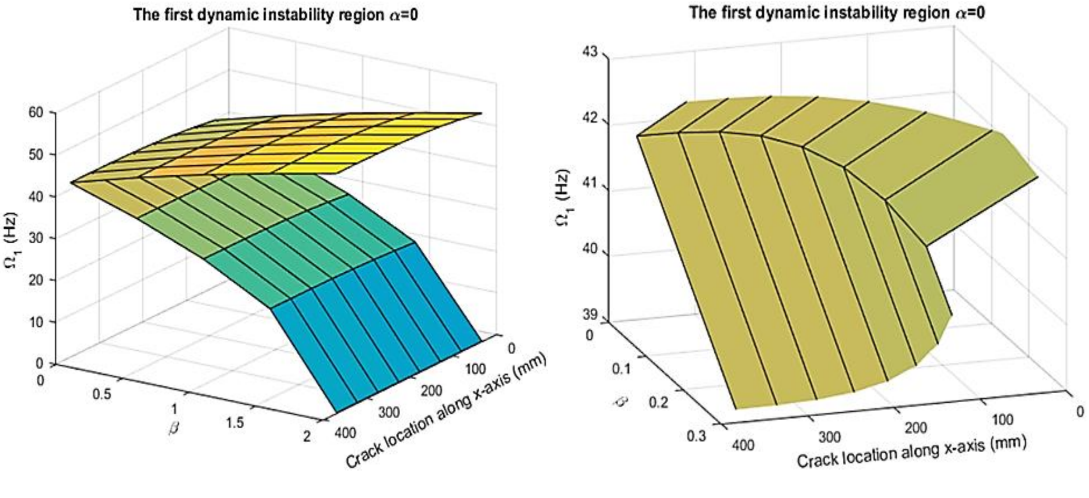

Figure 4.49 The effect of crack on the first dynamic instability region of the isotropic plate for α=0

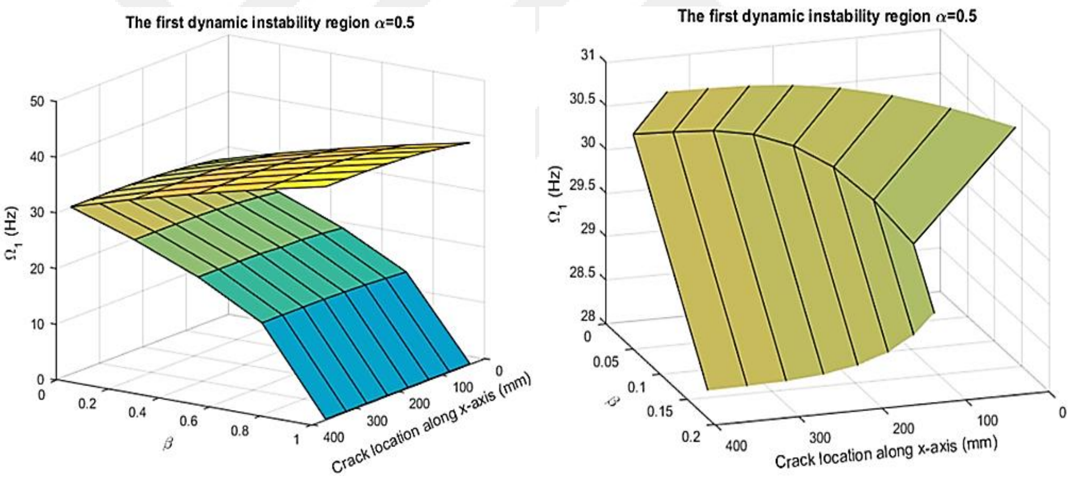

Figure 4.50 The effect of crack on the first dynamic instability region of the isotropic plate for α=0.5

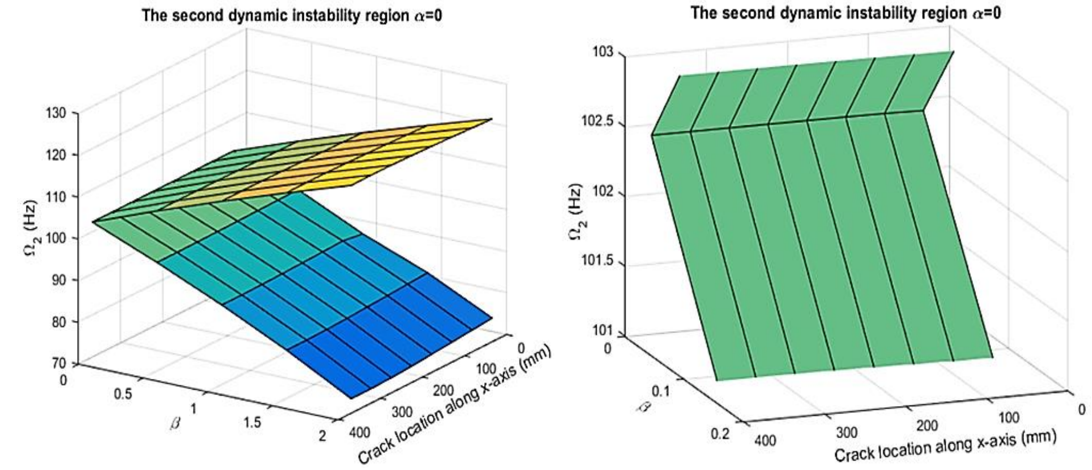

Figure 4.51 The effect of crack on the second dynamic instability region of the isotropic plate for α=0

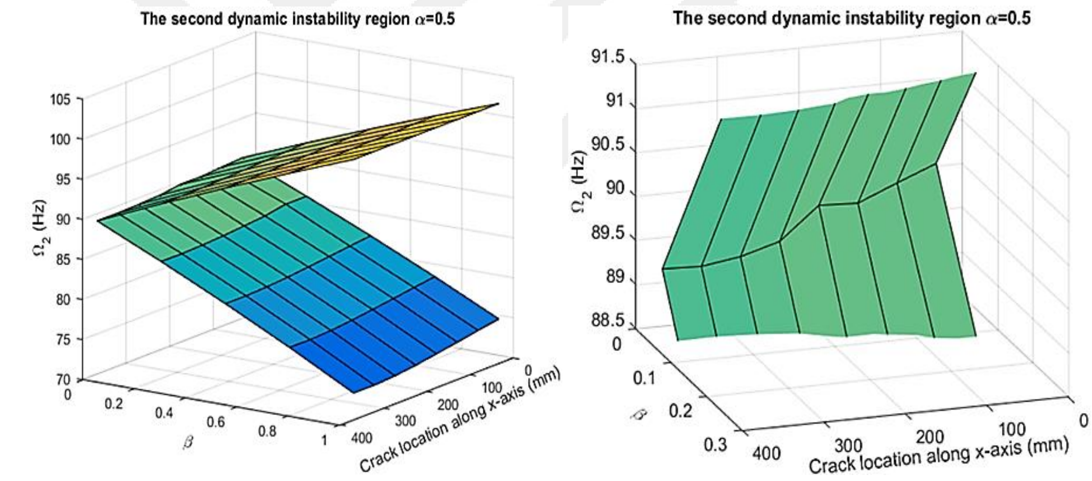

Figure 4.52 The effect of crack on the second dynamic instability region of the isotropic plate for α=0.5

Figures from 4.53 to 4.72 show the effects of the dynamic load factor, static load factor and the crack location on the first and second dynamic stability of cantilever composite plate, as 3D plots. The composite plates have been examined for the five different orientation angles which are denoted by C1, C2, C3, C4, C5. In these figures, the crack is located in the middle of y the axis and the crack is moved along the x axis of the cantilever composite plate. As seen from these figures, when the static load factor (α) is equal to 0.5, the dynamic load factor (β) is bounded between the values of 0 and 1. If the static load factor (α) is equal to 0, the dynamic load factor (β) is bounded between the values of 0 and 2. If the dynamic load factor (β) increases, the unstable region widens for C1, C2, C3, C4, C5. If the static load factor (α) is equal to 0, 0.5 and dynamic load factor (β) is equal to 1, 2, respectively, the first exciting frequencies constructing the lower border of the unstable region reach zero. It is observed that the crack does not change these situations.

In these figures, the crack changes the unstable region of cantilever composite plate for C1, C2, C3, C4, C5. It is observed for C2, C3, C4, C5 orientation angles that if the crack is moved away from the fixed support on the x axis direction, the first exciting frequency increases for each static load factor (α). It is also observed that when the crack is moved away from the fixed support on the x axis direction and static load factor (α) is equal to 0, the first exciting frequency increases for C1 orientation. As seen from figure 4.54, if the crack is moved away from the fixed support to 100 mm on the x axis direction and static load factor (α) is equal to 0.5, the effect of crack is less on the first exciting frequency for C1 orientation. If the crack is moved away from 100 to 400 mm, the first exciting frequency increases. In these figures, if static load factor (α) is equal to 0, the effect of crack is less on the second exciting frequency. If the crack is moved away from the fixed support to 350 mm on the x axis direction and static load factor (α) is equal to 0.5, the crack decreases the second exciting frequency. When the crack is moved away from 350 to 400 mm, the effect of crack is less on the second exciting frequency for C1, C2, C3, C4, C5.

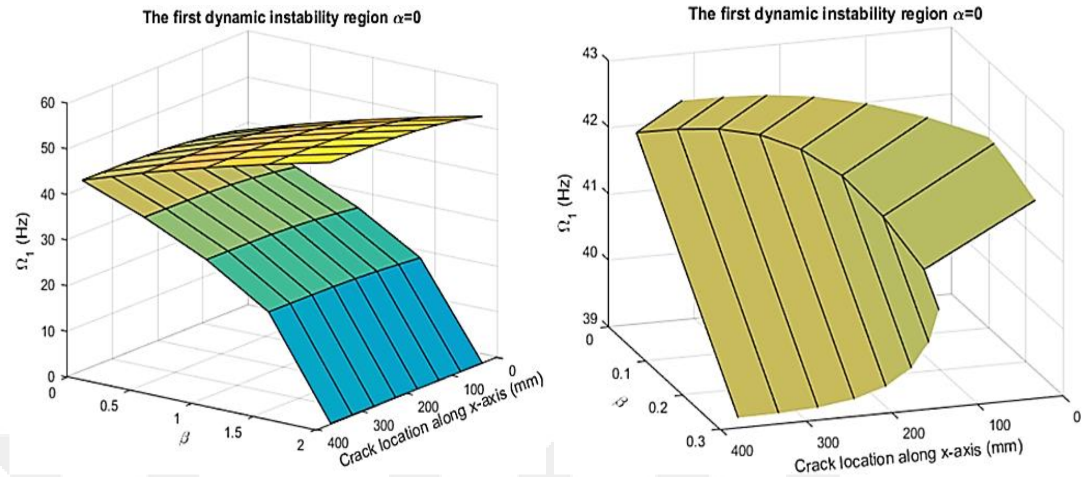

Figure 4.53 The effect of crack on the first dynamic instability region of the laminated composite plate [0°/0°/0°/0°] for α=0

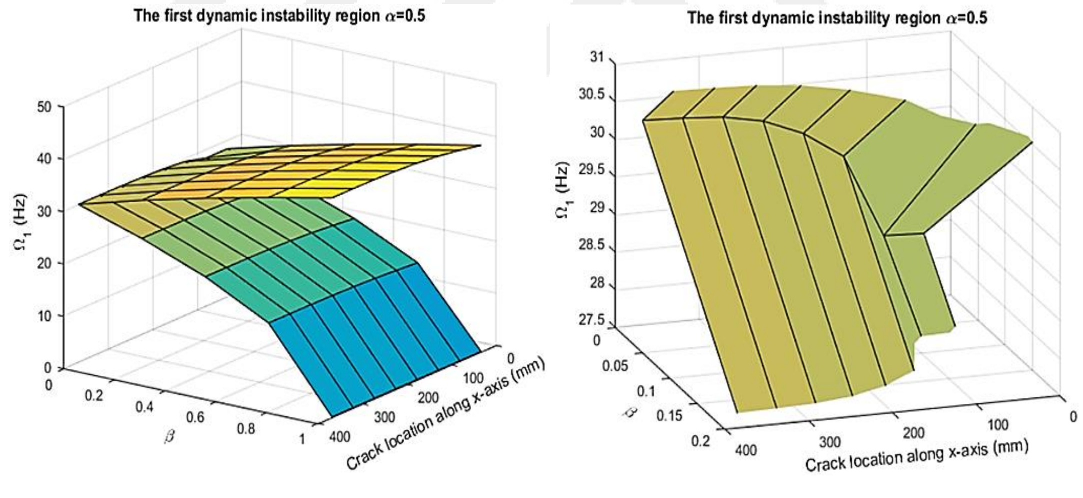

Figure 4.54 The effect of crack on the first dynamic instability region of the laminated composite plate [0°/0°/0°/0°] for α=0.5

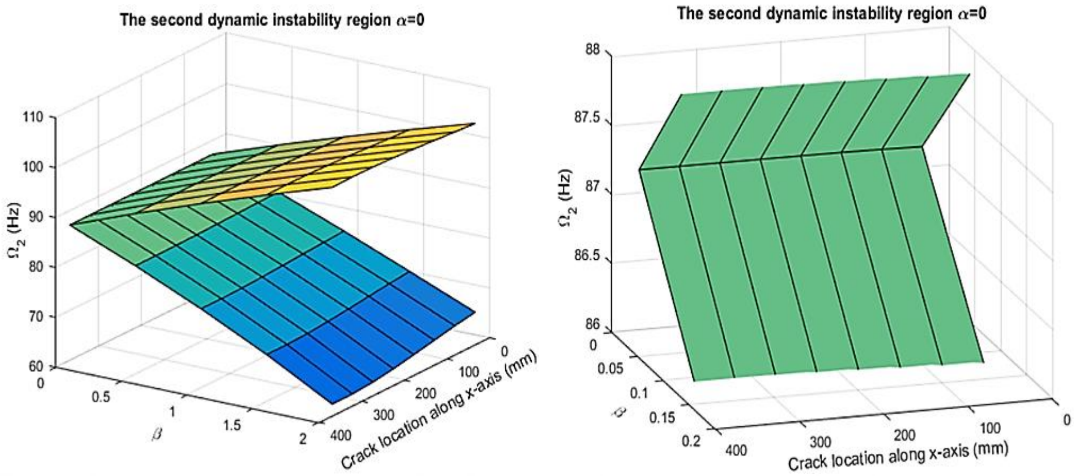

Figure 4.55 The effect of crack on the second dynamic instability region of the laminated composite plate [0°/0°/0°/0°] for α=0

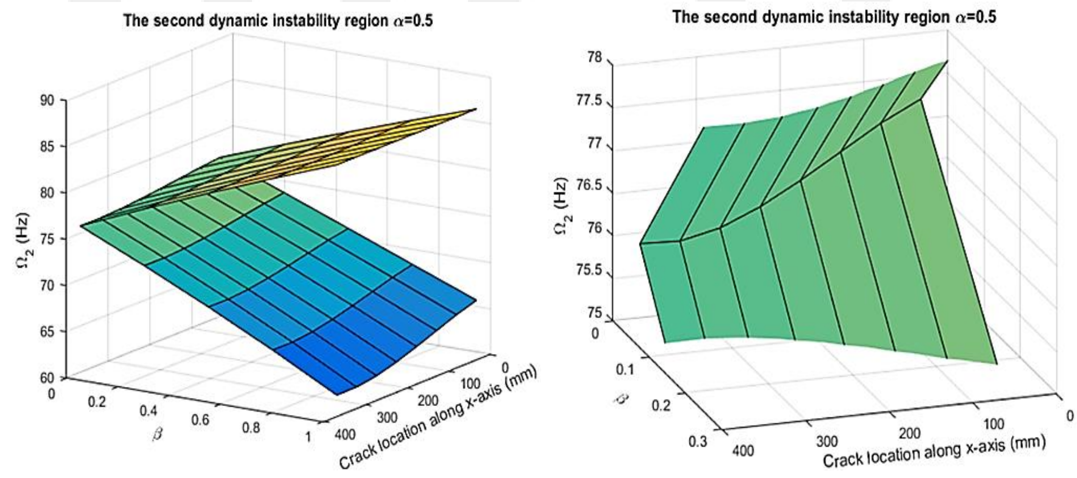

Figure 4.56 The effect of crack on the second dynamic instability region of the laminated composite plate [0°/0°/0°/0°] for α=0.5

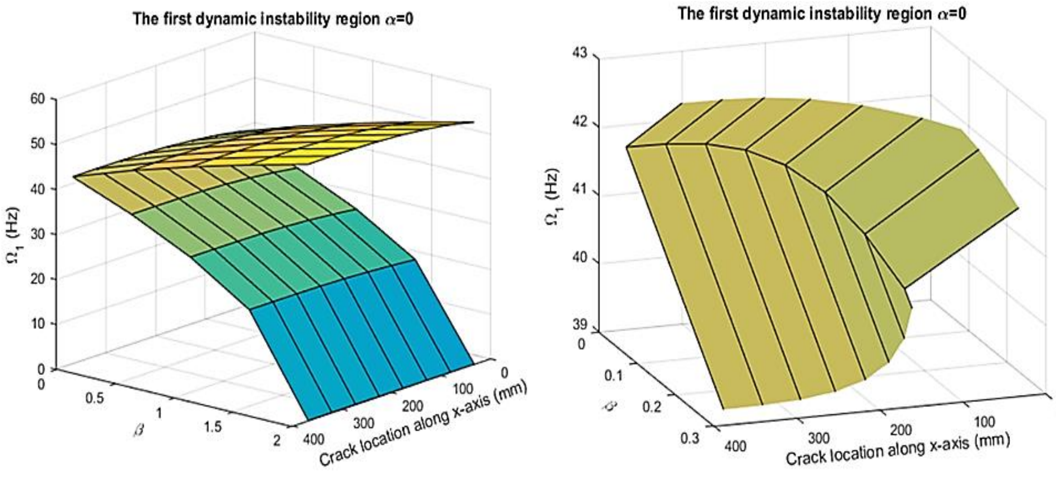

Figure 4.57 The effect of crack on the first dynamic instability region of the laminated composite plate [0°/30°/-30°/0°] for α=0

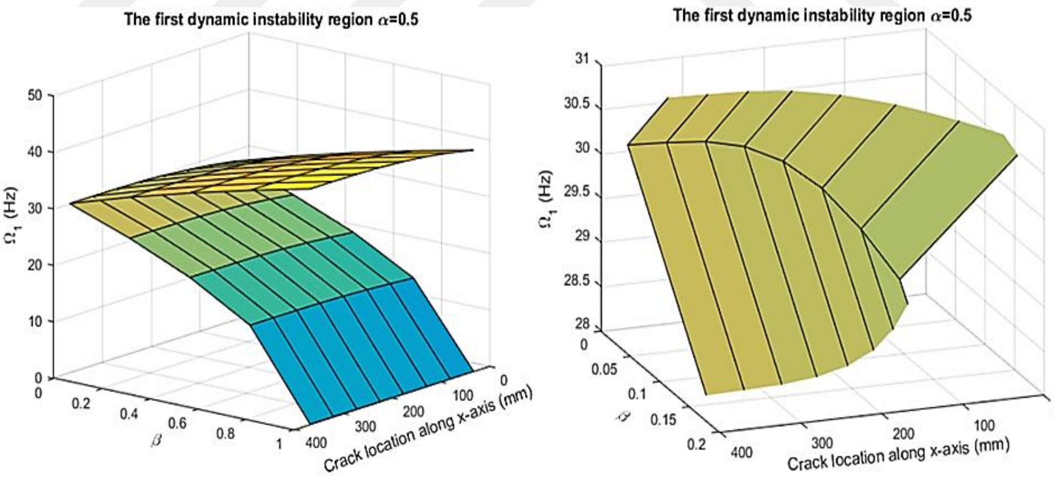

Figure 4.58 The effect of crack on the first dynamic instability region of the laminated composite plate [0°/30°/-30°/0°] for α=0.5

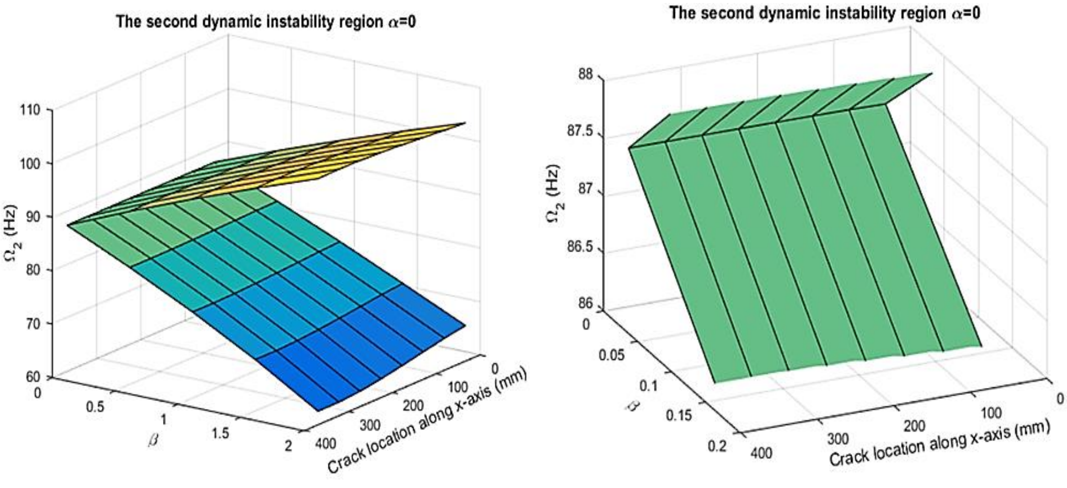

Figure 4.59 The effect of crack on the second dynamic instability region of the laminated composite plate [0°/30°/-30°/0°] for α=0

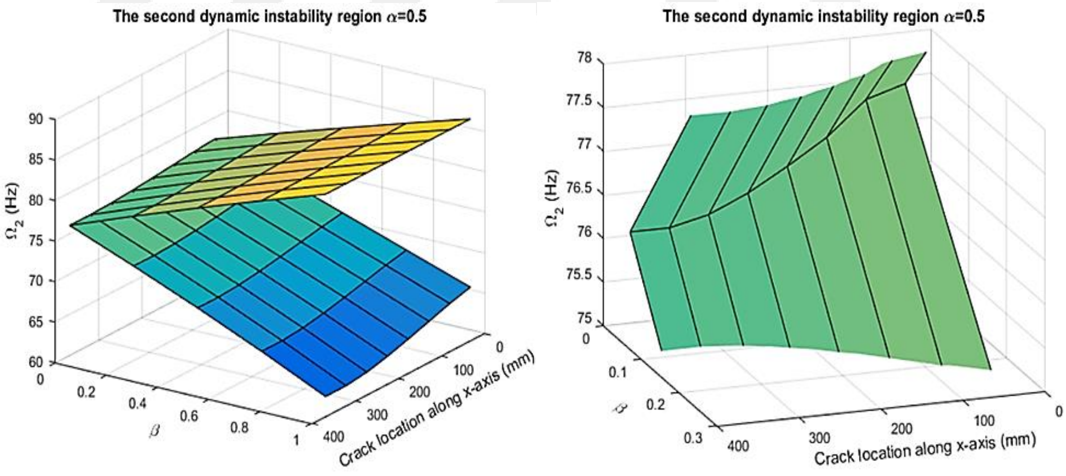

Figure 4.60 The effect of crack on the second dynamic instability region of the laminated composite plate [0°/30°/-30°/0°] for α=0.5

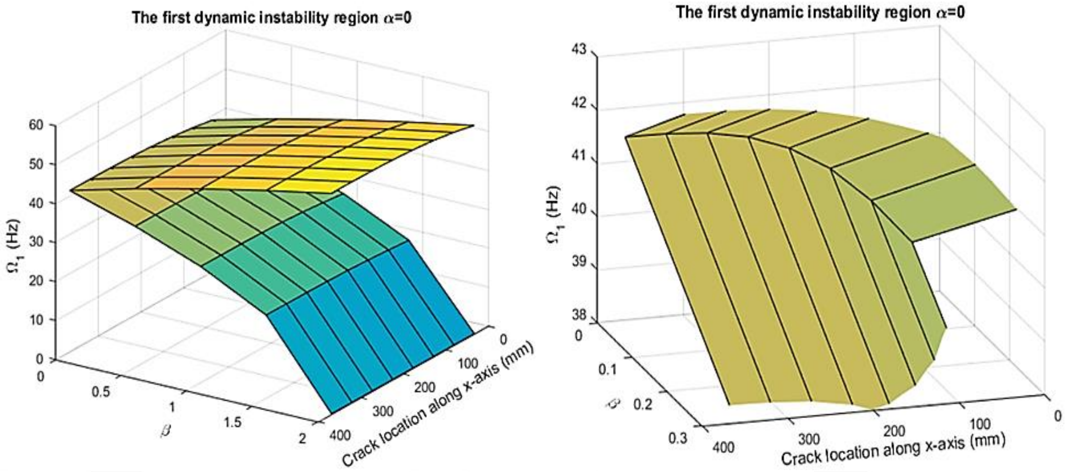

Figure 4.61 The effect of crack on the first dynamic instability region of the laminated composite plate [0°/45°/-45°/0°] for α=0

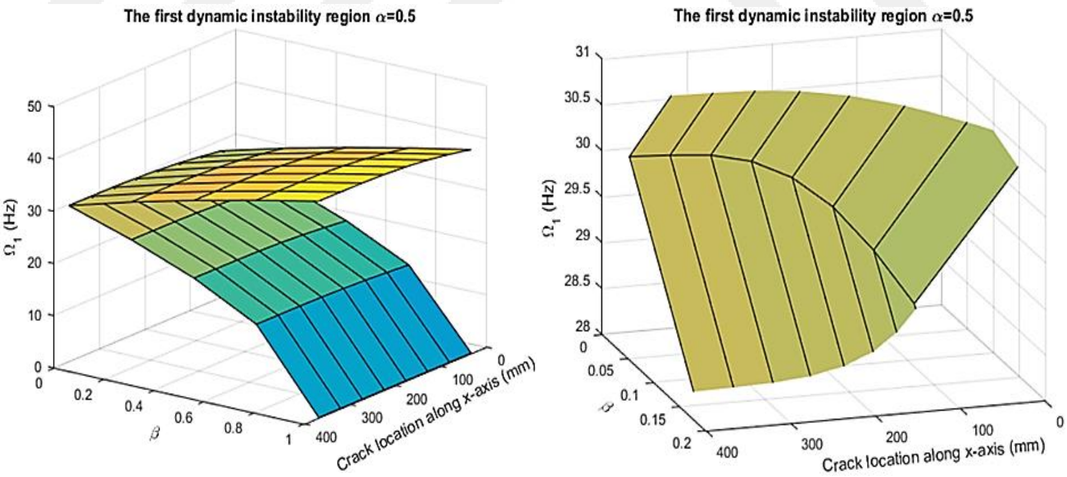

Figure 4.62 The effect of crack on the first dynamic instability region of the laminated composite plate [0°/45°/-45°/0°] for α=0.5

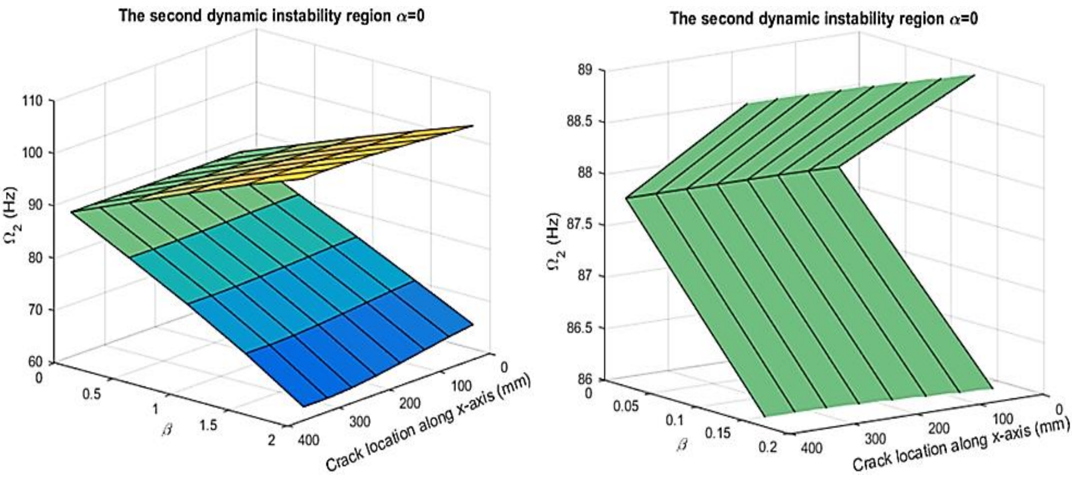

Figure 4.63 The effect of crack on the second dynamic instability region of the laminated composite plate [0°/45°/-45°/0°] for α=0

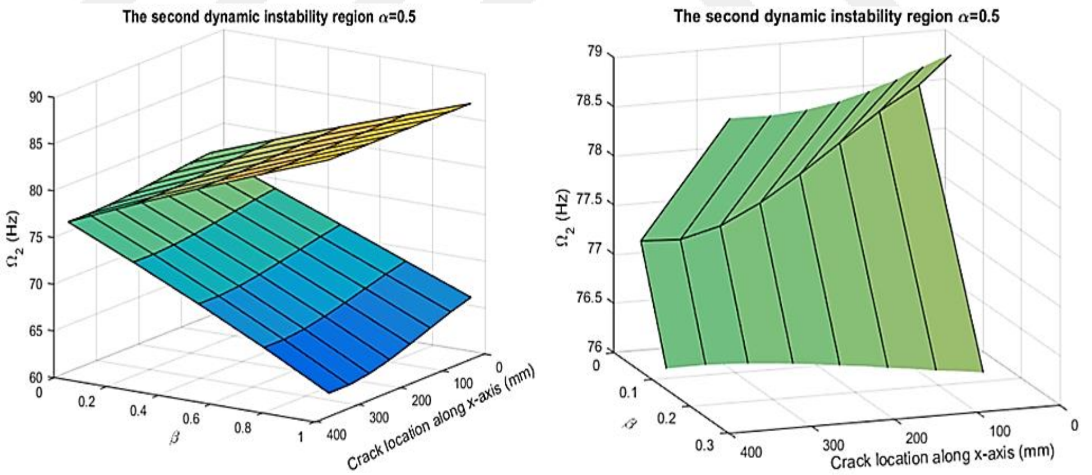

Figure 4.64 The effect of crack on the second dynamic instability region of the laminated composite plate [0°/45°/-45°/0°] for α=0.5

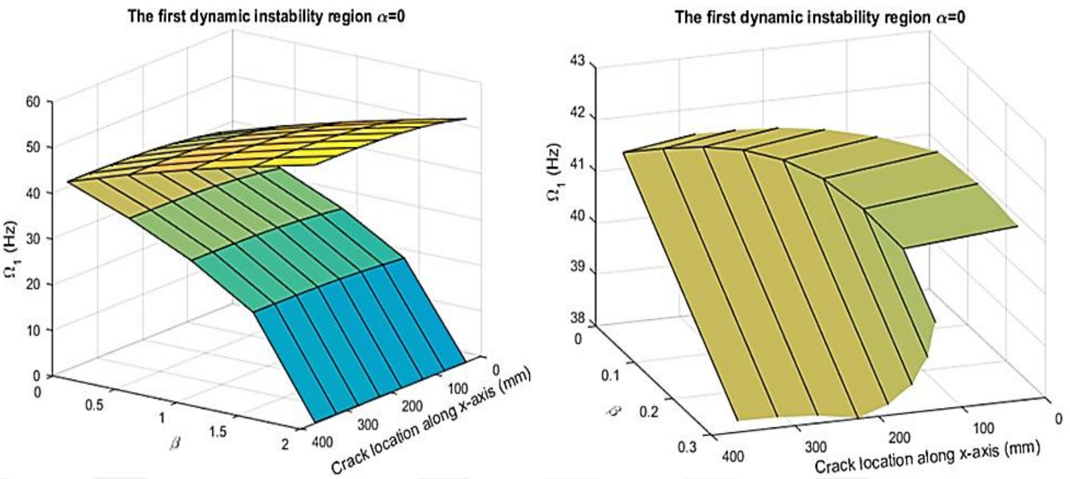

Figure 4.65 The effect of crack on the first dynamic instability region of the laminated composite plate [0°/60°/-60°/0°] for α=0

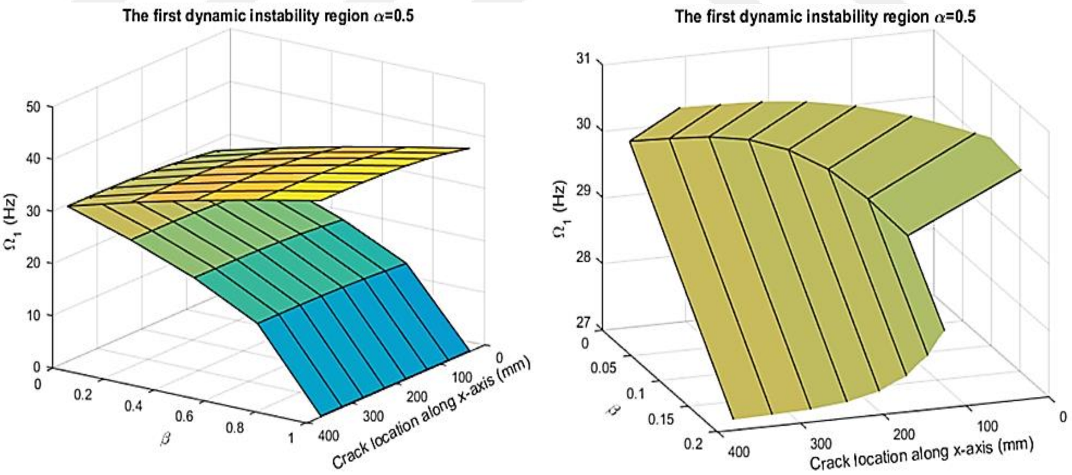

Figure 4.66 The effect of crack on the first dynamic instability region of the laminated composite plate [0°/60°/-60°/0°] for α=0.5

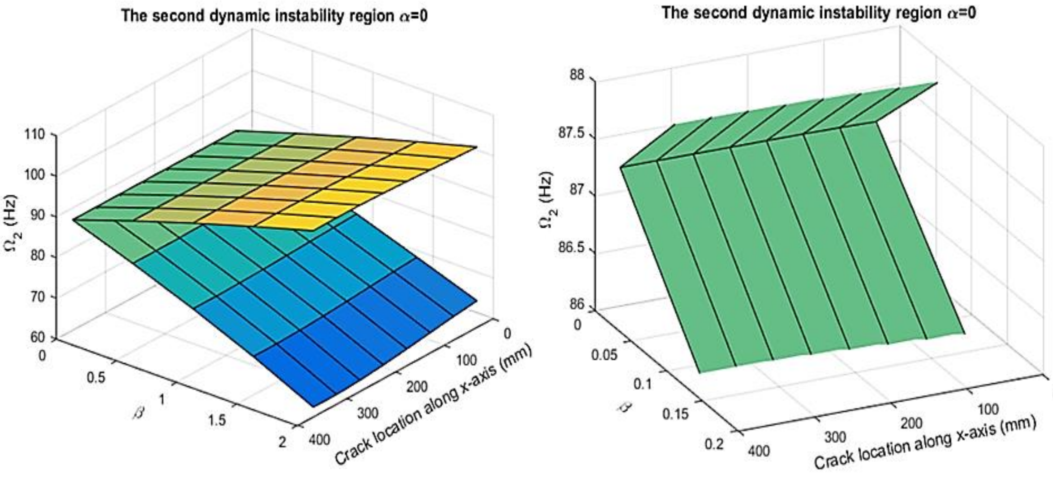

Figure 4.67 The effect of crack on the second dynamic instability region of the laminated composite plate [0°/60°/-60°/0°] for α=0

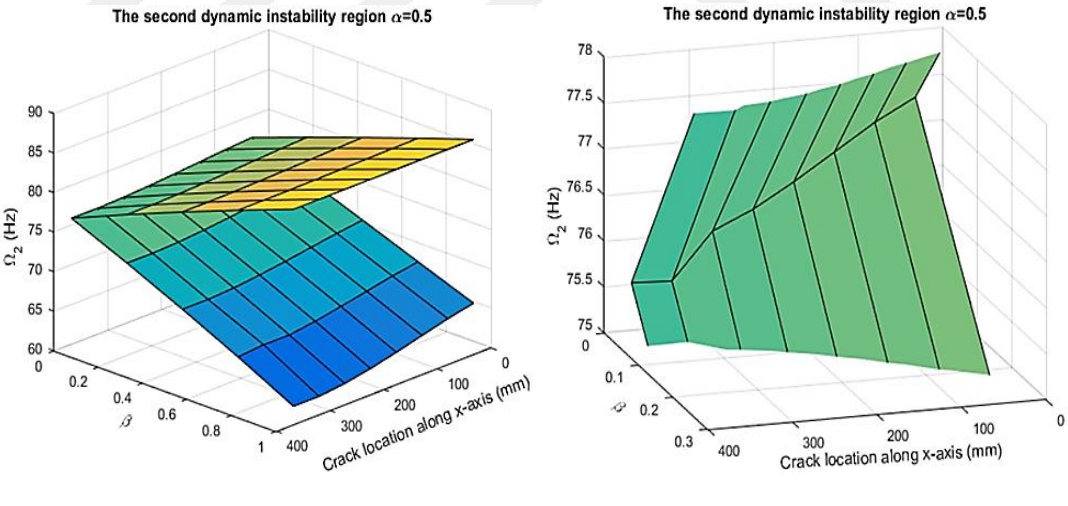

Figure 4.68 The effect of crack on the second dynamic instability region of the laminated composite plate [0°/60°/-60°/0°] for α=0.5

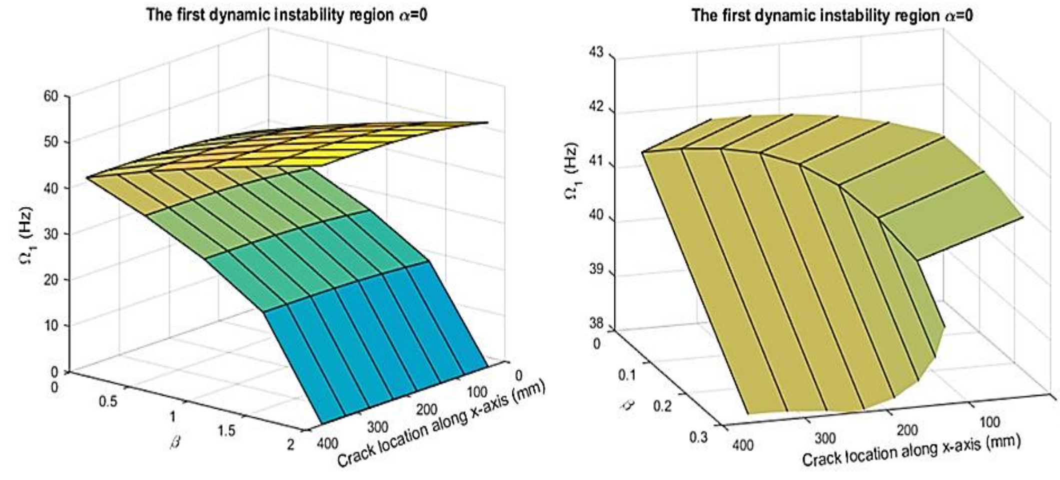

Figure 4.69 The effect of crack on the first dynamic instability region of the laminated composite plate [0°/90°/90°/0°] for α=0

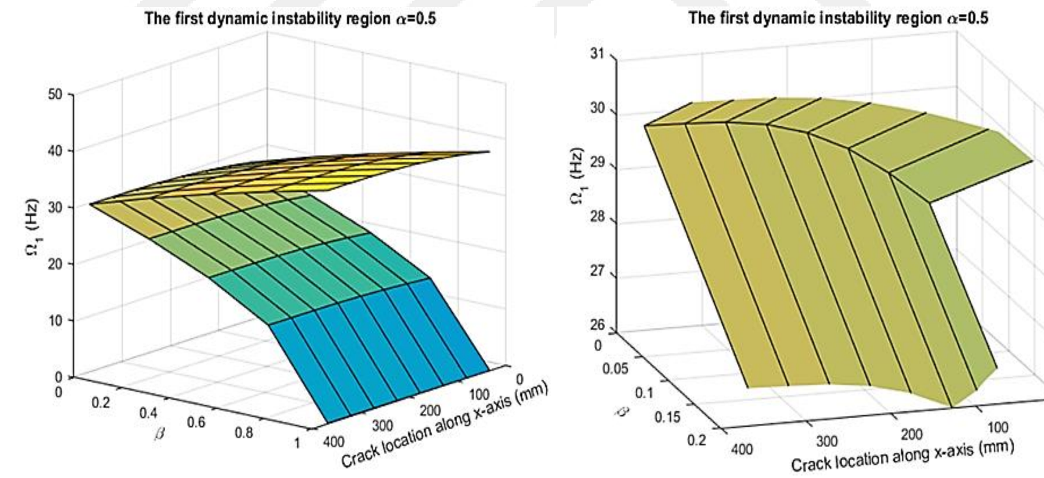

Figure 4.70 The effect of crack on the first dynamic instability region of the laminated composite plate [0°/90°/90°/0°] for α=0.5

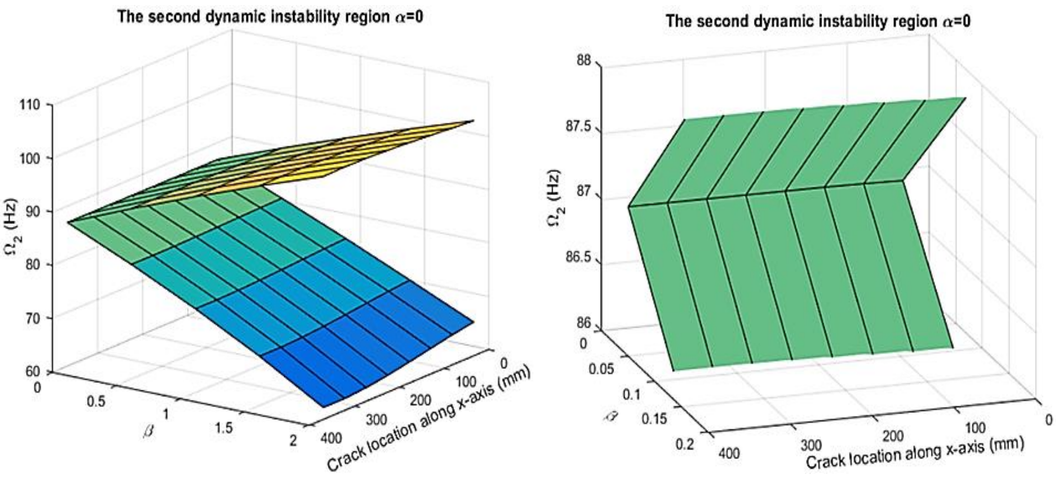

Figure 4.71 The effect of crack on the second dynamic instability region of the laminated composite plate [0°/90°/90°/0°] for α=0

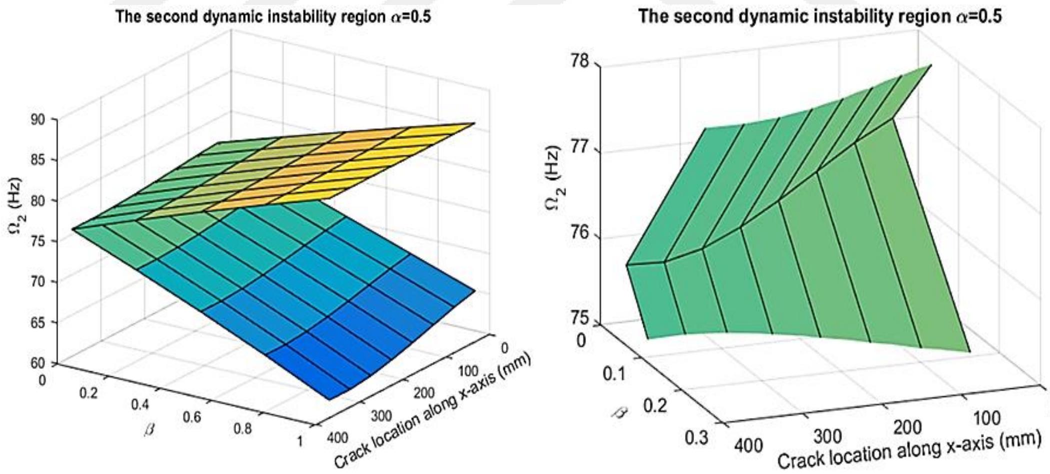

Figure 4.72 The effect of crack on the second dynamic instability region of the laminated composite plate [0°/90°/90°/0°] for α=0.5

CHAPTER FIVE
CONCLUSIONS

In this study, the effect of crack on the free vibration, buckling and dynamic stability analysis of isotropic and composite plates for the five different orientation angles have been investigated numerically by using the finite element method. The natural frequency and buckling load results obtained from the present work are compared with the results obtained from ANSYS software for the accuracy of the finite model.

The following conclusions are drawn:

When a crack occurs on the cantilever composite or isotropic plate, the first five modes of natural frequencies and the critical buckling load decrease albeit with different effects at each location.

The effect of the crack is different for each natural frequency mode.

The effect of the crack is different for each orientation angle.

If the composite plate is used to C1 orientation and the crack location is moved to the free end on the *x* axis, the first natural frequency is the maximum value for composite plate. If the crack location is moved to middle of fixed end and the cantilever composite plate is used to C5 orientation, the first natural frequency is the minimum value for composite plate.

If the crack occurs at the edge side regions of the composite plate and the crack location is moved away from the fixed side to the middle area on the *x* axis direction, the second natural frequency increases rapidly, especially for C1, C4, C5.

If the crack is moved along the *y* axis in a location close to a fixed support, the third natural frequency is minimum at the edge side regions of the composite plate.

The third natural frequency of C3 is lower than the other orientation angles in these regions. It is observed that if the crack location is moved from these regions to the middle area on the *y* axis, the third natural frequency increases. The change of the third natural frequency of C4 is slower than the other orientation in this region.

The effect of a crack is maximum in the middle of the plate. Therefore, the fourth natural frequency in this region is lower than the other regions. The fourth natural frequency of C2 is less than the other orientation angles in this region. When the crack location is moved to the fixed side in the middle of the *y* axis, the fourth natural frequency decreases.

When the crack is located at the edge side regions in the middle area, the fifth natural frequency is minimum for all five different orientations. The fifth natural frequency of C5 is lower than the other orientation angles in these regions.

If the crack location is moved to the middle of the fixed end, the critical buckling load decreases. The critical buckling load of the cantilever composite plate for C5 orientation is minimum.

When the static load factor (α) is equal to 0, the dynamic load factor (β) is bounded between the values of 0 and 2. If the static load factor (α) is equal to 0.5, the dynamic load factor (β) is bounded between the values of 0 and 1.

If the dynamic load factor (β) increases, the unstable region widens.

If the crack is moved from the fixed end to the free end on the *x* axis direction for C2, C3, C4, C5, the first exciting frequency increases for each static load factor (α). When the crack is moved from the fixed end to free end on the *x* axis direction and the static load factor (α) is equal to 0, the first exciting frequency increases for C1 orientation. If the crack is moved to the fixed end and static load factor (α) is equal to 0.5, the effect of the crack is less on the first exciting frequency for C1 orientation.

If the static load factor (α) is equal to 0, the effect of the crack is less on the second exciting frequency. If the crack is moved from the fixed end on the x axis direction and static load factor (α) is equal to 0.5, the second exciting frequency decreases. When the crack location is moved to the free end on the x axis, the effect of the crack is less on the second exciting frequency for C1, C2, C3, C4, C5.

For future studies, the study of the effect of crack on dynamic stability for the composite plate can be expanded using a curved plate instead of a flat plate. A recommendation for future studies, crack location, ply angle, static and dynamic load factor are considerable parameters for dynamic stability of cracked composite plates.

REFERENCES

Abbas, B. A. H. (1977). *Mechanical vibration and dynamic stability of complex structures by finite element method*. Ph.D. Thesis, Surrey University, Guildford.

Abramovich, H. (2017). *Stability and vibrations of thin-walled composite structures.* Cambridge: Woodhead.

Aggarwal, V. D. (2013). *Optimization of variable stiffness composite plate structures.* M.Sc. Thesis, San Diego State University, San Diego.

Anderson, T. L. (2005). *Fracture mechanics: fundamentals and applications* (3rd ed.). Boca Raton: CRC Press.

Avadutala, V. S. (2005). *Dynamic analysis of cracks in composite materials.* M.Sc. Thesis, Blekinge Institute of Technology, Karlskrona.

Bolotin, V. V. (1964). *The dynamic stability of elastic systems.* San Francisco: Holden-Day, Inc.

Chen, L. W., & Yang, J. Y. (1990). Dynamic stability of laminated composite plates by the finite element method. *Computers & Structures, 36* (5), 845-851.

Daniel, I. M., & Ishai, O. (2006). *Engineering mechanics of composite materials* (2nd ed.). New York: Oxford university Press.

Hutt, J. M. (1968). *Dynamic stability of plates by finite elements.* Ph.D. Thesis, Oklahoma State University, Oklahoma.

Khoei, A. R. (2015). *Extended finite element method: theory and applications.* West Sussex: John Wiley & Sons.

Krawczuk, M., & Ostachowicz, W. M. (1994). A finite plate element for dynamic analysis of a cracked plate. *Computer methods in applied mechanics and engineering*, *115* (1-2), 67-78.

Kwon, Y. W., & Bang, H. (1996). *The finite element method using MATLAB*. New York: CRC Press.

Oñate, E. (2013). *Structural analysis with the finite element method linear statics: volume 2. beams, plates and shells.* Barcelona: Springer.

Öztürk, H. (1999). *Effect of spring stiffness and spring position on the dynamic stability of cantilever, non-uniform cross-sectioned, Timoshenko beams subjected to periodic axial loading.* M.Sc. Thesis, Dokuz Eylül University, İzmir.

Radu, A. G., & Chattopadhyay, A. (2002). Dynamic stability analysis of composite plates including delaminations using a higher order theory and transformation matrix approach. *International Journal of Solids and Structures*, *39* (7), 1949-1965.

Reddy, J. N., (2003). *Mechanics of laminated composite plates theory and analysis* (2nd ed.). New York: CRC Press.

Semie, A. G. (2010). *Numerical modelling of thin plates using the finite element method.* M.Sc. Thesis, Addis Ababa University, Addis Ababa.

Soedel, W. (2004). *Vibrations of shells and plates* (3rd ed.). New York: Marcel Dekker, Inc.

Szilard, R. (2004). *Theories and applications of plate analysis: classical, numerical and engineering methods*. New Jersey: John Wiley & Sons.

Timoshenko, S. P., & Gere, J. M. (1961). *Theory of elastic stability* (2nd ed.). New York: McGraw- Hill Book Company, Inc.

Ventsel, E., & Krauthammer, T. (2001). *Thin plates and shells: theory, analysis and applications.* New York: Marcel Dekker, Inc.

Voyiadjis, G. Z., & Kattan, P. I. (2005). *Mechanics of composite materials with MATLAB.* Berlin: Springer.

APPENDICES

Appendix 1: Nomenclature

a_e	Length of the square plate element on the x-direction
$[A_e]$	Displacement matrix of square plate element
b_e	Width of the square plate element on the y-direction
$[\mathrm{B}_e]$	Strain displacement matrix of square plate element
$[C_e]$	Displacement model
d	Displacement matrix for corner of square plate element
$[\mathrm{D}_e]$	Rigidity matrix of square plate element
E	Young's modulus of isotropic plate
E_f	Young's modulus of fiber material
E_m	Young's modulus of matrix material
E_1	Longitudinal modulus of composite plate
E_2	Transverse modulus of composite plate
G	Shear modulus of isotropic plate
G_f	Shear modulus of fiber material
G_m	Shear modulus of matrix material
G_{12}	Shear modulus of the composite plate
h	Thickness of plate
K	Curvature
$[K_e]$	Global elastic stiffness matrix
$[K_e]^e$	Local elastic stiffness matrix
$[K_g^*]$	Global geometric stiffness matrix
$[K_g^*]^e$	Local geometric stiffness matrix
l_p	Length of plate
$[M]$	Global mass matrix
$[M]^e$	Local mass matrix
N_{cr}	Critical buckling load
$[N_e]$	Interpolation matrix

N_x	In-plane load per unit length on x axis
q	Generalized coordinates of plate
q_e	Generalized coordinates of square plate element
$[S]$	Displacement shape function matrix of square plate element
$[T]$	Transformation matrix
U	Strain energy
V	Kinetic energy
V_f	Volume fraction of fiber material
V_m	Volume fraction of matrix material
w	Translational displacement on z axis
w_p	Width of plate
α	Static load factor
$[\alpha^e]$	Coefficient matrix
β	Dynamic load factor
$[\mathcal{E}_e]$	Strain matrix of square plate element
ρ	Density of plate
φ	Rotational displacement on x axis
θ	Ply angle
v	Poisson's ratio of isotropic plate
v_f	Poisson's ratio of fiber material
v_m	Poisson's ratio of matrix material
v_{12}	Major poisson's ratio of composite plate
v_{21}	Minor poisson's ratio of composite plate
Ψ	Rotational displacement on y axis
ω	Natural frequency
Ω	Exciting frequency
ч	Dimensionless time
δ	Change of the virtual displacements
Λ	Loss of potential energy
Π	Total potential energy of the system